TESIS DOCTORAL

2022

Analysis of iterative algorithms based on KTG for transport properties of multicomponent mixtures.

ÓSCAR CÓRDOBA MUÑOZ

PROGRAMA DE DOCTORADO INTERUNIVERSITARIO EN MECÁNICA de FLUIDOS

DIRECTOR: MANUEL ARIAS ZUGASTI

Esta tesis está dedicada a Carmen y Luis,

a Mario y Rubén,

y a Cristina.

Madrid, Octubre de 2022

Agradecimientos

Esta tesis es el resultado del esfuerzo de muchos años, mío y de muchas personas sin cuya contribución este trabajo no habría salido adelante.

En primer lugar, mi mayor agradecimiento es para Manuel Arias-Zugasti. Ha dirigido esta tesis y la ha hecho posible iniciando esta línea de investigación, indicando el camino a seguir que él mismo había comenzado. Se ha encargado de realizar las correcciones oportunas de todos los manuscritos, ha prestado su ayuda siempre que se le ha requerido y ha aportado soluciones a los problemas que se han ido presentando. Me ha hecho partícipe del extraordinario campo de la teoría cinética de gases, que yo sin duda desconocía.

Asimismo, quiero agradecer también a las personas del departamento de Física y Mecánica de Fluidos de la UNED, Pedro García Ybarra y José Luis Castillo por sus consejos técnicos y su visión didáctica del transporte en mezclas de gases. Mi agradecimiento es también para la Escuela de Doctorado de la UNED y la oportunidad que me ha brindado de realizar este trabajo enmarcado dentro del programa #PID2019-108592RB-C44 del Ministerio de Ciencia e Innovación.

Mi agradecimiento es también para dos personas del CIEMAT. En primer lugar, Bertrand Naud, que ha contribuido en numerosas ocasiones aportando su propio trabajo, su visión y su conocimiento. En segundo lugar, Daniel Fernández Galisteo por su ayuda con la generación del fichero Chemkin del mecnismo de la reacción de siete pasos del hidrógeno.

Me gustaría agradecer a los revisores de las diferentes publicaciones a las que se han enviado algunas partes de este trabajo sus consejos, opiniones y críticas. Han conseguido que la consistencia y solidez del trabajo realizado sea muy superior. Agradezco también a los miembros de este tribunal por acceder a juzgar este trabajo.

Por último agradezco a mi mujer, Cristina, y a mis dos hijos, Mario y Rubén, su paciencia y comprensión durante la realización de este trabajo. Ha sido llevado a cabo en casa, fuera de mi horario laboral, dedicando mucha parte del tiempo que tendría que haberles dedicado a ellos.

Abstract

The purpose of this work is to provide an efficient and accurate algorithm to calculate the transport coefficients in mixtures of gases. This is specially important in combustion simulations with large number of components. The main transport parameters are the diffusion coefficients and the thermal conductivity. Diffusion is the transport phenomenon responsible for mixing at the molecular level, playing an important role in combustion. As is well known, diffusion fluxes are proportional to species concentration and temperature gradients, with Fick's law multicomponent diffusion coefficients D_{ij} $(i, j = 1, \ldots, N)$ and thermal diffusion coefficients D_{Ti} being the corresponding respective transport coefficients. Hence, accurate calculation of D_{ij} and D_{Ti} is the key for a correct evaluation of diffusion fluxes in multicomponent mixtures. The thermal conductivity is the main transport coefficient used in the energy equation of mixtures of gases. Once all the relevant physical processes taking place in a typical combustion environment are accurately represented (in particular multicomponent transport and chemical kinetics), it is possible to perform Direct Numerical Simulations (DNS) of laminar or turbulent flames, which may be considered as numerical experiments.

Resumen

El propósito de este trabajo es generar un algoritmo eficiente y preciso para calcular los coeficientes de transporte en mezclas de gases. Esto es especialmente importante en simulaciones de combustión con un número elevado de componentes. Los principales parámetros de transporte son los coeficientes de difusión y la conductividad térmica. La difusión es el fenómeno de transporte responsable de la mezcla a nivel molecular, jugando un papel importante en combustión. Como es conocido, los flujos de difusión son proporcionales a los gradientes de concentración y gradientes de temperatura, con los coeficientes de difusión correspondientes a la ley de Fick D_{ij} $(i, j = 1, \ldots, N)$ y los coeficientes de difusión térmica D_{Ti} $(i = 1, \ldots, N)$. Por tanto, un cálculo preciso de D_{ij} y D_{Ti} es la llave para una correcta evaluación de los flujos de difusión en mezclas multicomponente. La conductividad térmica es el principal coeficiente de transporte usado en la ecuación de la energía de mezclas de gases. Una vez que todos los procesos físicos relevantes que tienen lugar en los procesos de combustión son simulados de forma precisa (en particular el transporte multicomponente y la cinética química), es posible realizar Simulaciones Numéricas Directas (DNS) de llamas laminares o turbulentas, las cuales pueden ser consideradas como experimentos numéricos.

Contents

List of Figures

List of Tables

Chapter 1

Introduction and objectives

1.1 State of the art

In the case of mixtures of dilute gases, the kinetic theory of gases (KTG) [3, 4, 1] provides a general framework for the calculation of the multicomponent diffusion coefficients D_{ij} and D_{Ti}, thermal conductivity and viscosity, based on the knowledge of the molecular characteristics of all chemical species in the mixture (i.e., molecular masses, sizes and intermolecular interaction potentials among all different species in the mixture). Classical theory provides very good results on monatomic gases with low and medium density, assuming elastic interactions between molecules. For dense gases, the classical kinetic theory of gases is not so accurate. Within the kinetic theory of gases framework and based on the Chapman-Enskog expansion, a step forward was given in reference [5] to account for polar interactions, monopolar-polar interactions, non elastic interactions and polar resonant collisions. Based on this, in references [6, 7, 8], a formal kinetic theory for polyatomic gases requires the resolution of a linear system with $3N$ equations (or $2N + P$, where P is the number of non monatomic molecules). The solution of the aforementioned system poses no difficulty. However, since the evaluation of the transport properties must be evaluated at every time step and every node in the computational mesh, and the former linear system depends on mixture composition and temperature, the evaluation of transport properties can become computationally expensive if the number of components in the mixture is high, specially in unsteady 3D direct numerical simulations (DNS). The former difficulty has motivated the development of useful simplified approximations, such as *mixture averaged* transport properties, which becomes quite accurate in the dilute limit, or the use of constant Lewis numbers, which is useful in theoretical combustion analyses as it leads to simplified evolution equations [9, 10]. Recent works have tested simplified models using Lewis number in the stabilization effect of premixed flames [11]. In reference [12], the authors show the validation of the mixture averaged approximation in hydrogen flames with thermal diffusion. Although, the results of mixture averaged are valid

for certain types of simulations, they are not accurate enough for the transport coefficient calculation in detailed simulations. A proper evaluation of multicomponent transport properties is critical in accurate DNS of reactive flows. For instance, detailed multicomponent transport can have an important effect in turbulent flames in regions where the front experiences strong curvature [13] and in cases with Reynolds numbers between 600 and 8000 [14].

Regarding accuracy, it must be noted that kinetic theory of gases does not match experiments completely and this is the reason why iterative methods are so interesting. References [15, 16, 17] shows that multicomponent transport properties and test measurements are in a range of $\pm 5\%$. These results are found for several interaction potentials between particles and the correspondent collision integrals. On the other hand, in some cases the differences between the results for transport coefficients based on the mixture averaged approximation and the exact solution from the kinetic theory of gases can be quite significant, with errors over $\pm 100\%$ in some transport coefficients, which makes mixture averaged approximation clearly not suitable for accurate simulations. Therefore, multicomponent transport with iterative approximations are an adequate scope for the transport magnitudes calculation.

After the initial studies on multicomponent diffusion in combustion by Dixon-Lewis [18] followed by Jones and Boris [19] and Oran and Boris [20], the general problem of multicomponent transport is addressed in the well known works of Giovangigli (see, e.g., [21, 22, 23, 24, 25, 26]). In particular, the application of standard iterative methods for the calculation of the transport properties of multicomponent mixtures is investigated in reference [26]. For a review on the implementations for transport calculations available in 2011 see [15]. A different strategy is adopted by Xin et al. in a more recent work [27], based on a sensitivity analysis which determines the group of species whose diffusive transport has strongest impact on flame dynamics, thus allowing for a simplified treatment of the transport properties of the remaining species.

The calculation of the multicomponent Fick diffusion coefficients was also analyzed by Arias-Zugasti et al. [28], where two efficient new algorithms: Model 1 and Model 1+M, are derived for the calculation of D_{ij}. Both models are based on the KTG and make use of dimensionless variables, conveniently scaled with the correct characteristic quantities, thus allowing for an increased efficiency in the calculation of D_{ij}. In Model 1, based on [29], the multicomponent mixture is assumed to be dilute in 1 major species, and D_{ij} is given as a power series in terms of the remaining $N-1$ mole fractions in the mixture. As a natural extension of Model 1, in Model 1+M the mixture is assumed to contain a total of $1+M$ major species, and D_{ij} are computed as a power series in terms of the remaining $N-M-1$ mole fractions, which are assumed to be close to the dilute limit, thus avoiding the use of approximate methods regarding the major, non-dilute, species. The optimal implementation of Model 1+M was subsequently analyzed by Naud and Arias-Zugasti [30]. When the number of major species in the mixture is properly chosen, the leading order of Model 1+M provides

accurate results at a computational cost which is even lower than the corresponding mixture averaged approximation [30]. This extreme computational time reduction is a consequence of the structure of Model 1+M, which in its leading order approximation involves the evaluation of a reduced number of binary diffusion coefficients (i.e., only those involving at least one of the major species).

Model 1+M improves considerably the performance of the existing algorithms for the Fick diffusion coefficients calculations, such as mixture averaged or Ern Giovangigli method. The extrapolation of these ideas to the rest of the transport parameters promises good results for the thermal diffusion coefficients and thermal conductivity.

1.2 Objectives

The following list summarizes the objectives of this work:

- To review the kinetic theory of gases and to revisit the equations needed to obtain the multicomponent transport coefficients of multicomponent mixtures of ideal gases.
- To reuse the results of [28] and to apply the same ideas for those transport parameters not covered, i.e., the thermal diffusion coefficients and the thermal conductivity. Based on this, to design an efficient and accurate algorithm to calculate the transport coefficients of multicomponent mixtures.
- To implement and to validate the iterative algorithm for the transport coefficients calculations. The algorithm efficiency is studied and the operations count is reviewed and compared against a direct inversion algorithm and the conjugate gradients iterative algorithm.
- To study the convergence and stability of the proposed algorithm.
- To review the algorithm accuracy comparing the results against the exact KTG solution and the EGLib and mixture averaged approaches. To this end, two cases of interest in combustion science are considered, including a premixed hydrogen flame as a function of the equivalence ratio and a methane counterflow diffusion flame.

Summarizing the previous list, the purpose of this work is to provide a new simple, efficient and accurate iterative algorithm for the evaluation of the multicomponent transport coefficients of typical combustion gas mixtures. The general idea to achieve this goal is to formulate the problem in terms of dimensionless variables, based on the correct characteristic scales. The proposed solution makes use of the results shown in [28] and involves the inversion of new sub-matrices which are diagonally dominant, thus allowing for an efficient inversion based on the Neumann series.

This work presents the theoretical details for the calculation of the multicomponent thermal diffusion coefficients and the partial thermal conductivity. These new algorithms have been implemented in the software library package MuTLib (Multicomponent Transport Library), available for the transport properties calculations in third party applications. The algorithm performance improvements are shown in two different flames: a hydrogen premixed flame and a methane diffusion flame. The results are successfully compared against the library package EGLib (Ern Giovangigli Library, which considers the same physical effects as this work), and to the well known mixture averaged approximation, which is also briefly described in this work.

Chapter 2

Summary of the classical kinetic theory of gases

The notes in this chapter are extracted mostly from the reference Ferziger-Kaper, 1972. "The mathematical theory of transport processes in gases" [1].

2.1 Historical background

The kinetic theory of gases began in mid-19th century. The following are the most relevant milestones:

- 1859, Maxwell introduced the statistical approach to non equilibrium gases and the maxwellian velocity distribution.
  - Maxwell, J.C. (1860 A): Illustrations of the dynamical theory of gases. Part I. On the motions and collisions of perfectly elastic spheres. The London, Edinburgh, and Dublin Philosophical Magazine and Journal of Science, 4th Series, vol.19, pp.19-32, `https://doi.org/10.1080/14786446008642818`.
- 1872, Boltzmann was the first author mentioning the H-theorem and molecular collisions entropy increase. The Boltzmann H theorem relates the system entropy S with the number of states accessible to the the system W, $S = k_B \ln W$, where k_B is the Boltzmann constant ($1.380649 \cdot 10^{-23} \cdot \mathrm{m}^2 \cdot \mathrm{kg} \cdot \mathrm{s}^{-2} \cdot \mathrm{K}^{-1}$). Moreover, the evolution equation for the joint (position and velocity) probability density function (PDF) in non-equilibrium gases was derived from first principles (i.e., mass conservation and Newton's equation) by Boltzmann, and is known today as Boltzmann's equation.
  - Boltzmann, L. 1872, "Weitere Studien über das Wärmegleichgewicht unter Gasmolekülen", Wiener Berichte , 66, 275-370;

https://doi.org/10.1142/9781848161337_0015.

- 1887, Lorentz wrote a formal framework of the kinetic theory of nonuniform gases.
  - H.A. Lorentz, 1887, Über das Gleichgewicht der lebendigen Kraft unter Gasmolekülen Sitzungsberichte der Kaiserlichen Akademie der Wissenschaften in Wien 95: 115-152.
- 1910, Hilbert proved the existence and uniqueness of solution to Boltzmann equation, by reducing it to a certain linear integral equation of the second kind.
  - Hilbert, David, 1912, Grundzüge einer allgemeinen theorie der linearen integralgleichungen. Teubner, Leipzig, 1912;
    https://doi.org/10.1007/978-3-322-84410-1_1.
- 1917, independently, Chapman and Eskog, going further than Hilbert's work, deduced the same expressions for the transport coefficients.
  - Enskog, D., 1917, Kinetische theorie der vorgänge in mässig verdünnten gasen, Diss., Uppsala.
  - Chapman, S., 1916, On the Law of Distribution of Molecular Velocities, and on the Theory of Viscosity and Thermal Conduction, in a Non-Uniform Simple Monatomic Gas, Phil. Trans. Roy. Soc. London 216, 279-341;
    https://doi.org/10.1098/rsta.1916.0006.
  - Chapman, S., 1916, The Kinetic Theory of Simple and Composite Monatomic Gases: Viscosity, Thermal Conduction, and Diffusion, Phil. Trans. Roy. Soc. London 217, 118-192;
    https://doi.org/10.1098/rspa.1916.0046.
- 1935, Burnett deduced the second order approximation to Boltzmann equation's solution. In fact, he generated a methodology to solve any order of accuracy.
  - Burnett, D., 1935a, The distribution of velocities in a slightly non-uniform gas, Proc London Math. Soc. 39, 385-430;
    https://doi.org/10.1112/plms/s2-39.1.385.
  - Burnett, D., 1935b, The distribution of molecular and the mean motion in a non-uniform gas, Proc London Math. Soc. 40, 382-435;
    https://doi.org/10.1112/plms/s2-40.1.382.
- 1946, Bogoliubov, used different time scales. He generalized the Boltzmann equation for dense gases and liquids.

  - Bogoliubov, N. N., 1946, Problems of a dynamical theory in statistical physics (Russian), (Moscow).

- 1959, Wang-Chang, and Uhlenbeck established the basis for the KTG in polyatomic gases.

  - Wang-Chang, C. S. Uhlenbeck, G. E., 1959, Transport phenomena in polyatomic gases. CM-681, University of Michigan;
    `https://hdl.handle.net/2027.42/8195`.

- 1963. Monchick and Mason created the formal framework for polyatomic gases and generated the corresponding data tables for the collision integrals.

  - Monchick, L. Yun, K. S. Mason, E. A., 1963, Formal kinetic theory of transport phenomena in polyatomic gas mixtures. The Journal of Chemical Physics. 39, 654-669;
    `https://doi.org/10.1063/1.1734304`.

- After the Monchick and Mason works the Kinetic Theory of Gases is a well established branch of the Statistical Mechanics. The results validity is beyond any doubt and appear in two well known treatises:

  - 1964, Hirschfelder, Curtis, Bird. A compilation of the existing know-how in Kinetic Theory of Gases.
    * The mathematical theory of gases and liquids. New York NY, second edition, 1964.
  - 1972, Ferziger, Kaper. A modern and clear compilation about the state of the art in Kinetic Theory of Gases.
    * The mathematical theory of transport processes in gases. North Holland, 1972.

2.2 Properties of a gas

The starting point of the KTG is a statistical view of the particles existing in a fluid. The velocity function distribution $f(\boldsymbol{r}, \boldsymbol{c}, t)$ is defined in such way that $f(\boldsymbol{r}, \boldsymbol{c}, t)\, d^3r d^3c$ is the expected number of molecules in the volume element d^3r located at $\mathbf{r}$, whose velocities lie in d^3c about velocity $\mathbf{c}$. The number density $n(\boldsymbol{r}, t)$ is the number of particles per unit volume at point $\boldsymbol{r}$ at time t.

$$n(\boldsymbol{r}, t) = \int f(\boldsymbol{r}, \boldsymbol{c}, t)\, d^3c \tag{2.1}$$

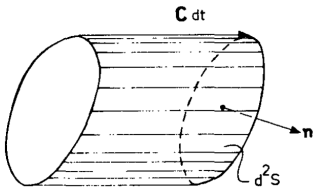

Figure 2.1: Cylinder containing molecules with peculiar velocity $\boldsymbol{C}$ surface element $\mathrm{d}^2\mathrm{S}$ during the time interval dt. Figure 2.1 from reference [1]

Since for a simple gas each particle has mass m, the mass density at $\boldsymbol{r}$ at time t is:

$$\rho\left(\boldsymbol{r},t\right)=mn\left(\boldsymbol{r},t\right) \tag{2.2}$$

The hydrodynamic (i.e., *barycentric*) velocity is defined as:

$$\boldsymbol{v}\left(\boldsymbol{r},t\right)=\frac{1}{\rho\left(\boldsymbol{r},t\right)}\int m\boldsymbol{c}f\left(\boldsymbol{r},\boldsymbol{c},t\right)d^{3}c \tag{2.3}$$

The peculiar velocity is defined as the difference with respect the hydrodynamic velocity $\boldsymbol{C}=\boldsymbol{c}-\boldsymbol{v}$. It is also important the definition of internal energy:

$$u\left(\boldsymbol{r},t\right)=\frac{1}{\rho\left(\boldsymbol{r},t\right)}\int\frac{1}{2}mC^{2}f\left(\boldsymbol{r},\boldsymbol{c},t\right)d^{3}c \tag{2.4}$$

and absolute temperature

$$\rho u=\frac{3}{2}nk_{B}T\qquad k_{B}\quad Boltzmann\quad constant. \tag{2.5}$$

The average of any function of velocity may be defined by:

$$\bar{\varphi}\left(\mathbf{r},t\right)=\frac{1}{n\left(\boldsymbol{r},t\right)}\int\varphi\left(\boldsymbol{c}\right)f\left(\boldsymbol{r},\boldsymbol{c},t\right)d^{3}c \tag{2.6}$$

Considering the variations over the hydrodynamic velocity (see Figure figure 2.1) the diffusion flux vector associated to property φ is (2.7).

$$\boldsymbol{\Phi}=\int\varphi f\boldsymbol{C}d^{3}c. \tag{2.7}$$

For instance, for the transport of mass $\varphi\left(C\right)=m$. By definition, the diffusion velocity average is zero.

$$\boldsymbol{\Phi}\left(\boldsymbol{r},t\right)=m\int f\boldsymbol{C}d^{3}c=nm\bar{\boldsymbol{C}}=0. \tag{2.8}$$

On the other hand, for the transport of the α component of momentum $\varphi\left(C\right)=mC_{\alpha}$ is

$$\mathbf{\Phi}\left(\boldsymbol{r},t\right)=mC_{\alpha}\int f\boldsymbol{C}d^{3}c=nm\overline{C_{\alpha}C}. \tag{2.9}$$

The nine components of the pressure tensor are:

$$\mathbf{P}=m\int\boldsymbol{C}\boldsymbol{C}fd^{3}c \tag{2.10}$$

and the hydrostatic pressure is defined as the normal pressure across the orthogonal planes

$$p=\frac{1}{3}\boldsymbol{P}:\boldsymbol{I}. \tag{2.11}$$

If the shear stresses are zero and the normal pressures are equal $\boldsymbol{P}=p\boldsymbol{I}$. Combining the relations (2.4) and (2.5) the well known perfect gas law is obtained:

$$p=nkT. \tag{2.12}$$

Finally, for the diffusive transport of kinetic energy $\varphi\left(C\right)=\frac{1}{2}mC^{2}$ we find

$$\boldsymbol{q}=\frac{1}{2}\int C^{2}f\boldsymbol{C}d^{3}c=\frac{1}{2}nm\overline{C^{2}\boldsymbol{C}}. \tag{2.13}$$

If now a mixture with N components is considered, the number of expected molecules of species i which, at time t, are situated in the volume element $d^{3}r$ is $f_{i}\left(\boldsymbol{r},c_{i},t\right)d^{3}rd^{3}c_{i}$. The number density is $n=\sum_{i=1}^{K}n_{i}$ and the mass density $\rho=\sum_{i=1}^{K}\rho_{i}=\sum_{i=1}^{K}n_{i}m_{i}$. The transport of the different macroscopic physical magnitudes are expressed in similar way as it is done for simple gas.

$$n\bar{\varphi}=\sum_{i}n_{i}\varphi_{i}=\sum_{i}\int f_{i}\varphi_{i}d^{3}c_{i}. \tag{2.14}$$

The diffusive transport of mass for a mixture is (2.15).

$$\rho\boldsymbol{v}=\sum_{i}m_{i}\int f_{i}c_{i}d^{3}c_{i}. \tag{2.15}$$

The corresponding diffusive momentum flux for a multicomponent mixture is (2.16),

$$\boldsymbol{P}=\sum_{i}m_{i}\int\boldsymbol{C}_{i}\boldsymbol{C}_{i}f_{i}d^{3}c_{i}\qquad p=\frac{1}{3}\boldsymbol{P}:\boldsymbol{I} \tag{2.16}$$

and the heat flux equation is (2.17).

$$\boldsymbol{q}=\sum_{i}\frac{1}{2}m_{i}\int C_{i}^{2}\boldsymbol{C}_{i}f_{i}d^{3}c_{i}. \tag{2.17}$$

2.3 Boltzmann´s equation and properties

2.3.1 Fundamentals

There are two basic assumptions for the Boltzmann's equation derivation.

1. Only pairs of particles may interact simultaneously and collisions are short duration events. As a consequence, this is only applicable for low density gases.

2. Stosszahlansatz or molecular chaos, means that particles are distributed in a statistical manner. The position of each particle is independent of the position of the rest of the particles. It permits calculation of the expected number of pairs of molecules which collide during a given time interval. The probability density function for two particles is the product of the two functions of each particle$f\left(\mathbf{r},\mathbf{c}_1,\mathbf{c}_2,t\right)=f_1\left(\mathbf{r},\mathbf{c}_1,t\right)f_2\left(\mathbf{r},\mathbf{c}_1,t\right)$. As a consequence, this approximation makes Boltzmann's equation irreversible in time, whereas the evolution equations governing the microscopic (i.e., molecular) interactions (Newton's law, Schrödinger equation) are time reversible.

In the usual case of gas in which each molecule of type i is subject to an external force $\boldsymbol{F}_i$ per unit mass, which is a function of $\boldsymbol{r}$ and t, but not of $\boldsymbol{c}_i$, in absence of collisions we have the probability conservation

$$f_i\left(\boldsymbol{r}+\mathbf{c}_i dt,\mathbf{c}_i+\boldsymbol{F}_i dt,t+dt\right)=f_i\left(\boldsymbol{r},\mathbf{c}_i,t\right). \tag{2.18}$$

With collisions the equality must be modified accordingly

$$f_i\left(\boldsymbol{r}+\mathbf{c}_i dt,\mathbf{c}_i+\boldsymbol{F}_i dt,t+dt\right)=f_i\left(\boldsymbol{r},\mathbf{c}_i,t\right)+\left(\frac{\partial f_i}{\partial t}\right)_{coll}dt \tag{2.19}$$

and dividing by dt and letting dt tend to zero

$$\left(\frac{\partial}{\partial t}+\boldsymbol{c}_i\cdot\nabla_r+\boldsymbol{F}_i\cdot\nabla_{\boldsymbol{c}_i}\right)f_i\left(\boldsymbol{r},\boldsymbol{c}_i,t\right)=\left(\frac{\partial f_i}{\partial t}\right)_{coll} \tag{2.20}$$

Assuming the collision collision scheme shown in Fig. 2.2 with the geometric parameters b, χ, ε and $d\varepsilon$ where the velocities before and after are g and g', the expected number of collisions in $d^3\mathbf{r}$ about $\mathbf{r}$, during a small interval dt, between molecules in the velocity ranges d^3c_1, d^3c_2, about c_1, c_2 with geometrical collision variables in the range db, $d\varepsilon$ about b, ε is

$$f_1\left(\mathbf{r},\mathbf{c}_1,t\right)f_2\left(\mathbf{r},\mathbf{c}_1,t\right)gbdbd\varepsilon d^3c_1d^3c_2d^3rdt, \tag{2.21}$$

which is a quadratic term that multiplies the individual probability density functions (molecular chaos) and introduce an irreversible term with respect to time. The rate at which the velocity distribution function f_1 for molecules of species 1 being altered by collisions is

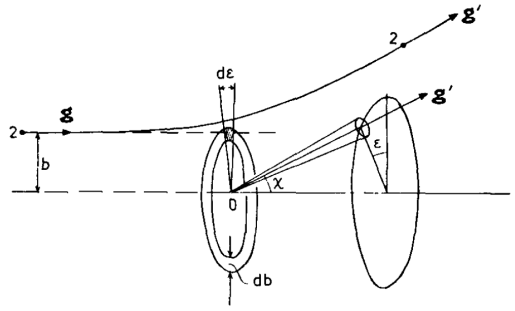

Figure 2.2: The geometry of a binary encounter; molecule 1 is at rest with its center at the origin. Figure 3.2 from reference [1]

$$\left(\frac{\partial f_1}{\partial t}\right)_{2,coll} = \iiint \left(f_1' f_2' - f_1 f_2\right) g b db d\varepsilon d^3 c_2 \tag{2.22}$$

Hence, the Boltzmann's equation for a simple gas is

$$\left(\frac{\partial}{\partial t} + \boldsymbol{c}\cdot\nabla_r + \boldsymbol{F}\cdot\nabla_{\boldsymbol{c}}\right) f\left(\boldsymbol{r},\boldsymbol{c},t\right) = \iiint \left(f' f_1' - f f_1\right) g b db d\varepsilon d^3 c_1 \tag{2.23}$$

and the Boltzmann's equation for a mixture is

$$\left(\frac{\partial}{\partial t} + \boldsymbol{c}_i\cdot\nabla_r + \boldsymbol{F}_i\cdot\nabla_{\boldsymbol{c}_i}\right) f_i\left(\boldsymbol{r},\boldsymbol{c}_i,t\right) = \sum_j \iiint \left(f_i' f_j' - f_i f_j\right) g b db d\varepsilon d^3 c_j \tag{2.24}$$

The Boltzmann equation in an abbreviated form is

$$\mathscr{D} f_i = \textstyle\sum_j J\left(f_i f_j\right) \tag{2.25}$$

where the streaming operator $\mathscr{D}$ and the collision operator J in (2.25) are defined as:

$$\begin{array}{l} \mathscr{D} f_i = \ \frac{\partial f_i}{\partial t} + \boldsymbol{c}_i\cdot\nabla_r f_i + \boldsymbol{F}_i\cdot\nabla_{\boldsymbol{c}_i} f_i \\ J\left(f_i f_j\right) = \iint \left(f_i' f_j' - f_i f_j\right) g b db d\varepsilon d^3 c_j \end{array} \tag{2.26}$$

2.3.2 Macroscopic conservation equations

With the Boltzmann equation, the conservation relations may be deduced. Assuming that Φ is an arbitrary function of $\mathbf{r}$, $\mathbf{c}$ and t for each component of the mixture $\left(\frac{\partial \phi_i}{\partial t}\right)_{coll}$ is defined as

$$\left(\frac{\partial \phi_i}{\partial t}\right)_{coll} = \frac{1}{n_i}\sum_j \int \phi_i J\left(f_i f_j\right) d^3 c_i. \tag{2.27}$$

If ϕ is a microscopic physical property, the integration with the velocity corresponds to the macroscopic physical property. Similarly, for the whole mixture

$$\left(\frac{\partial \phi}{\partial t}\right)_{coll} = \frac{1}{n}\sum_i n_i \left(\frac{\partial \phi_i}{\partial t}\right)_{coll} = \frac{1}{n}\sum_{i,j}\int \phi_i J\left(f_i f_j\right) d^3 c_i. \tag{2.28}$$

Using the definition of the collision operator is derived.

$$\left(\frac{\partial \phi}{\partial t}\right)_{coll} = \frac{1}{4n}\sum_{i,j}\iiiint \left(\phi_i + \phi_j - \phi_i' + \phi_j'\right)\left(f_i' f_j' - f_i f_j\right) g b db d\varepsilon d^3 c_j d^3 c_i \tag{2.29}$$

and multiplying Boltzmann equation by ϕ_i and integrate over c_i expression (2.30) is obtained.

$$\int \phi_i \mathscr{D} f_i d^3 c_i = n_i \left(\frac{\partial \phi_i}{\partial t}\right)_{coll} \tag{2.30}$$

Integrating by parts, equations of transfer are obtained

$$\frac{\partial\left(n_i \bar{\phi}_i\right)}{\partial t} = -\nabla_{\mathbf{r}} \cdot n_i \overline{\mathbf{c_i}\phi_i} + n_i \left\{\overline{\frac{\partial \phi_i}{\partial t}} + \overline{\mathbf{c_i}\cdot\nabla_{\mathbf{r}}\phi_i} + \overline{\mathbf{F_i}\cdot\nabla_{\mathbf{c_i}}\phi_i} + \left(\frac{\partial \phi_i}{\partial t}\right)_{coll}\right\} \tag{2.31}$$

where the summation over i verifies that

$$\frac{\partial\left(n\bar{\phi}\right)}{\partial t} = -\nabla_{\mathbf{r}} \cdot n\overline{\mathbf{c}\phi} + n\left\{\overline{\frac{\partial \phi}{\partial t}} + \overline{\mathbf{c}\cdot\nabla_{\mathbf{r}}\phi} + \overline{\mathbf{F}\cdot\nabla_{\mathbf{c}}\phi} + \left(\frac{\partial \phi}{\partial t}\right)_{coll}\right\}. \tag{2.32}$$

If ϕ only depends on the velocity, then

$$\frac{\partial\left(n\bar{\phi}\right)}{\partial t} = -\nabla_{\mathbf{r}} \cdot n\overline{\mathbf{c}\phi} + n\left\{\overline{\mathbf{F}\cdot\nabla_{\mathbf{c}}\phi} + \left(\frac{\partial \phi}{\partial t}\right)_{coll}\right\} \tag{2.33}$$

If the functions Φ summed over the molecules involved in a collision do not change during the collision then they are called summational invariants ψ. In the case of binary collisions, ψ is a summational invariant if

$$\psi_i\left(\mathbf{c}_i\right) + \psi_j\left(\mathbf{c}_j\right) = \psi_i\left(\mathbf{c}_i'\right) + \psi_j\left(\mathbf{c}_j'\right) \Rightarrow \left(\frac{\partial \psi}{\partial t}\right)_{coll} = 0. \tag{2.34}$$

The general conservation equation for a mixture is

$$\frac{\partial\left(\sum_i \int \psi_i f_i d^3 c_i\right)}{\partial t} + \nabla_{\mathbf{r}} \cdot \sum_i \int \psi_i \mathbf{c}_i f_i d^3 c_i = \sum_i \mathbf{F}\cdot \int f_i \nabla_{c_i} \psi_i f_i d^3 c_i \tag{2.35}$$

From the physical point of view, the invariants are deduced from the conservation laws, mass,

momentum and energy, so these are the parameters tried.

$$\begin{array}{ccc} & \psi_1 = m & \\ \psi_2 = mc_x & \psi_3 = mc_y & \psi_4 = mc_z \ . \\ & \psi_5 = \frac{1}{2}mc^2 & \end{array} \tag{2.36}$$

Inserting the invariants in (2.35) the conservation equations are obtained. Relation (2.37) is obtained for the mass, relations (2.38) for the momentum conservation and (2.39) for energy.

$$\frac{1}{\rho}\frac{d\rho}{dt} = -\nabla \cdot \mathbf{v} \tag{2.37}$$

$$\rho\frac{d\mathbf{v}}{dt} = \sum_i \rho_i \mathbf{F}_i - \nabla \cdot \mathbf{P} \tag{2.38}$$

$$\rho\frac{du}{dt} = -\nabla \cdot \mathbf{q} - \mathbf{P} : \nabla\mathbf{v} + \sum_i \rho_i \mathbf{F}_i \cdot \mathbf{V}_i \tag{2.39}$$

where $\frac{d}{dt} = \frac{\partial}{\partial t} + \mathbf{v} \cdot \nabla$ is the substantial derivative. The mass conservation equation for each individual specie is (2.40).

$$\frac{1}{\rho_i}\frac{d\rho_i}{dt} = -\nabla \cdot (\mathbf{v} + \mathbf{V}_i) - \frac{1}{\rho_i}\mathbf{V}_i \cdot \nabla\rho_i \qquad i = 1, \cdots, K \tag{2.40}$$

To summarize this section, the Boltzmann's equation with the associated hypotheses allows for the microscopic description of the system. With the help of the collision invariants, the macroscopic laws corresponding to conservation of mass, momentum and energy may be derived.

2.3.3 Boltzmann's H theorem

An important physical law that can be derived from Boltzmann's equation is the well known second principle of thermodynamics. In this regard, the relation between entropy and the number of accessible states of the system had been previously discovered by Boltzmann, and from the Boltzmann's equation the microscopic evolution of the system entropy may be derived. The H theorem justifies that every irreversible process increases entropy such as Clausius established previously.

Considering N identical molecules in a six dimensional space $x_i = (\mathbf{r}_i, \mathbf{c}_i)$ $i = 1, \cdots, I$, the probability of finding a certain set of occupation numbers $(N_1, \cdots, N_I)$ is

$$P_N = \frac{N!}{N_1! \cdots N_I!} (\triangle x)^N \ . \tag{2.41}$$

Taking logarithms and applying the Stirling's formula when $N \to \infty$, $\log n! \approx n \log n - n$

$$\log P_N \approx -\sum_i N_i log\left(N_i/N \triangle x\right). \tag{2.42}$$

Expressing N_i in terms of the distribution function and letting $\triangle x$ become $dx = d^3rd^3c$ it is obtained the *Boltzmann H-function*

$$\log P\left(f\right) = -\iint f \log f d^3rd^3c \Rightarrow H\left(f\right) = \iint f \log f d^3rd^3c. \tag{2.43}$$

In a gas mixture with functions f_i independent of $\mathbf{r}$ and no external forces, the Boltzmann equation reads as

$$\frac{\partial f_i}{\partial t} = \sum_j \iiint \left(f_i' f_j' - f_i f_j\right) gbdbd\varepsilon d^3c_j. \tag{2.44}$$

The *Boltzmann H-function* for a mixture is (2.45)

$$H = \sum_i \int f_i \log f_i d^3c_i. \tag{2.45}$$

Hence, the derivative of the *Boltzmann H-function* is

$$\frac{dH}{dt} = \sum_i \int \left(\log f_i + 1\right) \frac{\partial f_i}{\partial t} d^3c_i. \tag{2.46}$$

Using the previous relations in (2.28) and (2.29), the following relation is obtained

$$\begin{array}{c} \sum_{i,j} \int \left(\log f_i + 1\right) J\left(f_i f_j\right) d^3c_i = \\ -\frac{1}{4} \sum_{i,j} \iiint \left(f_i' f_j' - f_i f_j\right) \left(\log f_i' f_j' - \log f_i f_j\right) gbdbd\varepsilon d^3c_j \end{array}. \tag{2.47}$$

Thus, we find that Boltzmann's H-theorem is equivalent to the second law of thermodynamics. The *Boltzmann H-function* measures the approach to equilibrium. Entropy cannot decrease. The expression $(x - y)(\log x - \log y)$ is always positive except for $x = y$ where it is zero.

$$\frac{dH}{dt} \leqq 0 \tag{2.48}$$

2.3.4 Maxwellian function distribution

The objective in this section is to deduce the expression of the probability density function for a gas in equilibrium. The resultant normal distribution was discovered by Maxwell.

In equilibrium $\dfrac{dH}{dt} = 0$ and due to the nature of the Boltzmann equation with a product of two probability density functions the next expression must be fulfilled:

$$\log f_i + \log f_j = \log f_i' + \log f_j' \tag{2.49}$$

where $\log f$ is a summational invariant and therefore is a linear combination of the known summational invariants, mass, momentum and energy.

$$\log f_i = m_i \alpha_i^{(1)} + m_i \mathbf{c}_i \alpha_{\mathbf{i}}^{(\mathbf{2})} - \tfrac{1}{2} m_i c_i^2 \alpha_i^{(3)} \tag{2.50}$$

The coefficients $\alpha_i^{(1)}$, $\alpha_{\mathbf{i}}^{(\mathbf{2})}$ and $\alpha_i^{(3)}$ must be independent of $\mathbf{r}$ and t since the state of the gas is uniform and steady. Moreover, through the collision must be satisfied the conservation of momentum and energy

$$\begin{gathered} \alpha_{\mathbf{i}}^{(\mathbf{2})} = \alpha_{\mathbf{j}}^{(\mathbf{2})} = \alpha^{(\mathbf{2})} \quad \alpha_i^{(3)} = \alpha_j^{(3)} = \alpha^{(3)} \quad \mathbf{C}_i' = \mathbf{c}_i - \alpha^{(\mathbf{2})}/\alpha^{(3)} \\ f_i = \alpha_i^{(0)} \exp\left(-\tfrac{1}{2} m_i C_i'^2 \alpha^{(3)}\right) \qquad \alpha_i^{(0)} = \exp\left(m_i \alpha_i^{(1)} + \frac{1}{2} m_i \mathbf{c}_i \alpha^{(\mathbf{2})} \frac{\alpha^{(\mathbf{2})}}{\alpha^{(3)}}\right). \end{gathered} \tag{2.51}$$

Using the number density, hydrodynamic velocity and temperature, the coefficients of the unknowns coefficients from relation (2.50) are:

$$\begin{aligned} n_i = \int f_i d^3 c_i \Rightarrow n_i &= \alpha_i^{(0)} \left(2\pi/m_i \alpha^{(3)}\right)^{\frac{3}{2}} \\ \rho \mathbf{v} = \sum_{\mathbf{i}} \int m_i \mathbf{c}_i f_i d^3 c_i \Rightarrow \mathbf{v} &= \alpha^{(2)}/\alpha^{(3)} \\ \frac{3}{2} k_B T = \frac{1}{n} \sum_i \int \frac{1}{2} m_i C_i^2 f_i d^3 c_i \Rightarrow \alpha^{(3)} &= 1/k_B T. \end{aligned} \tag{2.52}$$

Inserting the coefficients $\alpha_i^{(1)}$, $\alpha_{\mathbf{i}}^{(\mathbf{2})}$ and $\alpha_i^{(3)}$ in (2.51), expression (2.53) is obtained.

$$f_i(c_i) = f_M = n_i \left(m_i/2\pi k_B T\right)^{\frac{3}{2}} \exp\left(-m_i C_i^2/2 k_B T\right). \tag{2.53}$$

The velocity distribution function at thermodynamic equilibrium is normally distributed about its mean value with variance $k_B T/m$. This was first written by Maxwell in 1860.

2.4 The non-uniform state of a simple gas

2.4.1 Hilbert's expansion

In 1912 Hilbert proved a uniqueness theorem for the Boltzmann equation. If the macroscopic gradients are small, the molecules in a small region will induce variations only on the macroscopic time scale and the dominant effect is that collisions drive the gas toward thermal equilibrium. The small parameter ε may introduce the Boltzmann equation as a perturbation problem:

$$\mathscr{D} f = \varepsilon^{-1} J(ff). \tag{2.54}$$

If ε is small, the preceding equation is a singular perturbation problem for the function f

$$f = f^{(0)} + \varepsilon f^{(1)} + \varepsilon^2 f^{(2)} + \cdots \tag{2.55}$$

Balancing the terms in the powers of ε^r, the following relation is obtained for $r = 0$

$$J\left(f^{(0)} f^{(0)}\right) = 0. \tag{2.56}$$

For $r = 1$

$$J\left(f^{(1)} f^{(0)}\right) + J\left(f^{(0)} f^{(1)}\right) = \left(\mathscr{D} f\right)^{(0)}. \tag{2.57}$$

and for $r = 2, r = 3, \ldots$

$$J\left(f^{(0)} f^{(r)}\right) + J\left(f^{(r)} f^{(0)}\right) = \mathscr{D} f^{(r-1)} - J\left(f^{(1)} f^{(r-1)}\right) - \cdots - J\left(f^{(r-1)} f^{(1)}\right). \tag{2.58}$$

The solution of (2.56) has already been discussed and is (2.53):

$$f^{(0)}(\boldsymbol{c}) = n^{(0)}\left(m/2\pi k T^{(0)}\right)^{\frac{3}{2}} \exp\left(-mC^2/2k_B T^{(0)}\right). \tag{2.59}$$

To obtain a solution Hilbert proposed solutions in the form $\phi^r = f^{(r)}/f^{(0)}$ and the expression (2.58) is

$$J\left(f^{(0)} f^{(r)}\right) + J\left(f^{(r)} f^{(0)}\right) = -\left(n^{(0)}\right)^2 I\left(\phi^r\right). \tag{2.60}$$

where $I(F)$ for a single gas is defined as:

$$I(F) = \frac{1}{n^2} \iiint f_M f_{M1} \left(F + F_1 - F' - F_1'\right) g b db d\varepsilon d^3 c_1 \tag{2.61}$$

and for a mixture

$$I_{ij}(F) = \frac{1}{n_i n_j} \iiint f_{Mi} f_{Mj} \left(F_i + F_j - F_i' - F_j'\right) g b db d\varepsilon d^3 c_j. \tag{2.62}$$

For a single gas, the bracket integral is defined as:

$$[F, G] = \int G I(F)\, d^3 c. \tag{2.63}$$

It may verified by symmetry of arguments that

$$[F, G] = \frac{1}{4n} \iiiint f_M f_{M1} \left(F + F_1 - F' - F_1'\right)\left(G + G_1 - G' - G_1'\right) g b db d\varepsilon d^3 c d^3 c_1. \tag{2.64}$$

Additional I functions are required to define the bracket integral in a mixture

$$I_{ij,i}(F) = \frac{1}{n_i n_j} \iiint f_{Mi} f_{Mj} (F_i - F_i') \, gbdbd\varepsilon d^3 c_j$$
$$I_{ij,j}(F) = \frac{1}{n_i n_j} \iiint f_{Mi} f_{Mj} \left(F_j - F_j'\right) gbdbd\varepsilon d^3 c_j$$

and finally

$$\begin{gathered} [F,G]_{ij}' = \int G_i I_{ij,i}(F) \, d^3 c_i \\ [F,G]_{ij}'' = \int G_i I_{ij,j}(F) \, d^3 c_i \\ [F,G] = \sum_{i,j} \frac{n_i n_j}{n^2} \left([F,G]_{ij}' + [F,G]_{ij}''\right). \end{gathered} \tag{2.65}$$

Hilbert showed that the problem may be reduced to a Fredholm integral equation of the second kind, for $r = 1, 2, \cdots$ and the solution exits if and only if

$$\int \psi \left\{ \mathscr{D} f^{(r-1)} - J\left(f^{(1)} f^{(r-1)}\right) - \ldots - J\left(f^{(r-1)} f^{(1)}\right) \right\} d^3 c = 0. \tag{2.66}$$

The solution is in the form

$$\phi^{(r)} = \bar{\phi}^{(r)} + \alpha^{(r)} \cdot \psi \phi^{(r)} \tag{2.67}$$

where $\bar{\phi}^{(r)}$ is a particular solution of the equation (2.58) and $\phi^{(r)}$ is uniquely determined if we require

$$\begin{gathered} \int \psi \bar{\phi}^{(r)} f^{(0)} d^3 c = 0 \\ \psi = \left\{ \begin{array}{c} 1 \\ mc_x \\ mc_y \\ mc_z \\ \frac{1}{2} mC^2 \end{array} \right\} \end{gathered} \tag{2.68}$$

For $r = 1$, the compatibility condition is

$$\int \psi \mathscr{D} f^{(0)} d^3 c = 0 \tag{2.69}$$

and the conservation equations lead to Euler equations

$$\begin{gathered} \mathbf{P}^{(0)} = p^{(0)} \mathbf{I} \qquad p^{(0)} = n^{(0)} k T^{(0)} \\ \mathbf{q}^{(0)} = 0 \\ \left(1/\rho^{(0)}\right) \left(d\rho^{(0)}/dt\right) = -\nabla \cdot \mathbf{v}^{(0)} \\ \rho^{(0)} \left(dv^{(0)}/dt\right) = \rho^{(0)} \mathbf{F} - \nabla p^{(0)} \\ (d/dt) \left(\rho^{(0)} / T^{(0)\frac{3}{2}}\right) = 0 \end{gathered} \tag{2.70}$$

The vectors with different moments are defined as:

$$\beta^{(r)} = \int \boldsymbol{\psi} f^{(r)} d^3c \tag{2.71}$$

and using (2.67)

$$f^{(r)} = f^{(0)} \left\{ \bar{\phi}^{(r)} + \boldsymbol{\alpha}^{(r)} \cdot \boldsymbol{\psi} \right\} \Rightarrow \beta^{(r)} = \int \boldsymbol{\psi}\boldsymbol{\psi} f^{(0)} d^3c \cdot \boldsymbol{\alpha}^{(r)} \tag{2.72}$$

The formal Hilbert expansion technique yields a unique solution to the Boltzmann equation provided that initial values are assigned to all vectors $\beta^{(0)}, \beta^{(1)}, \cdots$. In the Hilbert class of normal solutions to the Boltzmann equation a velocity distribution function is uniquely determined by the values of its first five velocity moments at any instant $t = t_0$. Although the Hilbert's method for order zero obtains the Euler equations it does not generate the Navier Stokes equations in the first order and it is limited therefore.

2.4.2 Chapman-Enskog method

Based on Hilbert work, simultaneously, Chapman and Enskog tried a different perturbation approach to the Boltzmann equation. Different hypotheses and ideas were tried to obtain the Navier Stokes equations for the first order of approximation. Keeping in mind the definition of the moment $\boldsymbol{\beta} = \int \boldsymbol{\psi} f d^3c$, the Enskog hypotheses are:

- Time does not enter explicitly among the arguments of f and $\partial\boldsymbol{\beta}/\partial t$
- Time enters implicitly through $\boldsymbol{\beta}$ and the spatial gradients of $\boldsymbol{\beta}$
- $f(\boldsymbol{r}, \boldsymbol{c}, t) \equiv f(\boldsymbol{r}, \boldsymbol{c}|\boldsymbol{\beta}, \boldsymbol{\nabla}_r\boldsymbol{\beta}, \cdots)$
- $(\partial/\partial t)\,\boldsymbol{\beta}(r, t) \equiv \boldsymbol{\Phi}(\boldsymbol{r}|\boldsymbol{\beta}, \boldsymbol{\nabla}_r\boldsymbol{\beta}, \cdots)$

The dots indicate higher order spacial derivatives of β. The reasoning behind these hypotheses is that collisions do not affect to the macroscopic variables directly. They will stay constant in a time of the order of the mean free time and in this sense they can be regarded as constants of motion on the kinetic time scale. According to the singular perturbation scheme,

$$\boldsymbol{\Phi} = \boldsymbol{\Phi}^{(0)} + \varepsilon\boldsymbol{\Phi}^{(1)} + \varepsilon^2\boldsymbol{\Phi}^{(2)} + \cdots \tag{2.73}$$

Applying the chain rule for derivation next expression is obtained

$$\frac{\partial f}{\partial t} = \boldsymbol{\Phi} \cdot \boldsymbol{\nabla}_\beta f + (\boldsymbol{\nabla}_r\boldsymbol{\Phi}) : (\boldsymbol{\nabla}_{\nabla_r\beta} f) + \ldots \tag{2.74}$$

The operator $\dfrac{\partial_i}{\partial t}$ is defined as:

$$\frac{\partial_i}{\partial t} = \boldsymbol{\Phi}^{(i)} \cdot \boldsymbol{\nabla}_\beta + \boldsymbol{\nabla}_r\boldsymbol{\Phi} : \boldsymbol{\nabla}_{\nabla_r\beta} + \cdots \tag{2.75}$$

and the streaming operator may be defined as:

$$(\mathscr{D}f)^{(i)}_{Enskog} = \frac{\partial_i f^{(0)}}{\partial t} + \ldots + \frac{\partial_0 f^{(i)}}{\partial t} + c \cdot \boldsymbol{\nabla}_r f^{(i)} + \boldsymbol{F} \cdot \boldsymbol{\nabla}_c f^{(i)}. \tag{2.76}$$

The following equation contains the streaming operator for comparison with the Hilbert expansion

$$(\mathscr{D}f)^{(i)}_{Hilbert} = \frac{\partial f^{(i)}}{\partial t} + c \cdot \boldsymbol{\nabla}_r f^{(i)} + \boldsymbol{F} \cdot \boldsymbol{\nabla}_c f^{(i)}. \tag{2.77}$$

Again, the coefficients like powers of ε are equated in the Boltzmann equation (2.54). The expression for $r = 0$ is again (2.56) and for $r = 1$ is (2.57). The resultant equation is soluble if and only if $\boldsymbol{\psi}$ the summational invariants and the orthogonality condition is given by

$$\int \psi \, (\mathscr{D}f)^{(r-1)} \, d^3c = 0. \tag{2.78}$$

Operating with the different terms of the Boltzmann equation and the orthogonality conditions the next expression is obtained:

$$\begin{gathered} \frac{\partial \boldsymbol{\beta}}{\partial t} + \boldsymbol{\nabla}_r \cdot \sum_{j=0}^{r} \varepsilon^j \int \boldsymbol{c\psi} f^{(j)} d^3c - \sum_{j=0}^{r} \varepsilon^j \int \boldsymbol{c} \cdot (\boldsymbol{\nabla_r \psi}) f^{(j)} d^3c - \\ F \cdot \sum_{j=0}^{r} \varepsilon^j \int (\boldsymbol{\nabla_c \psi}) f^{(j)} d^3c = 0. \end{gathered} \tag{2.79}$$

The particular solutions for the differential equation may be selected as follows:

$$\begin{gathered} \textstyle\int \psi f^{(0)} d^3c = \int \psi f d^3c = \boldsymbol{\beta} \\ \textstyle\int \psi f^{(r)} d^3c = 0 \quad r = 1, 2, \ldots \end{gathered} \tag{2.80}$$

After trivial manipulations, the following set of partial differential equations are obtained:

$$\begin{gathered} \frac{1}{\rho}\frac{d\rho}{dt} = -\nabla \cdot \mathbf{v} \\ \rho \frac{d\mathbf{v}}{dt} = \rho \mathbf{F} - \sum_{j=0}^{r} \nabla \cdot \mathbf{P^{(j)}} \\ \rho \frac{du}{dt} = -\left(\sum_{j=0}^{r} \nabla \cdot \mathbf{q}^{(j)} + \sum_{j=0}^{r} \mathbf{P}^{(j)} : \nabla \mathbf{v} \right) \\ \mathbf{P^{(j)}} = \varepsilon^j \int m \boldsymbol{CC} f^{(j)} d^3c \qquad \boldsymbol{q^{(j)}} = \varepsilon^j \int \frac{1}{2} m C^2 \boldsymbol{C} f^{(j)} d^3c \end{gathered} \tag{2.81}$$

The Hilbert's method is formally equivalent to Chapman Enskog method but there are two main drawbacks:

- The evaluation of the successive coefficients $f^{(r)}$ involve the solution of an integral

equation. In Chapman-Enskog method $f^{(r)}$ is computed in terms of $\boldsymbol{\beta}$ (i.e., in terms of macroscopic observable n, $\boldsymbol{v}$ and T).

- The Navier Stokes fluid equations are not obtained explicitly.

Chapman Enskog method provides a unique method of determining successive approximations to the solution of the Boltzmann equation and yields the equations of fluid dynamics in such a form that they can be explicitly evaluated to each order of approximation.

2.4.3 Chapman-Enskog method: first order approximation

We have already shown that the zero-order approximation to f is a local Maxwellian function and the conservation equations lead to Euler hydrodynamic equations. For the first order approximation the following term of the Boltzmann equation must be satisfied:

$$J\left(f^{(1)}f^{(0)}\right) + J\left(f^{(0)}f^{(1)}\right) = (\mathscr{D}f)^{(0)}\,. \tag{2.82}$$

Using $f^{(1)} = f^{(0)}\phi^{(1)}$ the term of the Boltzmann equation is

$$-n^2 I\left(\phi^{(1)}\right) = (\mathscr{D}f)^{(0)} \tag{2.83}$$

and the streaming operator is

$$(\mathscr{D}f)^{(0)} = \partial_0 f^{(0)}/\partial t + \boldsymbol{c}\cdot\boldsymbol{\nabla}_r f^{(0)} + \boldsymbol{F}\cdot\boldsymbol{\nabla}_c f^{(0)}. \tag{2.84}$$

Instead of $\boldsymbol{c}$, the peculiar velocity $\boldsymbol{C}$, may be used. An equivalent expression with the help of the substantial derivative definition is:

$$\begin{aligned}(\mathscr{D}f)^{(0)} = f^{(0)}\Bigg\{&\frac{d_0 \log f^{(0)}}{dt} + \boldsymbol{C}\cdot\nabla_r \log f^{(0)} + \left(F - \frac{d_0 v}{dt}\right)\cdot\nabla_c \log f^{(0)} \\ &- \left(\boldsymbol{\nabla}_c \log f^{(0)}\right)\boldsymbol{C} : \boldsymbol{\nabla}\boldsymbol{v}\Bigg\}.\end{aligned} \tag{2.85}$$

From Maxwell distribution function

$$\log f^{(0)} = \log n - \frac{3}{2}\log T - mC^2/2k_BT + \text{constant}. \tag{2.86}$$

Using Euler equations obtained from the zero order approximation (Euler equations (2.70)) the next relation is obtained.

$$\frac{d_0 \log f^{(0)}}{dt} = \frac{1}{n}\frac{d_0 n}{dt} + \left(\frac{mC^2}{2k_BT} - \frac{3}{2}\right)\frac{1}{T}\frac{d_0 T}{dt} = -\frac{mC^2}{3k_BT}\boldsymbol{\nabla}\cdot\boldsymbol{v}\ . \tag{2.87}$$

Further, one verifies easily that

$$\nabla_r \log f^{(0)} = \nabla \log n + \left(\frac{mC^2}{2k_B T} - \frac{3}{2} \right) \boldsymbol{\nabla} \log T \tag{2.88}$$

and

$$\boldsymbol{\nabla}_c \log f^{(0)} = -\frac{m}{k_B T} \boldsymbol{C}. \tag{2.89}$$

By substitution, the expression (2.85) becomes:

$$(\mathscr{D} f)^{(0)} = f^{(0)} \left\{ \left(\frac{mC^2}{2k_B T} - \frac{5}{2} \right) \boldsymbol{C} \cdot \boldsymbol{\nabla} \log T + \frac{m}{k_B T} \left(\boldsymbol{CC} - \frac{1}{3} C^2 \boldsymbol{I} \right) : \boldsymbol{\nabla v} \right\}. \tag{2.90}$$

It must be noted that external force $\boldsymbol{F}$ does not occur in this expression. Relation (2.83) is then:

$$-n^2 I\left(\phi^{(1)}\right) = f^{(0)} \left\{ \left(\tfrac{mC^2}{2k_B T} - \tfrac{5}{2} \right) \boldsymbol{C} \cdot \boldsymbol{\nabla} \log T + \tfrac{m}{k_B T} \left(\boldsymbol{CC} - \tfrac{1}{3} C^2 \boldsymbol{I} \right) : \boldsymbol{\nabla v} \right\} . \tag{2.91}$$

Additional restrictions have to be added since to any particular solution one may add a linear combination of the summational invariants which are the solutions of the homogeneous equation. The particular solutions will fulfill $\int \psi f^{(1)} d^3 c = 0$ and looking at the integral equation (2.91) the solution must be in the form

$$\phi^{(1)} = -\frac{1}{n} \boldsymbol{A} \cdot \boldsymbol{\nabla} \log T - \frac{1}{n} \boldsymbol{B} : \boldsymbol{\nabla v} + \boldsymbol{\alpha}^{(1)} \cdot \boldsymbol{\psi}. \tag{2.92}$$

$\boldsymbol{A}$ and $\boldsymbol{B}$ are vector and a tensor functions of $\boldsymbol{C}$, $\boldsymbol{\alpha}^{(1)}$ is a vector independent of the velocity variable. The components of $\boldsymbol{\nabla} \log T$ and $\boldsymbol{\nabla v}$ are all linearly independent and therefore the two following expressions have to be satisfied.

$$nI\left(\boldsymbol{A}\right) = f^{(0)} \left(\frac{mC^2}{2k_B T} - \frac{5}{2} \right) \boldsymbol{C} \tag{2.93}$$

$$nI\left(\boldsymbol{B}\right) = f^{(0)} \tfrac{m}{k_B T} \left(\boldsymbol{CC} - \tfrac{1}{3} C^2 \boldsymbol{I} \right) . \tag{2.94}$$

Accounting the additional constraint for the summational invariants may be showed that

$$\phi^{(1)} = -\frac{1}{n} A\left(C\right) \boldsymbol{C} \cdot \boldsymbol{\nabla} \log T - \frac{1}{n} B\left(C\right) \left(\boldsymbol{CC} - \frac{1}{3} C^2 \boldsymbol{I} \right) : \boldsymbol{\nabla v} \tag{2.95}$$

$$\int f^{(0)} A\left(C\right) C^2 d^3 c = 0 \tag{2.96}$$

$$\boldsymbol{P}^{(1)} = -\frac{m}{5n}\int f^{(0)} B\left(C\right)\left(\boldsymbol{CC} - \frac{1}{3}C^2\boldsymbol{I}\right) : \left(\boldsymbol{CC} - \frac{1}{3}C^2\boldsymbol{I}\right) d^3c\boldsymbol{S} \tag{2.97}$$

where $\boldsymbol{S}$ is the rate-of-shear tensor, symmetric traceless component of $\boldsymbol{\nabla v}$

$$S_{\alpha\beta} = \frac{1}{2}\left(\frac{\partial v_\beta}{\partial x_\alpha} + \frac{\partial v_\alpha}{\partial x_\beta}\right) - \frac{1}{3}\nabla \cdot v\delta_{\alpha\beta} \tag{2.98}$$

$$\boldsymbol{P}^{(1)} = -\frac{1}{5}k_B T\int \boldsymbol{B} : I\left(\boldsymbol{B}\right) d^3c\boldsymbol{S} = -\frac{1}{5}k_B T\left[\boldsymbol{B},\boldsymbol{B}\right]\boldsymbol{S}$$

and defining the coefficient of viscosity as

$$\eta = \frac{1}{10}kT\left[\boldsymbol{B},\boldsymbol{B}\right] \tag{2.99}$$

the Newton's law is

$$\boldsymbol{P} = p\mathbf{I} - 2\eta\mathbf{S}. \tag{2.100}$$

In a similar way

$$\boldsymbol{q}^{(1)} = -\frac{m}{6n}\int f^{(0)} A\left(C\right) C^4 d^3c\boldsymbol{\nabla}\log T \tag{2.101}$$

$$\boldsymbol{q}^{(1)} = -\frac{1}{3}kT\left[\boldsymbol{A},\boldsymbol{A}\right]\boldsymbol{\nabla}\log T. \tag{2.102}$$

The thermal of conductivity is defined as

$$\lambda = \frac{1}{3}k\left[\boldsymbol{A},\boldsymbol{A}\right] \tag{2.103}$$

and the Fourier's law is

$$q = -\lambda\boldsymbol{\nabla}T. \tag{2.104}$$

The Chapman-Enskog first order approximation results in the Navier Stokes equations:

$$\frac{1}{\rho}\frac{d\rho}{dt} = -\nabla \cdot \boldsymbol{v} \tag{2.105}$$

$$\rho\frac{d\boldsymbol{v}}{dt} = \rho\boldsymbol{F} - \boldsymbol{\nabla}p + 2\eta\boldsymbol{\nabla}\cdot\mathbf{S} \tag{2.106}$$

$$\rho\frac{dT}{dt} = -\frac{2m}{3k}\left(-\boldsymbol{\nabla}\cdot\lambda\boldsymbol{\nabla}T + p\boldsymbol{\nabla}\cdot\boldsymbol{v} - 2\eta\boldsymbol{S} : \boldsymbol{\nabla v}\right) \tag{2.107}$$

The derivation of the Navier Stokes equations is what made so important the Chapman Enskog method and it is why its use is so extensive. The kinetic theory of gases relies on

the Chapman Enskog approximation to the solution of the Boltzmann equation to obtain the transport variables.

2.4.4 Calculation of the dynamic viscosity and thermal conductivity

The expressions 2.93 and 2.94 represent the integral equations to solve the Boltzmann's equation. This problem cannot be solved in the general case and approximation methods must be used. Enskog, in his original work, tried to expand in powers of C^2 without completely successful results. The use of Sonine polynomials and variational principles addressed this issue. The advantages of Sonine polynomials (Nikolai Sonine) or associated Laguerre polynomials were pointed out by Burnett [31, 32]. The Sonine polynomials $S_\nu^{(n)}(x)$ of order n (integer) and index ν are defined as

$$S_\nu^{(n)}(x) = \sum_{p=0}^{n} \frac{\Gamma(\nu+n+1)}{(n-p)!p!\Gamma(\nu+p+1)}(-x)^p. \tag{2.108}$$

In particular, for any value of the index ν,

$$S_\nu^{(0)}(x) = 1; \quad S_\nu^{(1)}(x) = \nu + 1 + x. \tag{2.109}$$

These polynomials are the coefficients in the expansion

$$(1-s)^{-\nu-1}\exp\left(-\frac{xs}{1-s}\right) = \sum_{n=0}^{\infty} S_\nu^{(n)}(x)\, s^n \tag{2.110}$$

and satisfy the orthogonality relation

$$\int_0^\infty e^{-x} S_\nu^{(p)}(x)\, S_\nu^{(q)}(x)\, x^\nu = 0 \qquad if\ p \neq q \tag{2.111}$$

The use of variational methods is because we are not so much interested in the complete solutions of $\boldsymbol{A}$ and $\boldsymbol{B}$, but rather, in particular functions of the solutions, i.e., the bracket integrals that occur in the definitions of η and λ. Considering the local entropy density of the gas

$$s = -k_B \int f \log f d^3c \tag{2.112}$$

The rate of change of s due to collisions is given by

$$(\partial s/\partial t)_{coll} = k\left\{\frac{1}{3}[\boldsymbol{A},\boldsymbol{A}]\,|\boldsymbol{\nabla}\log T|^2 + \frac{1}{5}[\boldsymbol{B},\boldsymbol{B}]\,\boldsymbol{S}:\boldsymbol{S}\right\} = \lambda\,|\boldsymbol{\nabla}\log T|^2 + (2\eta/T)\,\boldsymbol{S}:\boldsymbol{S}. \tag{2.113}$$

Supposing that vector $\boldsymbol{a} \equiv a(C)\,\boldsymbol{C}$ satisfies the condition

$$[\boldsymbol{a}, \boldsymbol{a}] = [\boldsymbol{a}, \boldsymbol{A}] \tag{2.114}$$

it follows that

$$[\boldsymbol{a}, \boldsymbol{a}] \leqq [\boldsymbol{A}, \boldsymbol{A}] \,. \tag{2.115}$$

Similarly if $\boldsymbol{b} \equiv b\,(C)\left(\boldsymbol{CC} - \frac{1}{3}C^2\boldsymbol{I}\right)$ satisfies the condition

$$[\boldsymbol{b}, \boldsymbol{b}] = [\boldsymbol{b}, \boldsymbol{B}] \tag{2.116}$$

then

$$[\boldsymbol{b}, \boldsymbol{b}] \leqq [\boldsymbol{B}, \boldsymbol{B}] \tag{2.117}$$

The maximum principle for non-equilibrium systems is applied. The distribution of the molecular velocities is such that, for given temperature and velocity gradients, the rate of change of the entropy density due to collisions is as large as possible. An additional constraint will be considered:

$$\int f^{(0)} a\,(C)\, C^2 d^3c = 0 \tag{2.118}$$

The exact solution of $\boldsymbol{A}$ is given by the vector $\boldsymbol{a}$ which maximizes the bracket $[\boldsymbol{a}, \boldsymbol{a}]$ with respect to all the available parameters in the trial function $\boldsymbol{a}$. The exact solution of $\boldsymbol{B}$ is given by the tensor $\boldsymbol{b}$ which maximizes the bracket $[\boldsymbol{b}, \boldsymbol{b}]$ with respect to all the available parameters in the trial function $\boldsymbol{b}$.

As the trial functions $\boldsymbol{a}$ in the computation of $\boldsymbol{A} \equiv a\,(C)\,\boldsymbol{C}$ we take a finite linear combination of Sonine polynomials,

$$\boldsymbol{a} \equiv a\,(C)\,\boldsymbol{C} = -\left(\frac{m}{2k_BT}\right)^{\frac{1}{2}} \sum_{p=0}^{n} a_p^{(n)} S_{\frac{3}{2}}^{(p)}\left(\mathcal{C}^2\right)\boldsymbol{\mathcal{C}} \tag{2.119}$$

where $\boldsymbol{\mathcal{C}}$ is the dimensionless velocity variable.

$$\boldsymbol{\mathcal{C}} = (m/2k_BT)^{\frac{1}{2}}\,\mathbf{C} \tag{2.120}$$

To satisfy the additional constraint

$$0 = \frac{1}{n}\int f^{(0)} a\,(C)\, C^2 d^3c = -\frac{3}{2}a_0^{(n)}. \tag{2.121}$$

Thus, it is only necessary to require that $a_0^{(n)} = 0$. For a given n, the statement of the variational criterion is

$$\delta g = 0 \tag{2.122}$$

where g is the bracket integral formed from the trial function:

$$g \equiv [\boldsymbol{a}, \boldsymbol{a}] = \frac{75k}{16} \sum_{q=1}^{n} \sum_{r=1}^{n} \Lambda^{qr} a_q^{(n)} a_r^{(n)} \tag{2.123}$$

The coefficient $\Lambda^{qr}$is

$$\Lambda^{qr} = \frac{8m}{75k_B^2 T} \left[S_{\frac{3}{2}}^{(q)} \left(\mathcal{C}^2 \right) \boldsymbol{\mathcal{C}}, S_{\frac{3}{2}}^{(r)} \left(\mathcal{C}^2 \right) \boldsymbol{\mathcal{C}} \right] \qquad \Lambda^{qr} = \Lambda^{rq}. \tag{2.124}$$

Minimizing with the help of the Lagrange multipliers method, the following system of linear equation is obtained:

$$\sum_{q=1}^{n} \Lambda^{pq} a_q^{(n)} = \frac{4}{5k_B} \delta_{p1} \qquad p = 1, \ldots, n. \tag{2.125}$$

For the trial functions $\boldsymbol{b}$

$$\boldsymbol{b} \equiv b\left(C\right) \left(\boldsymbol{CC} - \frac{1}{3} C^2 \boldsymbol{I} \right) = \sum_{p=0}^{n-1} b_p^{(n)} S_{\frac{5}{2}}^{(p)} \left(\mathcal{C}^2 \right) \left(\boldsymbol{\mathcal{C}\mathcal{C}} - \frac{1}{3} \mathcal{C}^2 \boldsymbol{I} \right). \tag{2.126}$$

In a similar way, the variational principle stands

$$g \equiv [\boldsymbol{b}, \boldsymbol{b}] = \frac{5}{2} k_B T \sum_{q=0}^{n-1} \sum_{r=0}^{n-1} H^{qr} b_q^{(n)} b_r^{(n)} \tag{2.127}$$

where the coefficients H^{qr} are defined as

$$H^{qr} = \frac{2}{5k_B T} \left[S_{\frac{5}{2}}^{(q)} \left(\mathcal{C}^2 \right) \left(\boldsymbol{\mathcal{C}\mathcal{C}} - \frac{1}{3} \mathcal{C}^2 \boldsymbol{I} \right), S_{\frac{5}{2}}^{(r)} \left(\mathcal{C}^2 \right) \left(\boldsymbol{\mathcal{C}\mathcal{C}} - \frac{1}{3} \mathcal{C}^2 \boldsymbol{I} \right) \right] \qquad H^{qr} = H^{rq}. \tag{2.128}$$

Again, using the method of Lagrangian multipliers the coefficients $b_p^{(n)}$ can be solved from the following set of linear algebraic equations

$$\sum_{q=0}^{n-1} H^{pq} b_q^{(n)} = \frac{2}{k_B T} \delta_{p0} \qquad p = 1, \ldots, n-1 \tag{2.129}$$

The transport coefficients are

$$\left[\lambda\right]_n = \frac{1}{3} k_B \left[\boldsymbol{a}, \boldsymbol{a} \right] = \frac{5}{4} k_B a_1^{(n)} \tag{2.130}$$

$$[\eta]_n = \frac{1}{10} k_B T \left[\boldsymbol{b}, \boldsymbol{b}\right] = \frac{1}{2} k_B T b_0^{(n)}. \tag{2.131}$$

In particular, for $n = 1$ we find

$$[\lambda]_1 = \frac{5}{4} k a_1^{(1)} = \left(\Lambda^{11}\right)^{-1} \tag{2.132}$$

$$[\eta]_1 = \frac{1}{2} k T b_0^{(1)} = \left(H^{00}\right)^{-1} \tag{2.133}$$

and for $n = 2$

$$[\lambda]_2 = \frac{5}{4} k_B a_1^{(2)} = \left(1 + \frac{\Lambda^{12}\Lambda^{21}}{\Lambda^{11}\Lambda^{22} - \Lambda^{12}\Lambda^{21}}\right) \frac{1}{\Lambda^{11}} \tag{2.134}$$

$$[\eta]_2 = \frac{1}{2} k T b_0^{(2)} = \left(1 + \frac{H^{10}H^{01}}{H^{00}H^{11} - H^{01}H^{10}}\right) \frac{1}{H^{00}} \tag{2.135}$$

Taking $n = 1, 2, \ldots$ it is generated a sequence of numerical approximations to the transport coefficients λ and η.

2.5 The non-uniform state of a gas mixture

An extension to simple gases will be applied to multicomponent gases in this section. Back to the Boltzmann equation, following the same procedure as for a simple gas, balancing the same order terms in the perturbation approximations the next relations are obtained:

$$\begin{gathered} \mathscr{D} f_i = \sum_{j=1}^{N} J\left(f_i f_j\right) \qquad f_i = f_i^{(0)} + \varepsilon f_i^{(1)} + \varepsilon^2 f_i^{(2)} + \ldots \\ f_i\left(\boldsymbol{r}, \boldsymbol{c}_i, t\right) \equiv f_i\left(\boldsymbol{r}, \boldsymbol{c}_i | \boldsymbol{\beta}, \boldsymbol{\nabla}_r \boldsymbol{\beta}, \ldots\right) \\ \left(\partial/\partial t\right) \boldsymbol{\beta}\left(\boldsymbol{r}, t\right) = \boldsymbol{\Phi}\left(\boldsymbol{r} | \boldsymbol{\beta}, \boldsymbol{\nabla}_r \boldsymbol{\beta}, \ldots\right) \end{gathered} \tag{2.136}$$

where the hypothesis of the Chapman-Enskog method are used in the same way as for simple gases. The zero order approximation, $r = 0$ to the Boltzmann equation for multicomponent gases is

$$\sum_{j=1}^{N} J\left(f_i^{(0)} f_j^{(0)}\right) = 0 \qquad i = 1, \ldots, N \tag{2.137}$$

and the higher orders $r = 1, r = 2, \ldots$,

$$\sum_{j=1}^{N} J\left(f_i^{(0)} f_j^{(r)}\right) + \sum_{j=1}^{N} J\left(f_i^{(r)} f_j^{(0)}\right) = (\mathscr{D} f_i)^{(r-1)} - \sum_{j=1}^{N} J\left(f_i^{(1)} f_j^{(r-1)}\right) - \ldots - \sum_{j=1}^{N} J\left(f_i^{(r-1)} f_j^{(1)}\right) \qquad i = 1, \ldots, N. \tag{2.138}$$

The solution follows the same steps as in the case of a simple gas

$$f_i^{(0)} = n_i \left(m_i / 2\pi k_B T\right)^{\frac{3}{2}} \exp\left(-m_i C_i^2 / 2 k_B T\right) \qquad i = 1, \ldots, K \ . \tag{2.139}$$

The function ϕ is defined for a simpler notation.

$$\phi_i^{(r)} = f_i^{(r)} / f_i^{(0)} \qquad \sum_{j=1}^{N} J\left(f_i^{(0)} f_j^{(r)}\right) + \sum_{j=1}^{N} J\left(f_i^{(r)} f_j^{(0)}\right) = -\sum_{j=1}^{N} n_i n_j I_{ij}\left(\phi^{(r)}\right). \tag{2.140}$$

Searching for the continuity equations, a similar analysis than the performed for a single gas leads to the following:

$$\begin{aligned} \frac{1}{\rho_i}\frac{d\rho_i}{dt} &= -\boldsymbol{\nabla}\cdot\boldsymbol{v} - \sum_{j=0}^{r} \boldsymbol{\nabla}\cdot\boldsymbol{V}_i^{(j)} - \sum_{j=0}^{r} \boldsymbol{V}_i^{(j)} \cdot \frac{1}{\rho_i}\boldsymbol{\nabla}\rho_i \qquad i = 1, \ldots, K \\ \rho\frac{d\boldsymbol{v}}{dt} &= \sum_{i=0}^{N} \rho_i \boldsymbol{F}_i - \sum_{j=0}^{r} \boldsymbol{\nabla}\cdot\boldsymbol{P}^{(j)} \\ \rho\frac{du}{dt} &= -\sum_{j=0}^{r} \boldsymbol{\nabla}\cdot\boldsymbol{q}^{(j)} - \sum_{j=0}^{r} \boldsymbol{P}^{(j)} : \boldsymbol{\nabla}\boldsymbol{v} + \sum_{i=1}^{N}\sum_{j=0}^{r} \rho_i \boldsymbol{F}_i \cdot \boldsymbol{V}_i^{(j)} \end{aligned} \tag{2.141}$$

where $\boldsymbol{V}_i^{(j)}$, $P_i^{(j)}$ and $\boldsymbol{q}^{(j)}$ are the jth order contributions to the diffusion velocity vector of species i, the pressure tensor and the heat flow vector of the mixture, respectively,

$$n_i V_i^{(j)} = \varepsilon^j \int \boldsymbol{C}_i f_i^{(j)} d^3 c_i \tag{2.142}$$

$$P^{(j)} = \sum_{i=1}^{N} P_i^{(j)} = \varepsilon^j \sum_{i=1}^{N} \int m_i \boldsymbol{C}_i \boldsymbol{C}_i f_i^{(j)} d^3 c_i \tag{2.143}$$

$$q^{(j)} = \sum_{i=1}^{N} q_i^{(j)} = \varepsilon^j \sum_{i=1}^{N} \int m_i C_i^2 \boldsymbol{C}_i f_i^{(j)} d^3 c_i \tag{2.144}$$

where ε is merely a scaling factor for the density in the Boltzmann equation and eventually it will be taken as unity.

As $\sum_{i=1}^{K} \rho_i V_i^{(j)} = 0$ for all j, multiplying the mass conservation equation by ρ_i and summing

over all i

$$\sum_{i=1}^{N} \frac{d\rho_i}{dt} = -\sum_{i=1}^{N} \rho_i \boldsymbol{\nabla} \cdot \boldsymbol{v} - \sum_{j=0}^{r} \boldsymbol{\nabla} \cdot \sum_{i=1}^{N} \rho_i \boldsymbol{V}_i^{(j)} - \sum_{j=0}^{r} \sum_{i=1}^{N} \rho_i \boldsymbol{V}_i^{(j)} \cdot \frac{\boldsymbol{\nabla}\rho_i}{\rho_i} \tag{2.145}$$

$$\frac{1}{\rho}\frac{d\rho}{dt} = -\boldsymbol{\nabla} \cdot \boldsymbol{v} \tag{2.146}$$

The last equations account the mass conservation for multicomponent gases. The diffusion velocity $\boldsymbol{V}_i$ is a new concept which is absent in the case of a simple gas.

2.5.1 Zero order approximation

The general solution to the zero-order equation (2.137) is given by (2.139). Each f_i is a local Maxwellian corresponding to local conditions. Diffusion velocities, pressure tensor and heat flow vector are:

$$\begin{gathered} \boldsymbol{V}_i^{(0)} = 0 \\ \boldsymbol{P}^{(0)} = p\boldsymbol{I} \qquad p = nk_BT \\ \boldsymbol{q}^{(0)} = 0 \end{gathered} \tag{2.147}$$

The substitution of these zero-order results in the general conservation equations satisfy the Euler hydrodynamic equations.

$$\begin{gathered} \frac{1}{\rho_i}\frac{d\rho_i}{dt} = -\nabla \cdot v \qquad i = 1, \ldots, N \\ \frac{1}{\rho}\frac{d\rho}{dt} = -\nabla \cdot v \qquad i = 1, \ldots, N \\ \rho\frac{d\boldsymbol{v}}{dt} = \sum_{i=1}^{N} \rho_i \boldsymbol{F}_i - \boldsymbol{\nabla} p \\ \frac{d}{dt}\left(\rho T^{-\frac{3}{2}}\right) = 0 \end{gathered} \tag{2.148}$$

The last equation is expressed sometimes in the form $p\rho^{\gamma} = \text{cte}$, where γ is the well known adiabatic coefficient $\gamma = \frac{c_p}{c_v}$.

2.5.2 First order approximation

The expressions (2.149) are the integral equations from which the coefficients $f_i^{(1)}$ are to be found .

$$-\sum_{j=1}^{N} n_i n_j I_{ij}\left(\phi^{(1)}\right) = \left(\mathscr{D} f_i\right)^{(0)} \qquad i = 1, \ldots, N. \tag{2.149}$$

For each i the right member is:

$$(\mathscr{D}f_i)^{(0)} = \partial_0 f_i^{(0)}/\partial t + \boldsymbol{c}_i \cdot \boldsymbol{\nabla}_r f_i^{(0)} + \boldsymbol{F}_i \cdot \nabla_{ci} f_i^{(0)}. \tag{2.150}$$

If $f_i^{(0)}$ is regarded as a function of $\boldsymbol{r}$, $\boldsymbol{C}_i$ and t, instead of $\boldsymbol{r}$, $\boldsymbol{c}_i$ and t

$$\begin{aligned}(\mathscr{D}f_i)^{(0)} = f_i^{(0)} \Bigg\{ \frac{d_0 \log f_i^{(0)}}{dt} + \boldsymbol{C}_i \cdot \log f_i^{(0)} + \left(\boldsymbol{F}_i - \frac{d_0 v}{dt} \right) \cdot \boldsymbol{\nabla}_{C_i} \log f_i^{(0)} \\ - \left(\boldsymbol{\nabla} \log f_i^{(0)} \right) C_i : \nabla v \Bigg\}.\end{aligned} \tag{2.151}$$

As for a simple gas

$$\frac{d_0 \log f_i^{(0)}}{dt} = -\frac{m_i C_i^2}{3 k_B T} \boldsymbol{\nabla} \cdot \boldsymbol{v} \tag{2.152}$$

further,

$$\nabla_r f_i^{(0)} = \nabla \log n_i + \left(\frac{m_i C_i^2}{2 k_B T} - \frac{3}{2} \right) \nabla \log T \tag{2.153}$$

and

$$\boldsymbol{\nabla}_{c_i} \log f_i^{(0)} = -\frac{m_i}{k_B T} \mathbf{C}_i. \tag{2.154}$$

Hence

$$\begin{aligned}(\mathscr{D}f_i)^{(0)} = f_i^{(0)} \Bigg\{ \boldsymbol{C}_i \cdot \left[\boldsymbol{\nabla} \log n_i + \frac{m_i}{\rho k_B T} \left(-\boldsymbol{\nabla} p + \sum_N \rho_k \boldsymbol{F}_k \right) - \frac{m_i}{k_B T} \boldsymbol{F}_i + \left(\frac{m_i C_i^2}{2 k_B T} - \frac{3}{2} \right) \boldsymbol{\nabla} \log T \right] \\ + \frac{m_i}{k_B T} \left(\boldsymbol{C}_i \boldsymbol{C}_i - \frac{1}{3} C_i^2 \boldsymbol{I} \right) : \boldsymbol{\nabla} \boldsymbol{v} \Bigg\}\end{aligned} \tag{2.155}$$

Using the mole fractions n_i/n and the hydrostatic pressure p. Since $p = n k_B T$, one has

$$\nabla \log n_i = \nabla \log (n_i/n) + \nabla \log p - \nabla \log T \tag{2.156}$$

Equation (2.155) is equivalent to

$$(\mathscr{D}f_i)^{(0)} = f_i^{(0)} \left\{ \frac{n}{n_i} \boldsymbol{C}_i \cdot \boldsymbol{d}_i + \left(\frac{m_i C_i^2}{2 k_B T} - \frac{5}{2} \right) \boldsymbol{C}_i \cdot \boldsymbol{\nabla} \log T + \frac{m_i}{k_B T} \left(\boldsymbol{C}_i \boldsymbol{C}_i - \frac{1}{3} C_i^2 \boldsymbol{I} \right) : \boldsymbol{\nabla} \boldsymbol{v} \right\} \tag{2.157}$$

where $d_i$is the diffusion driving force

$$d_i = \nabla\left(\frac{n_i}{n}\right) + \left(\frac{n_i}{n} - \frac{\rho_i}{\rho}\right)\nabla \log p - \frac{\rho_i}{p}\left(F_i - \sum_j \frac{\rho_j}{\rho} F_j\right) \tag{2.158}$$

Since $\sum_i \left(\frac{n_i}{n}\right) = 1$ and $\sum_i \left(\frac{n_i}{n}\right) = 1$, the following identity is obtained

$$\sum_i \boldsymbol{d}_i = 0. \tag{2.159}$$

The equation (2.149) becomes

$$\begin{aligned}\sum_{j=1}^{N} n_i n_j I_{ij}\left(\phi^{(1)}\right) = -f_i^{(0)}\Bigg\{&\frac{n}{n_i}\boldsymbol{C}_i \cdot \boldsymbol{d}_i + \left(\frac{m_i C_i^2}{2k_B T} - \frac{5}{2}\right)\boldsymbol{C}_i \cdot \boldsymbol{\nabla} \log T \\ &+ \tfrac{m_i}{k_B T}\left(\boldsymbol{C}_i\boldsymbol{C}_i - \tfrac{1}{3}C_i^2 \boldsymbol{I}\right) : \boldsymbol{\nabla}\boldsymbol{v}\Bigg\}\end{aligned} \tag{2.160}$$

The vector $d_1, \ldots, d_k$ are linearly dependent dependent and therefore

$$d_i = d_i^* - \gamma_i \sum_j d_j^* \tag{2.161}$$

where $\gamma_1, \ldots, \gamma_N$are arbitrary constants such that

$$\sum_i \gamma_i = 1 \tag{2.162}$$

A convenient choice is given by

$$\gamma_i = \rho_i/\rho \qquad i = 1, \ldots, N \tag{2.163}$$

As I is a linear rotationally invariant operator

$$\phi_i^{(1)} = -\frac{1}{n}\sum_j \boldsymbol{D}_i^j \cdot \boldsymbol{d}_j^* - \frac{1}{n}\boldsymbol{A}_i \cdot \boldsymbol{\nabla} \log T - \frac{1}{n}\boldsymbol{B}_i : \boldsymbol{\nabla}\boldsymbol{v} \tag{2.164}$$

$\boldsymbol{D}_i^j$ and $\boldsymbol{A}_i$ are vector functions of $\boldsymbol{C}_i$ and $\boldsymbol{B}_i$ is a traceless tensor function of $\boldsymbol{C}_i$

$$\boldsymbol{D}^j = D^j(C)\,\boldsymbol{C} \quad \boldsymbol{A} = A(C)\,\boldsymbol{C} \quad \boldsymbol{B} = B(C)\left(\boldsymbol{C}\boldsymbol{C} - \frac{1}{3}C^2\boldsymbol{I}\right) \tag{2.165}$$

Comparing the coefficients of corresponding terms:

$$\sum_j \frac{n_i n_j}{n^2} I_{ij}\left(\boldsymbol{D}^k\right) = \frac{1}{n_i} f_i^{(0)}\left(\delta_{ik} - \frac{\rho_i}{\rho}\right)\boldsymbol{C}_i \quad i, k = 1, \ldots, N \tag{2.166}$$

$$\sum_j \frac{n_i n_j}{n^2} I_{ij}(\boldsymbol{A}) = \frac{1}{n} f_i^{(0)}\left(\frac{m_i C_i^2}{2k_B T} - \frac{5}{2}\right)\boldsymbol{C}_i \quad i = 1, \ldots, N \tag{2.167}$$

$$\sum_j \frac{n_i n_j}{n^2} I_{ij}(\boldsymbol{B}) = \frac{m_i}{n k_B T} f_i^{(0)} \left(\boldsymbol{C}_i \boldsymbol{C}_i - \frac{1}{3} C_i^2 \boldsymbol{I} \right) \quad i = 1, \ldots, N \tag{2.168}$$

The set of vectors D^k is such that the linear combination $\sum_k (\rho_k/\rho) \boldsymbol{D}^k$is a summational invariant.

$$\sum_K (\rho_k/\rho) \boldsymbol{D}^k = 0$$

The solution of (2.160) is given by

$$\phi_i^{(1)} = -\frac{1}{n} \sum_j \boldsymbol{D}_i^j \cdot \boldsymbol{d}_j - \frac{1}{n} \boldsymbol{A}_i \cdot \boldsymbol{\nabla} \log T - \frac{1}{n} \boldsymbol{B}_i : \boldsymbol{\nabla v} \tag{2.169}$$

If $\mathbf{d}^l$ and $\boldsymbol{a}$ are vector functions and $\mathbf{b}$ is a tensor function defined for each constituent of the mixture, then

$$\left[\boldsymbol{D}^k, \boldsymbol{d}^k \right] = \frac{1}{n_k} \sum_i \int f_k^{(0)} \boldsymbol{d}_k^l \cdot \mathbf{C}_k d^3 c_k - \frac{1}{\rho} \sum_i m_i \int f_i^{(0)} \boldsymbol{d}_i^l \cdot \mathbf{C}_i d^3 c_i \tag{2.170}$$

$$[\boldsymbol{A}, \boldsymbol{a}] = \frac{1}{n} \sum_i \int f_i^{(0)} \left(\frac{m_i C_i^2}{2kT} - \frac{5}{2} \right) \boldsymbol{a}_i \cdot \mathbf{C}_i d^3 c_i \tag{2.171}$$

$$[\boldsymbol{B}, \boldsymbol{b}] = \frac{1}{nkT} \sum_i m_i \int f_i^{(0)} \left(\boldsymbol{C}_i \boldsymbol{C}_i - \frac{1}{3} C^2 \boldsymbol{I} \right) : \boldsymbol{b}_i d^3 c_i \tag{2.172}$$

From the vectorial calculus

$$\begin{aligned} \boldsymbol{V}_i^{(1)} = \boldsymbol{V}_i = \tfrac{1}{n_i} \textstyle\int C_i^2 f_i^{(1)} d^3 c_i = -\tfrac{1}{3nn_i} \textstyle\sum_j \int f_i^{(0)} C_i^2 D_i^j d^3 c_i \boldsymbol{d}_j \\ -\frac{1}{3nn_i} \sum_j \int f_i^{(0)} C_i^2 A_i d^3 c_i \nabla \log T \end{aligned} \tag{2.173}$$

Comparing to the previous integral brackets expressions,

$$D_{ij} = \frac{1}{3n} \left[\boldsymbol{D}^i, \boldsymbol{D}^j \right] \tag{2.174}$$

$$D_{Ti} = \frac{1}{3n} \left[\boldsymbol{D}^i, \boldsymbol{A} \right] \tag{2.175}$$

D_{ij} are the multicomponent diffusion coefficients and D_{Ti} are the multicomponent thermal diffusion coefficients. The expression for the diffusion velocity may be written as:

$$\boldsymbol{V}_i = -\sum_j D_{ij} \boldsymbol{d}_j - D_{Ti} \boldsymbol{\nabla} \log T \tag{2.176}$$

where the term $-\sum_j D_{ij}\boldsymbol{d}_j$ is the Fick diffusion and the term $-D_{Ti}\boldsymbol{\nabla}\log T$ is the thermal diffusion.

$$D_{ij} = D_{ji}.$$

As $\sum_K (\rho_k/\rho)\,\boldsymbol{D}^k = 0$, not all the diffusion coefficients are independent. There are $\frac{1}{2}N\,(N-1)$ independent diffusion coefficients and $N-1$ independent thermal diffusion coefficients because the compatibility equation must be fulfilled

$$\sum_i (\rho_i/\rho)\,D_{ij} = 0. \tag{2.177}$$

In principle, thermal diffusion could be considered as an unexpected phenomenon, although it is fully compatible with Onsager reciprocal relations. Enskog [1911] was the first to predict thermal diffusion on purely theoretical grounds. Chapman [1917] made the same prediction. It was confirmed experimentally on a binary mixture by Chapman and Dootson [1917]. As in the Fick diffusion, the compatibility expression for the thermal diffusion coefficients is

$$\sum_i (\rho_i/\rho)\,D_{Ti} = 0\ . \tag{2.178}$$

In the evaluation of the pressure tensor from (2.143), the next expression is obtained.

$$\boldsymbol{P}^{(1)} = -\frac{1}{5}k_BT\,[\boldsymbol{B},\boldsymbol{B}]\,\boldsymbol{S}. \tag{2.179}$$

The coefficient of viscosity may be defined as

$$\eta = \frac{1}{10}k_BT\,[\boldsymbol{B},\boldsymbol{B}] \tag{2.180}$$

and the first-order approximation to the pressure tensor is then

$$\boldsymbol{P} = p\boldsymbol{I} - 2\eta\boldsymbol{S} \tag{2.181}$$

The remaining magnitude to evaluate is the heat flow vector $\mathbf{q}$. The definition of the partial thermal conductivity is

$$\lambda' = \frac{1}{3}k_B\,[\boldsymbol{A},\boldsymbol{A}]\,. \tag{2.182}$$

Substituting in (2.144)

$$\boldsymbol{q} = -\lambda'\boldsymbol{\nabla}T - p\sum_i D_{Ti}\boldsymbol{d}_i + \frac{5}{2}kT\sum_i n_i\boldsymbol{V}_i \tag{2.183}$$

and eliminating $\boldsymbol{d}_i$

$$\boldsymbol{q} = -\lambda \boldsymbol{\nabla} T + p \sum_i \left(k_{Ti} + \frac{5}{2} \frac{n_i}{n} \right) \boldsymbol{V}_i \tag{2.184}$$

The relation between the partial thermal conductivity and the thermal conductivity is

$$\lambda = \lambda' - nk \sum_i k_{Ti} D_{Ti} \tag{2.185}$$

where the values $k_{Ti}$are the thermal diffusion ratios

$$\sum_j D_{ij} k_{Tj} = D_{Ti} \qquad i = 1, \ldots, N \tag{2.186}$$

$$\sum_i k_{Ti} = 0 \tag{2.187}$$

In this section, the derivation of the expressions for the first order of the Chapman Enskog approximation to the solution of the Boltzmann's equation for multicomponent gases has been showed. The definition of the transport parameter has also been presented.

2.5.3 Calculation of the multicomponent transport coefficients

With the transport coefficients definition, more elaborated relations for practical transport coefficients will be described. They will be expressed as systems of equations with terms that are defined in terms of functions of the bracket integrals. The beginning is the entropy production due to collisions.

$$\begin{aligned} \left(\frac{\partial s}{\partial t} \right)_{coll} = nk \textstyle\sum_{i,j} D_{ij} \left(d_i + k_{Ti} \nabla \log T \right) \cdot \left(d_j + k_{Tj} \nabla \log T \right) \\ + \lambda \left| \nabla \log T \right|^2 + \left(2\eta / T \right) \boldsymbol{S} : \boldsymbol{S}. \end{aligned} \tag{2.188}$$

A similar analysis as that performed for a simple gas drives to the following relations:

$$\boldsymbol{d}^k \equiv d^k \left(C \right) \boldsymbol{C} \quad \left[\boldsymbol{d}^k, \boldsymbol{d}^l \right] \leqq \left[\boldsymbol{D}^k, \boldsymbol{D}^l \right] \tag{2.189}$$

$$\boldsymbol{a} \equiv a \left(C \right) \boldsymbol{C} \quad [\boldsymbol{a}, \boldsymbol{a}] \leqq [\boldsymbol{A}, \boldsymbol{A}] \tag{2.190}$$

$$\boldsymbol{b} \equiv b \left(C \right) \left(\boldsymbol{CC} - \frac{1}{3} C^2 \boldsymbol{I} \right) \quad [\boldsymbol{b}, \boldsymbol{b}] \leqq [\boldsymbol{B}, \boldsymbol{B}] \,. \tag{2.191}$$

The maximum principle for multicomponent gases implies that the distribution of the molecular velocities is such that, for given gradients of concentration, pressure, temperature and velocity, the rate of change of the entropy density due to collision is as large as possible.

$$\boldsymbol{d}_i^k \equiv d_i^k\left(C_i\right)\boldsymbol{C}_i = \left(\frac{m_i}{2kT}\right)^{\frac{1}{2}} \sum_{p=0}^{n-1} d_{i,p}^{k(p)} S_{\frac{3}{2}}^{(r)}\left(\mathcal{C}^2\right)\boldsymbol{\mathcal{C}}_i$$

The variational principle stands

$$\delta\left\{g^{kl}\right\} = 0 \tag{2.192}$$

$$g^{kl} = \left[\boldsymbol{d}^k, \boldsymbol{d}^l\right] = \frac{75k_B}{16}\sum_{i,j=1}^{N}\sum_{q,r=0}^{n-1}\Lambda_{ij}^{qr} d_{i,q}^{k(n)} d_{j,r}^{l(n)} \tag{2.193}$$

with

$$\begin{aligned}\Lambda_{ij}^{qr} = \frac{8m_i^{\frac{1}{2}}m_j^{\frac{1}{2}}}{75k_B^2T}\Bigg\{\delta_{ij}\sum_h \frac{n_i n_h}{n^2}\left[S_{\frac{3}{2}}^{(q)}\left(\mathcal{C}^2\right)\boldsymbol{\mathcal{C}}, S_{\frac{3}{2}}^{(r)}\left(\mathcal{C}^2\right)\boldsymbol{\mathcal{C}}\right]_{ih}^{'} \\ + \frac{n_i n_j}{n^2}\left[S_{\frac{3}{2}}^{(q)}\left(\mathcal{C}^2\right)\boldsymbol{\mathcal{C}}, S_{\frac{3}{2}}^{(r)}\left(\mathcal{C}^2\right)\boldsymbol{\mathcal{C}}\right]_{ij}^{''}\Bigg\}.\end{aligned} \tag{2.194}$$

These Λ coefficients have the properties:

$$\Lambda_{ij}^{qr} = \Lambda_{ji}^{rq} \qquad \sum_i \Lambda_{ij}^{q0} = 0 \quad \sum_i \Lambda_{ij}^{0r}. \tag{2.195}$$

Minimizing with the help of the Lagrange multipliers method

$$\sum_{j=1}^{n}\sum_{q=0}^{n-1}\Lambda_{ij}^{pq} d_{j,q}^{k(n)} = \frac{8}{25k_B}\left(\delta_{ik} - \frac{\rho_i}{\rho_0}\right)\delta_{p0} \qquad \begin{matrix} i = 1,\ldots,N \\ p = 0,\ldots,n-1 \end{matrix}. \tag{2.196}$$

The compatibility equation is

$$\sum_i \left(\rho_i/\rho\right) d_{i,0}^{k(n)} = 0. \tag{2.197}$$

In a similar way, the trial functions $\boldsymbol{a}_i$

$$\boldsymbol{a}_i \equiv a_i\left(C_i\right)\boldsymbol{C}_i = -\left(\frac{m_i}{2kT}\right)^{\frac{1}{2}}\sum_{p=0}^{n} a_{i,p}^{(n)} S_{\frac{3}{2}}^{(p)}\left(\mathcal{C}^2\right)\boldsymbol{\mathcal{C}} \tag{2.198}$$

$$\delta\left\{g\right\} = 0 \qquad g = \left[\boldsymbol{a}, \boldsymbol{a}\right] = \frac{75k_B}{16}\sum_{i,j=1}^{N}\sum_{q,r=0}^{n}\Lambda_{ij}^{qr} a_{i,q}^{(n)} a_{j,r}^{(n)} \tag{2.199}$$

The resultant systems of linear equations provides the coefficients $a_{i,p}^{(n)}$

$$\begin{array}{c} \sum_{j=1}^{N}\sum_{q=0}^{n}\Lambda_{ij}^{pq}a_{j,q}^{(n)}=\frac{4}{5k_B}\frac{n_i}{n}\delta_{p1} \qquad i=1,\ldots,N \\ p=0,\ldots,n \\ \sum_i\left(\rho_i/\rho\right)a_{i,0}^{(n)}=0 \end{array}. \tag{2.200}$$

For the trial functions $\boldsymbol{b}_i$

$$\boldsymbol{b}_i\equiv b_i\left(C_i\right)\left(\boldsymbol{C}_i\boldsymbol{C}_i-\frac{1}{3}C_i^2\boldsymbol{I}\right)=\sum_{p=0}^{n-1}b_{i,p}^{(n)}S_{\frac{5}{2}}^{(p)}\left(\mathcal{C}_i^2\right)\left(\boldsymbol{\mathcal{C}}_i\boldsymbol{\mathcal{C}}_i-\frac{1}{3}\mathcal{C}_i^2\boldsymbol{I}\right) \tag{2.201}$$

$$\delta g=0 \qquad g\equiv[\boldsymbol{b},\boldsymbol{b}]=\frac{5}{2}kT\sum_{i,j=1}^{K}\sum_{q,r=0}^{n-1}H_{ij}^{qr}b_{i,q}^{(n)}b_{j,r}^{(n)} \tag{2.202}$$

$$\begin{array}{c} H_{ij}^{qr}=\frac{2}{5kT}\left\{\delta_{ij}\sum_h\frac{n_in_h}{n^2}\left[S_{\frac{5}{2}}^{(q)}\left(\mathcal{C}^2\right)\left(\boldsymbol{\mathcal{C}}_i\boldsymbol{\mathcal{C}}_i-\frac{1}{3}\mathcal{C}_i^2\boldsymbol{I}\right),S_{\frac{5}{2}}^{(r)}\left(\mathcal{C}^2\right)\left(\boldsymbol{\mathcal{C}}_i\boldsymbol{\mathcal{C}}_i-\frac{1}{3}\mathcal{C}_i^2\boldsymbol{I}\right)\right]_{ih}^{'}\right. \\ \left.+\frac{n_in_j}{n^2}\left[S_{\frac{5}{2}}^{(q)}\left(\mathcal{C}^2\right)\left(\boldsymbol{\mathcal{C}}_i\boldsymbol{\mathcal{C}}_i-\frac{1}{3}\mathcal{C}_i^2\boldsymbol{I}\right),S_{\frac{5}{2}}^{(r)}\left(\mathcal{C}^2\right)\left(\boldsymbol{\mathcal{C}}_i\boldsymbol{\mathcal{C}}_i-\frac{1}{3}\mathcal{C}_i^2\boldsymbol{I}\right)\right]_{ij}^{''}\right\} \end{array} \tag{2.203}$$

$$H_{ij}^{qr}=H_{ji}^{rq}. \tag{2.204}$$

The resultant systems of linear equations provides the coefficients $b_{i,p}^{(n)}$

$$\sum_{j=1}^{N}\sum_{q=0}^{n-1}H_{ij}^{pq}b_{j,q}^{(n)}=\frac{2}{k_BT}\frac{n_i}{n}\delta_{p0} \qquad \begin{array}{c} i=1,\ldots,N \\ p=0,\ldots,n-1 \end{array} \tag{2.205}$$

The bracket integrals are the key for the multicomponent transport coefficients calculation

$$\left[\boldsymbol{d}^k,\boldsymbol{d}^l\right]=\frac{3}{2}d_{l,0}^{k(n)} \qquad \left[\boldsymbol{d}^k,\boldsymbol{d}^l\right]=\frac{3}{2}d_{k,0}^{l(n)} \qquad \left[D_{kl}\right]_n=\frac{1}{2n}d_{l,0}^{k(n)}=\frac{1}{2n}d_{k,0}^{l(n)} \tag{2.206}$$

$$\left[\boldsymbol{d}^k,\boldsymbol{a}\right]=-\frac{3}{2}a_{k,0}^{(n)} \qquad \left[D_{Tk}\right]_n=-\frac{1}{2n}a_{k,0}^{(n)} \tag{2.207}$$

$$\left[\boldsymbol{d}^k,\boldsymbol{a}\right]=-\frac{15}{4}\sum_{i=1}^{N}\left(n_i/n\right)d_{i,1}^{k(n)} \qquad \left[D_{Tk}\right]_n=-\frac{5}{4n}\sum_{i=1}^{N}\left(n_i/n\right)d_{i,1}^{k(n)} \tag{2.208}$$

$$[\boldsymbol{a},\boldsymbol{a}]=\frac{15}{4}\sum_{i=1}^{N}\left(n_i/n\right)a_{i,1}^{(n)} \qquad \left[\lambda'\right]_n=\frac{5}{4}k_B\sum_{i=1}^{N}\left(n_i/n\right)a_{i,1}^{(n)} \tag{2.209}$$

$$[\boldsymbol{b},\boldsymbol{b}] = 5\sum_{i=1}^{N}(n_i/n)\,b_{i,0}^{(n)} \qquad [\eta]_n = \frac{1}{2}k_BT\sum_{i=1}^{N}(n_i/n)\,b_{i,0}^{(n)} \tag{2.210}$$

2.6 The transport coefficients.

In this section, some issues related to the bracket integrals and integral collisions will be addressed. With the evaluation of such integrals, the system of equations to derive the transport coefficients from the kinetic theory of gases is completely defined. The expressions of Λ parameters described in the previous chapter as a function of the integral collisions will be showed.

2.6.1 Expressions of the integral collisions

The initial point is the dynamics of binary collision. The interaction force between $\mathbf{F}$ is derived from the potential φ, $\mathbf{F} = -\nabla\varphi$. The equations of motion for the two particles are

$$m_i\frac{d^2\mathbf{r}_i}{dt^2} = \mathbf{F}\left(|\mathbf{r}_i - \mathbf{r}_j|\right) \qquad m_j\frac{d^2\mathbf{r}_j}{dt^2} = \mathbf{F}\left(|\mathbf{r}_i - \mathbf{r}_j|\right) \tag{2.211}$$

It helps the use of the center of mass and relative coordinates,

$$\mathbf{R} = \frac{m_i\mathbf{r}_i + m_j\mathbf{r}_j}{m_i + m_j}, \qquad r = r_i - r_j \tag{2.212}$$

In this coordinates, the equations of motion are

$$\frac{d^2\mathbf{R}}{dt^2} = 0 \tag{2.213}$$

$$m_{ij}\frac{d^2\mathbf{r}}{dt^2} = \mathbf{F}\left(r\right) \tag{2.214}$$

where m_{ij} is the reduced molecular mass

$$m_{ij} = \frac{m_im_j}{m_i + m_j}. \tag{2.215}$$

The trajectory of a force, function of $\mathbf{r}$, lies in a plane and polar coordinates can be used. Taking the scalar product of (2.214) with $\dfrac{d\mathbf{r}}{dt}$ and integrating,

$$\frac{1}{2}m_{ij}\left[\left(\frac{dr}{dt}\right)^2 + r^2\left(\frac{d\theta}{dt}\right)^2\right] + \varphi\left(r\right) = \frac{1}{2}m_{ij}g^2 \tag{2.216}$$

where $\boldsymbol{g} = \boldsymbol{c}_j - \boldsymbol{c}_i$ is the center of mass velocity for a pair of species.

The angular momentum is constant in the motion

$$m_{ij}r^2\frac{d\theta}{dt} = m_{ij}gb \tag{2.217}$$

where $m_{ij}gb$ is the constant in the infinite, figure 2.2. The motion equation is then

$$\frac{1}{2}m_{ij}\left(\frac{dr}{dt}\right)^2 + \left[\varphi(r) + \frac{1}{2}\frac{m_{ij}g^2b^2}{r^2}\right] + = \frac{1}{2}m_{ij}g^2. \tag{2.218}$$

Dividing by $\dfrac{d\theta}{dt}$ and rearranging

$$\frac{dr}{d\theta} = \left[\frac{r^4}{b^2} - r^2 - \frac{2r^4}{m_{ij}g^2b^2}\varphi(r)\right]^{\frac{1}{2}}. \tag{2.219}$$

Taking into account the symmetry about the point of closest approach

$$\chi = \pi - 2b\int_{r_0}^{\infty} \frac{{}^{dr}/_{r^2}}{\left[1 - ({}^{b^2}/_{r^2}) - 2\varphi(r)/m_{ij}g^2\right]^{\frac{1}{2}}}. \tag{2.220}$$

For potentials given by

$$\varphi(r) = \left(\frac{\sigma}{r}\right)^{\nu} \tag{2.221}$$

we have

$$\chi_{ij} = \pi - 2b\int_{r_0}^{\infty} \frac{dr/r^2}{\left[1 - ({}^{b^2}/_{r^2}) - 2\left(\sigma_{ij}/r\right)^{\nu}/m_{ij}g^2\right]^{\frac{1}{2}}}. \tag{2.222}$$

Introducing the variables

$$y = {}^{b}/_{r}, \quad y_0 = {}^{b}/_{r0}, \quad z = (b/\sigma_{ij})\left(m_{ij}g^2/2\nu\right)^{1/\nu}, \tag{2.223}$$

$$\chi_{ij} = \pi - 2\int_{r_0}^{\infty}\left[1 - y^2 - \nu^{-1}(y/z)\right]^{-\frac{1}{2}}dy \tag{2.224}$$

and taking into account that the dimensionless center of mass velocity is

$$\tilde{\boldsymbol{g}} = (m_{ij}/2kT)^{\frac{1}{2}}\,\boldsymbol{g} \tag{2.225}$$

the integral Q is defined as

$$Q_{ij}^{(l)} \equiv Q_{ij}^{(l)}(\tilde{g}) = 2\pi\int\left\{1 - cos^l\chi_{ij}(b,\tilde{g})\right\}bdb. \tag{2.226}$$

and the definition of the Ω integrals is

The partial bracket integral $[S_{\frac{3}{2}}^{(p)}(\mathscr{C}^2)\mathscr{C},\ S_{\frac{3}{2}}^{(q)}(\mathscr{C}^2)\mathscr{C}]'_{ij}$ for $p, q = 0, 1, 2$

	$[S_{\frac{3}{2}}^{(p)}(\mathscr{C}^2)\mathscr{C}, S_{\frac{3}{2}}^{(q)}(\mathscr{C}^2)\mathscr{C}]'_{ij}$
$p = 0, q = 0$	$8\mu_j \Omega_{ij}^{(1,1)}$,
$p = 0, q = 1$	$8\mu_j^2(\frac{5}{2}\Omega_{ij}^{(1,1)} - \Omega_{ij}^{(1,2)})$,
$p = 1, q = 1$	$8\mu_j[\frac{5}{4}(6\mu_i^2 + 5\mu_j^2)\Omega_{ij}^{(1,1)} - 5\mu_j^2\Omega_{ij}^{(1,2)} + \mu_j^2\Omega_{ij}^{(1,3)} + 2\mu_i\mu_j\Omega_{ij}^{(2,2)}]$,
$p = 0, q = 2$	$4\mu_j^3(\frac{35}{4}\Omega_{ij}^{(1,1)} - 7\Omega_{ij}^{(1,2)} + \Omega_{ij}^{(1,3)})$,
$p = 1, q = 2$	$8\mu_j^2[\frac{35}{16}(12\mu_i^2 + 5\mu_j^2)\Omega_{ij}^{(1,1)} - \frac{21}{8}(4\mu_i^2 + 5\mu_j^2)\Omega_{ij}^{(1,2)} + \frac{19}{4}\mu_j^2\Omega_{ij}^{(1,3)} - \frac{1}{2}\mu_j^2\Omega_{ij}^{(1,4)} + 7\mu_i\mu_j\Omega_{ij}^{(2,2)} - 2\mu_i\mu_j\Omega_{ij}^{(2,3)}]$,
$p = 2, q = 2$	$8\mu_j[\frac{35}{64}(40\mu_i^4 + 168\mu_i^2\mu_j^2 + 35\mu_j^4)\Omega_{ij}^{(1,1)} - \frac{7}{8}\mu_j^2(84\mu_i^2 + 35\mu_j^2)\Omega_{ij}^{(1,2)} + \frac{1}{8}\mu_j^2(108\mu_i^2 + 133\mu_j^2)\Omega_{ij}^{(1,3)} - \frac{7}{2}\mu_j^4\Omega_{ij}^{(1,4)} + \frac{1}{4}\mu_j^4\Omega_{ij}^{(1,5)} + \frac{7}{2}\mu_i\mu_j(4\mu_i^2 + 7\mu_j^2)\Omega_{ij}^{(2,2)} - 14\mu_i\mu_j^3\Omega_{ij}^{(2,3)} + 2\mu_i\mu_j^3\Omega_{ij}^{(2,4)} + 2\mu_i^2\mu_j^2\Omega_{ij}^{(3,3)}]$.

Table 2.1: Bracket integrals ' as function of the integral collisions for $p, q = 0, 1, 2$. Table 7.3 from reference [1].

$$\Omega_{ij}^{(l,r)} = \left(\frac{kT}{\pi m_{ij}}\right)^{\frac{1}{2}} \int_0^\infty \exp\left(-\tilde{g}^2\right) \tilde{g}^{2r+3} Q_{ij}^{(l)} d\tilde{g} \tag{2.227}$$

2.6.2 Expressions of the bracket integrals

The bracket integrals may be written as function of the Ω integrals, see Table 2.1 for $\left[S_{\frac{3}{2}}^{(p)}(\mathcal{C}^2)\boldsymbol{\mathcal{C}}, S_{\frac{3}{2}}^{(q)}(\mathcal{C}^2)\boldsymbol{\mathcal{C}}\right]'_{ij}$ and Table 2.2 for $\left[S_{\frac{3}{2}}^{(p)}(\mathcal{C}^2)\boldsymbol{\mathcal{C}}, S_{\frac{3}{2}}^{(q)}(\mathcal{C}^2)\boldsymbol{\mathcal{C}}\right]''_{ij}$, where $\mu_i = \frac{m_i}{m_i+m_j}$ and $\mu_j = \frac{m_j}{m_i+m_j}$. The tables for $\left[S_{\frac{5}{2}}^{(p)}(\mathcal{C}^2)\left(\boldsymbol{\mathcal{C}}_i\boldsymbol{\mathcal{C}}_i - \frac{1}{3}\mathcal{C}_i^2\boldsymbol{I}\right), S_{\frac{5}{2}}^{(q)}(\mathcal{C}^2)\left(\boldsymbol{\mathcal{C}}_i\boldsymbol{\mathcal{C}}_i - \frac{1}{3}\mathcal{C}_i^2\boldsymbol{I}\right)\right]'_{ij}$ and $\left[S_{\frac{5}{2}}^{(p)}(\mathcal{C}^2)\left(\boldsymbol{\mathcal{C}}_i\boldsymbol{\mathcal{C}}_i - \frac{1}{3}\mathcal{C}_i^2\boldsymbol{I}\right), S_{\frac{5}{2}}^{(q)}(\mathcal{C}^2)\left(\boldsymbol{\mathcal{C}}_i\boldsymbol{\mathcal{C}}_i - \frac{1}{3}\mathcal{C}_i^2\boldsymbol{I}\right)\right]''_{ij}$ may be also found in [1].

In general Ω integrals cannot be evaluated analytically due to the complicated dependence of χ on b and g. However, there are explicit expressions for the rigid sphere model,

$$\cos\frac{1}{2}\chi = b/\sigma_{ij} \tag{2.228}$$

$$\left[\Omega_{ij}^{(l,r)}\right]_{r.s.} = \left(\frac{kT}{\pi m}\right)^{\frac{1}{2}} \frac{(r+1)!}{2}\left[1 - \frac{1+(-1)^l}{2(l+1)}\right]\pi\sigma_{ij}^2 \tag{2.229}$$

where $\sigma_{ij} = \frac{1}{2}(\sigma_i + \sigma_j)$ is the separation of the centers of the two molecules with diameters σ_i and σ_j. It is possible to define the reduced values:

The partial bracket integral $[S_{\frac{3}{2}}^{(p)}(\mathscr{C}^2)\mathscr{C}, S_{\frac{3}{2}}^{(q)}(\mathscr{C}^2)\mathscr{C}]_{ij}''$ for $p, q = 0, 1, 2$

	$[S_{\frac{3}{2}}^{(p)}(\mathscr{C}^2)\mathscr{C}, S_{\frac{3}{2}}^{(q)}(\mathscr{C}^2)\mathscr{C}]_{ij}''$
$p=0, q=0$	$-8\mu_i^{\frac{1}{2}}\mu_j^{\frac{1}{2}}\Omega_{ij}^{(1,1)}$,
$p=0, q=1$	$-8\mu_i^{\frac{3}{2}}\mu_j^{\frac{1}{2}}(\frac{5}{2}\Omega_{ij}^{(1,1)}-\Omega_{ij}^{(1,2)})$,
$p=1, q=1$	$-8\mu_i^{\frac{3}{2}}\mu_j^{\frac{3}{2}}(\frac{5\,5}{4}\Omega_{ij}^{(1,1)}-5\Omega_{ij}^{(1,2)}+\Omega_{ij}^{(1,3)}-2\Omega_{ij}^{(2,2)})$,
$p=0, q=2$	$-4\mu_i^{\frac{3}{2}}\mu_j^{\frac{1}{2}}(\frac{3\,5}{4}\Omega_{ij}^{(1,1)}-7\Omega_{ij}^{(1,2)}+\Omega_{ij}^{(1,3)})$,
$p=1, q=2$	$-8\mu_i^{\frac{3}{2}}\mu_j^{\frac{3}{2}}(\frac{5\,0\,5}{1\,6}\Omega_{ij}^{(1,1)}-\frac{1\,8\,9}{8}\Omega_{ij}^{(1,2)}+\frac{1\,9}{4}\Omega_{ij}^{(1,3)}-\frac{1}{2}\Omega_{ij}^{(1,4)}-7\Omega_{ij}^{(2,2)}+2\Omega_{ij}^{(2,3)})$,
$p=2, q=2$	$-8\mu_i^{\frac{3}{2}}\mu_j^{\frac{3}{2}}(\frac{8\,5\,0\,5}{6\,4}\Omega_{ij}^{(1,1)}-\frac{8\,3\,3}{8}\Omega_{ij}^{(1,2)}+\frac{2\,4\,1}{8}\Omega_{ij}^{(1,3)}-\frac{7}{2}\Omega_{ij}^{(1,4)}$ $+\frac{1}{4}\Omega_{ij}^{(1,5)}-\frac{7\,7}{2}\Omega_{ij}^{(2,2)}+14\Omega_{ij}^{(2,3)}-2\Omega_{ij}^{(2,4)}+2\Omega_{ij}^{(3,3)})$.

Table 2.2: Bracket integrals " as function of the integral collisions for $p, q = 0, 1, 2$. Table 7.4 from reference [1].

$$\Omega_{ij}^{*(l,r)} = \Omega_{ij}^{(l,r)} / \left[\Omega_{ij}^{(l,r)}\right]_{r.s.} \tag{2.230}$$

There are certain combinations of the reduced Ω integrals which occur frequently in transport property calculations:

$$\begin{aligned} A_{ij}^* &= \Omega_{ij}^{(2,2)*}/\Omega_{ij}^{(1,1)*} \\ B_{ij}^* &= \left[5\Omega_{ij}^{(1,2)*} - 4\Omega_{ij}^{(1,3)*}\right]/\Omega_{ij}^{(1,1)*} \\ C_{ij}^* &= \Omega_{ij}^{(1,2)*}/\Omega_{ij}^{(1,1)*} \\ E_{ij}^* &= \Omega_{ij}^{(2,3)*}/\Omega_{ij}^{(2,2)*} \\ F_{ij}^* &= \Omega_{ij}^{(3,3)*}/\Omega_{ij}^{(1,1)*} \end{aligned} \tag{2.231}$$

2.6.3 Explicit expressions for the transport coefficients

The expression of the coefficient of viscosity of a simple gas in terms of a single Sonine expansion coefficient for the nth approximation is

$$[\eta]_n = \frac{1}{2} k_B T b_0^{(n)} \tag{2.232}$$

The Sonine expansion coefficients $b_0^{(n)} \ldots b_{n-1}^{(n)}$ must be calculated by the resolution of the linear system of equations (2.205) with $i = j = N = 1$. To build the system, the values H^{pq} have to be known and they are defined in terms of the bracket integrals.

The first approximation to the coefficient of viscosity of a simple gas in terms of the reduced Ω integrals is

$$[\eta]_1 = \frac{5}{16} \frac{(\pi m k_B T)^{\frac{1}{2}}}{\pi \sigma^2 \Omega^{(2,2)*}}. \tag{2.233}$$

The nth approximation of a simple gas in terms of single Sonine expansion coefficient is

$$[\lambda]_n = \frac{5}{4} k_B a_1^{(n)} \tag{2.234}$$

where $a_1^{(n)}$ is obtained from the solution of the system of linear equations (2.200) with $i = j = N = 1$, for the unknowns $a_1^{(n)}, \ldots, a_n^{(n)}$. The coefficients $\Lambda^{pq}$are also defined in terms of the bracket integral. The first approximation to the coefficient of thermal conductivity is

$$[\lambda]_1 = \frac{25}{32} \frac{(\pi m k_B T)^{\frac{1}{2}}}{\pi \sigma^2 \Omega^{(2,2)*}} \frac{3k_B}{2m}. \tag{2.235}$$

For analogy to simple gases, the following multicomponent quantities are defined

$$[\eta_{ij}]_1 = \frac{5}{16} \frac{(2\pi m_{ij} k_B T)^{\frac{1}{2}}}{\pi \sigma_{ij}^2 \Omega_{ij}^{(2,2)*}} \tag{2.236}$$

$$[\lambda_{ij}]_1 = \frac{25}{32} \frac{(2\pi m_{ij} k_B T)^{\frac{1}{2}}}{\pi \sigma_{ij}^2 \Omega_{ij}^{(2,2)*}} \frac{3k_B}{2m_{ij}} \tag{2.237}$$

The Fick diffusion coefficients for a gas mixture are given by:

$$[D_{kl}]_n = [D_{lk}]_n = \frac{1}{2n} d_{l,0}^{k(n)} \tag{2.238}$$

where $d_{l,0}^{k(n)}$ are obtained from the system of equations (2.196). The coefficients Λ_{ij}^{pq} are defined in terms of partial bracket integrals and can be written as linear combinations of Ω integrals:

$$\Lambda_{ii}^{00} = \sum_{\substack{l=1 \\ (l \neq i)}}^{K} \frac{x_i x_l}{2A_{il}^* [\lambda_{il}]_1} \quad \Lambda_{ij}^{00} = -\frac{x_i x_j}{2A_{ij}^* [\lambda_{ij}]_1} \qquad (i \neq j) \tag{2.239}$$

$$\Lambda_{ii}^{01} = \Lambda_{ii}^{10} = -\sum_{\substack{l=1 \\ (l \neq i)}}^{K} \frac{x_i x_l}{4A_{ij}^* [\lambda_{il}]_1} \frac{m_l}{m_i + m_l} (6C_{il}^* - 5) \tag{2.240}$$

$$\Lambda_{ij}^{01} = \Lambda_{ji}^{10} = \frac{x_i x_j}{4A_{ij}^* [\lambda_{ij}]_1} \frac{m_i}{m_i + m_j} \left(6C_{ij}^* - 5\right) \qquad (i \neq j) \tag{2.241}$$

$$\Lambda_{ii}^{11} = \frac{x_i^2}{[\lambda_i]_1} + \sum_{\substack{l=1 \\ (l \neq i)}}^{K} \frac{x_i x_l}{2A_{ij}^* [\lambda_{il}]_1} \frac{\frac{15}{2} m_i^2 + \frac{25}{4} m_l^2 - 3m_l^2 B_{il}^* + 4m_i m_l A_{il}^*}{(m_i + m_l)^2} \tag{2.242}$$

$$\Lambda_{ij}^{11} = -\frac{x_i x_j}{2A_{ij}^* \left[\lambda_{ij}\right]_1} \frac{m_i m_j}{\left(m_i + m_j\right)^2} \left(\frac{55}{4} - 3B_{ij}^* - 4A_{ij}^*\right) \qquad (i \neq j) \tag{2.243}$$

The thermal diffusion in a mixture are given by(2.207) and the values $a_{k,0}^{(n)}$ are obtained from the system of equations (2.200). The coefficients Λ_{ij}^{pq} are defined in (2.239), (2.240), (2.241), (2.242) and (2.243). From the system (2.200) may be also calculated the coefficients $a_{k,1}^{(n)}$ to derive the partial thermal conductivity (2.209).

Chapter 3

Polyatomic modifications to the classical kinetic theory of gases

As in the previous chapter the main reference is [1]. However, the polyatomic modifications are only developed for simple gases. The extension to mixtures has been written taking into account the references [8, 18].

3.1 Boltzmann equation generalization

Although polyatomic effects are negligible for Fick diffusion coefficients calculation, it is important in the thermal diffusion coefficients and thermal conductivity evaluation. The polyatomic effects contributions are due to:

- Inelastic collisions
- Long relaxation times for the internal degrees of freedom
- Resonant exchange for rotational energy

The procedure to account for polyatomic effects follows the Chapman Enskog method, but instead of considering only the translational velocity distribution function, we also consider each quantum state of each species as a separate entity, thus considering also the internal degrees of freedom of polyatomic molecules, rotational and vibrational. If E_I is the energy associated with the internal state I, the average internal energy per unit mass, u, is

$$\rho_i u_i = \sum_I \int \left(\frac{1}{2} m_i C_i^2 + E_{iI} \right) f_{iI} d^3 c_i \tag{3.1}$$

The distribution $f_{i_I}(\boldsymbol{r}, \boldsymbol{c}_i, E_{iI}, t)$ for the velocity $\boldsymbol{c}_i$ and the internal energy state E_{iI} for the species i is the given in terms of the collision integrals by the generalized Boltzmann equation.

We let $\sigma_{IJ}^{KL}(g,\chi,\varepsilon)$ be the cross section for scattering molecules in internal states I and J with respective speed g, that after the collision have the internal states K and L with the relative velocity rotated a polar angle χ and azimuthal angle ε (molecules are not spherically symmetric).

The number of collisions per unit volume and unit time involving molecules in state I with velocities in d^3c about $\boldsymbol{c}$ and molecules in state J with velocities d^3c_1 about $\boldsymbol{c}_1$, such that after collision, the molecules are in the states K and L respectively, and have their velocity oriented in a direction in $\sin\chi d\chi$ about χ and $d\varepsilon$ about $d\varepsilon$ with respect to their initial relative velocity, is:

$$g\sigma_{IJ}^{KL}(g,\chi,\varepsilon)\, f_I(\boldsymbol{r},\boldsymbol{c},t)\, f_J(\boldsymbol{r},\boldsymbol{c}_1,t)\, d^3c d^3c_1 \sin\chi d\chi d\varepsilon \tag{3.2}$$

Using the relation

$$d^2\Omega = \sin\chi d\chi d\varepsilon \tag{3.3}$$

the generalization of the Boltzmann equation is

$$\begin{gathered}\left(\frac{\partial}{\partial t} + \boldsymbol{c}_i\cdot\nabla_r + \boldsymbol{F}\cdot\nabla_{\boldsymbol{c}}\right) f_{iI}(\boldsymbol{r},\boldsymbol{c}_i,u_{iI},t) = \\ \sum_j \sum_{JKL} \iint \left(f'_{iK} f'_{1jL} - f_{iI} f_{1jJ}\right) g\sigma_{IJ}^{KL}(g,\chi,\varepsilon)\, d^2\Omega d^3c_j\end{gathered} \tag{3.4}$$

which is known as the Wang Chang-Uhlenbeck equation. In abbreviated notation:

$$\mathscr{D} f_{iI} = \sum_{j=1}^{N} \sum_{JKL} J_{IJ}^{KL}(f_i f_j)\,. \tag{3.5}$$

When the internal energy states are considered, the equilibrium Boltzmann distribution function is given by

$$f_{iI}^{(0)} = n_i \left(\frac{m_i}{2\pi k_B T}\right)^{\frac{3}{2}} \frac{\exp\left[-\left(m_i C_i^2/2k_B T\right) - \left(E_{iI}/k_B T\right)\right]}{\sum_I \exp\left(-E_{iI}/k_B T\right)} \tag{3.6}$$

The function

$$Z_{int,i} = \sum_I \exp\left(-E_{iI}/k_B T\right) \tag{3.7}$$

is recognized as the mechanical partition function for the internal degrees of freedom.

The internal energy for a species i is

$$\rho_i u_i = \frac{3}{2} n_i k_B T + \rho_i u_{int,i} \tag{3.8}$$

with

$$\rho_i u_{int,i} = n_i \bar{E}_i = n_i \frac{\sum_I E_{iI} \exp\left(-E_{iI}/k_B T\right)}{\sum_I \exp\left(-E_{iI}/k_B T\right)} \tag{3.9}$$

The parameters $\mathcal{E}_{Ii}$ and $\bar{\mathcal{E}}_i$ are the dimensionless energy variables

$$\mathcal{E}_{Ii} = \frac{E_{iI}}{k_B T}; \quad \bar{\mathcal{E}}_i = \frac{\bar{E}_i}{k_B T} = \frac{\sum_I \mathcal{E}_{Ii} \exp\left(-\mathcal{E}_{Ii}\right)}{\sum_I \exp\left(-\mathcal{E}_{Ii}\right)} \tag{3.10}$$

c_v and $c_{v,int}$ are the coefficients of specific heat defined by

$$c_{vi} = \left(\frac{\partial u_i}{\partial t}\right) = (3k_B/2m_i) + c_{v,int} \tag{3.11}$$

$$c_{vi,int} = \left(\frac{\partial u_{i,int}}{\partial t}\right) = \frac{k_B}{m_i}\left(\overline{\mathcal{E}_i^2} - \bar{\mathcal{E}}_i^2\right) = \frac{k_B}{m_i} \frac{\sum_I \left(\mathcal{E}_{Ii} - \bar{\mathcal{E}}_i\right) \exp\left(-\mathcal{E}_{Ii}\right)}{\sum_I \exp\left(-\mathcal{E}_{Ii}\right)} \tag{3.12}$$

The first order perturbation expansion for the Boltzmann equation is

$$f_{iI} \approx f_{iI}^{(0)} \left(1 + \phi_{iI}\right) \tag{3.13}$$

$$\sum_j \sum_{JKL} \iint f_{iI}^{(0)} f_{jJ}^{(0)} \left(\phi_{iI}\phi_{1jJ} - \phi'_{iK}\phi'_{1jL}\right) g \sigma_{IJ}^{KL}\left(g, \chi, \varepsilon\right) d^2\Omega d^3 c_j =$$

$$-f_{iI}^{(0)} \left\{ \left[\left(\mathcal{C}_i^2 - \tfrac{5}{2}\right) + \left(\mathcal{E}_{Ii} - \bar{\mathcal{E}}_i\right) \right] \boldsymbol{C}_i \cdot \boldsymbol{\nabla} \log T + 2\left(\boldsymbol{\mathcal{C}}_i \boldsymbol{\mathcal{C}}_i - \tfrac{1}{3}\mathcal{C}_i^2 \boldsymbol{I}\right) : \boldsymbol{\nabla} \boldsymbol{v} + \right. \tag{3.14}$$

$$\left. \left[\frac{2}{3} \frac{c_{vi,int}}{c_{vi}} \left(\mathcal{C}_i^2 - \frac{3}{2}\right) - \frac{k_B/m_i}{c_{vi}} \left(\mathcal{E}_{Ii} - \bar{\mathcal{E}}_i\right) \right] \boldsymbol{\nabla} \cdot \boldsymbol{v} + \frac{n}{n_i} \boldsymbol{C}_i \cdot \boldsymbol{d}_i \right\}$$

with

$$\phi_{iI} = -\frac{1}{n} \mathbf{A}_{iI} \cdot \boldsymbol{\nabla} \log T - \frac{1}{n} \boldsymbol{B}_{iI} : \boldsymbol{\nabla} \boldsymbol{v} - \frac{1}{n} \sum_j \boldsymbol{D}_{iI}^j \cdot \boldsymbol{d}_j^* - \frac{1}{n} \Gamma_{iI} \boldsymbol{\nabla} \cdot \boldsymbol{v} \tag{3.15}$$

where the vector functions $\mathbf{A}_{iI}$ and $\boldsymbol{D}_{iI}$, the tensor function $\boldsymbol{B}_{iI}$ and the scalar function Γ_{iI} are to be determined. As in the classical Chapman Enskog theory $\mathbf{A}_{iI}$ and $\boldsymbol{D}_{iI}^j$ must be proportional to $\boldsymbol{C}_i$ while $\boldsymbol{B}_{iI}$, which is symmetric and traceless, must be proportional to $\left(\boldsymbol{\mathcal{C}}_i \boldsymbol{\mathcal{C}}_i - \frac{1}{3}\mathcal{C}_i^2 \boldsymbol{I}\right)$. The functions expansion is this case is a double series (finite) of orthogonal polynomials:

$$
\begin{aligned}
\mathbf{A}_{iI} = A_{iI}\left(\mathcal{C}_i, \mathcal{E}_{iI}\right)\boldsymbol{\mathcal{C}}_i &= \sum_p \sum_q a_{i,pq} S^{(p)}_{\frac{3}{2}}\left(\mathcal{C}_i^2\right) P^{(q)}\left(\mathcal{E}_{iI}\right)\boldsymbol{\mathcal{C}}_i \\
\boldsymbol{B}_{iI} = \boldsymbol{B}_{iI}\left(\mathcal{C}_i, \mathcal{E}_{iI}\right)\left(\boldsymbol{\mathcal{C}}_i\boldsymbol{\mathcal{C}}_i - \tfrac{1}{3}\mathcal{C}^2\boldsymbol{I}\right) &= \sum_p \sum_q b_{iI,pq} S^{(p)}_{\frac{5}{2}}\left(\mathcal{C}_i^2\right)\left(\boldsymbol{\mathcal{C}}_i\boldsymbol{\mathcal{C}}_i - \frac{1}{3}\mathcal{C}_i^2\boldsymbol{I}\right) \\
\mathbf{D}^k_{iI} = D^k\left(\mathcal{C}_i, \mathcal{E}_{iI}\right)\boldsymbol{\mathcal{C}}_i &= \sum_p \sum_q d^k_{iI,pq} S^{(p)}_{\frac{3}{2}}\left(\mathcal{C}^2\right) P^{(q)}\left(\mathcal{E}_{iI}\right)\boldsymbol{\mathcal{C}}_i \\
\Gamma_{iI} = \Gamma_{iI}\left(\mathcal{C}_i, \mathcal{E}_{iI}\right) &= \sum_p \sum_q \gamma_{iI,pq} S^{(p)}_{\frac{1}{2}}\left(\mathcal{C}^2\right) P^{(q)}\left(\mathcal{E}_{iI}\right)
\end{aligned}
\tag{3.16}
$$

where $S_s^{(p)}\left(\mathcal{C}_i^2\right)$ is a Sonine polynomial and $P^{(q)}\left(\mathcal{E}_{iI}\right)$ is the qth order polynomial used by Wang Chang and Uhlenbeck and by Waldman an Trübenbacher, with the two first expressions:

$$
\begin{aligned}
P^{(0)} &= 1 \\
P^{(1)} &= \mathcal{E}_{Ii} - \bar{\mathcal{E}}_i
\end{aligned}
\tag{3.17}
$$

Application of the variational procedure for mixtures leads to sets of linear algebraic equations for the expansion coefficients $a_{i,pq}$, $b_{iI,pq}$, $d^k_{iI,pq}$ and $\gamma_{iI,pq}$. We will focus on the thermal diffusion coefficients and the thermal conductivity. In these transport coefficients the second order terms are relevant and the impact of polyatomic effects is important. This is because if the zero order is considered in the Chapman-Enskog expansion, the resultant homogeneous system leads to the trivial solution for $\left[D_{Ti}\right]_{(0)}$ and λ'. Hence, at least the first correction in the Chapman-Enskog expansion must be used.

3.2 Thermal diffusion coefficients

Identifying the terms in $\boldsymbol{\nabla}\log T$ of 3.14 with the compatibility equation:

$$
\begin{aligned}
\frac{1}{n}\sum_j \sum_{JKL} \iint f^{(0)}_{iI} f^{(0)}_{jJ}\left(A_{iI}A_{1jJ} - A'_{iK}A'_{1jL}\right) g\sigma^{KL}_{IJ}\left(g, \chi, \varepsilon\right) d^2\Omega d^3c_j = \\
f^{(0)}_{iI}\left[\left(\mathcal{C}_i^2 - \tfrac{5}{2}\right) + \left(\mathcal{E}_{Ii} - \bar{\mathcal{E}}_i\right)\right]\boldsymbol{C}_i \\
\sum_i \sqrt{m_i}\sum_I \int f^{(0)}_{iI} A_{iI}\left(\mathcal{C}_i, \mathcal{E}_{iI}\right)\mathcal{C}_i^2 d^3c = 0
\end{aligned}
\tag{3.18}
$$

After the minimization process with the help of the Lagrange multipliers method, the following system of equations is obtained:

$$
\begin{aligned}
\sum_{j=1}^{N}\sum_{mn}\Lambda^{rs,mn}_{ij} a^{(1)}_{j,mn} = \left(\delta_{r1} + \delta_{s1}\right)x_i; \qquad & i = 1, \ldots, N \\
& rs, mn = 00, 10, 01 \\
\sum_{j=1}^{N} y_j a^{(1)}_{00j} = 0 &
\end{aligned}
\tag{3.19}
$$

The first Chapman Enskog approximation of the multicomponent diffusion coefficient D_{Tk} may be written as (3.20).

$$[D_{Ti}]_{(1)} = -\frac{1}{2n} a_{i,00}^{(1)} \tag{3.20}$$

3.3 $\mathbf{\Lambda}$ coefficients

The coefficients $\Lambda_{ij}^{rs,mn}$ in Eq. (3.19) are given by mole fraction weighted sums of several microscopic properties of the chemical species in the mixture (see [8]), depending on the molecular sizes, masses, elastic collision integrals—defined in terms of the corresponding interaction potentials, specific molecular heat, inelastic collision parameters and resonant self diffusion parameters. As a consequence, these coefficients depend on mixture composition and temperature. These Λ coefficients can be written in terms of the well known *binary* diffusion coefficients ($\mathscr{D}_{ij}$)

$$\mathscr{D}_{ij} = \frac{3}{8n\sigma_{ij}^2 \Omega_{ij}^{(1,1)*}} \left(\frac{k_B T}{2\pi m_{ij}} \right)^{1/2} \tag{3.21}$$

by means of

$$\Lambda_{ij}^{rs,mn} = \frac{1}{5n} \sum_{\ell=1}^{N} \frac{x_i x_\ell}{\mathscr{D}_{i\ell}} F_{ij\ell}^{rs,mn}; \qquad rs, mn = 00, 10, 01 \tag{3.22}$$

where σ_{ij} is the differential collision cross-section of chemical species i and j, $m_{ij}^{-1} = m_i^{-1} + m_j^{-1}$ denotes the reduced mass. In the former expression Eq. (3.22) the dimensionless functions $F_{ij\ell}^{rs,mn}$ depend on temperature, but not on mixture composition. The expressions of functions $F_{ij\ell}$ are given by

$$F_{ij\ell}^{00,00} = \delta_{ij} - \delta_{j\ell} \tag{3.23}$$

$$F_{ij\ell}^{00,10} = \left(\frac{5}{2} - 3C_{i\ell}^* \right) \frac{m_{i\ell}}{m_j} \left(\delta_{ij} - \delta_{j\ell} \right) \tag{3.24}$$

$$F_{ij\ell}^{10,00} = \left(\frac{5}{2} - 3C_{i\ell}^* \right) \frac{m_{i\ell}}{m_i} \left(\delta_{ij} - \delta_{j\ell} \right) \tag{3.25}$$

$$\begin{aligned} F_{ij\ell}^{10,10} = & \left\{ 4A_{i\ell}^* \left(\delta_{ij} + \delta_{j\ell} \right) + \left[\left(\frac{25}{4} - 3B_{i\ell}^* \right) \frac{m_\ell}{m_j} + \frac{15}{2} \frac{m_j}{m_\ell} \right] \left(\delta_{ij} - \delta_{j\ell} \right) \right\} \frac{m_{i\ell}^2}{m_i m_\ell} \\ & + \frac{20}{3} \frac{m_{i\ell}^2}{m_i m_\ell} A_{i\ell}^* \left(\delta_{ij} + \delta_{j\ell} \right) \left(\frac{c_{i,\text{rot.}}}{\pi k_B \zeta_{i\ell}} + \frac{c_{\ell,\text{rot.}}}{\pi k_B \zeta_{\ell i}} \right) \end{aligned} \tag{3.26}$$

$$\frac{c_{j,\text{int.}}}{k_B} F_{ij\ell}^{10,01} = -\frac{10 m_j A_{i\ell}^*}{(m_i + m_\ell)} \left(\delta_{j\ell} + \delta_{ij} \right) \frac{c_{j,\text{rot.}}}{\pi k_B \zeta_{j\ell}} \tag{3.27}$$

$$\frac{c_{i,\text{int.}}}{k_B} F_{ij\ell}^{01,10} = -\frac{10 m_i A_{i\ell}^*}{(m_i + m_\ell)} \left(\delta_{j\ell} + \delta_{ij}\right) \frac{c_{i,\text{rot.}}}{\pi k_B \zeta_{i\ell}} \tag{3.28}$$

$$\left(\frac{c_{i,\text{int.}}}{k_B}\right)^2 F_{ij\ell}^{01,01} = \frac{25}{4} \left\{ \frac{c_{i,\text{int.}}}{k_B} \frac{\mathscr{D}_{i\ell}}{\mathscr{D}_{i\,\text{int.},\ell}} + \frac{12}{5} \frac{m_i A_{i\ell}^*}{m_\ell} \frac{c_{i,\text{rot.}}}{\pi k_B \zeta_{i\ell}} \right\} \delta_{ij} \tag{3.29}$$

The dimensionless functions A_{ij}^*, B_{ij}^*, C_{ij}^*, which appear in the former definitions, are given by the corresponding ratios of reduced collision integrals (see [1]: Eqs. (7.1-31)-(7.1-33)), with values tabulated by (e.g.) reference [6]. These tables account for polar molecules and the input parameters are reduced temperature T^* and the reduced dipole moment δ^*, given by

$$T_{ij}^* = \frac{k_B T}{\epsilon_{ij}} \tag{3.30}$$

$$\delta_{ij}^* = \frac{1}{2} \frac{\mu_i \mu_j}{\epsilon_{ij} \sigma_{ij}^3} \tag{3.31}$$

where ϵ is the Lennard Jones potential well depth ($\frac{\varepsilon}{k_B}$) and μ is the dipole moment. In the case that species i, j are either both polar or both non polar, the Lennard Jones potential well depth ϵ_{ij} and the differential collision cross-section σ_{ij} are given by

$$\epsilon_{ij} = \sqrt{\epsilon_i \epsilon_j} \tag{3.32}$$

$$\sigma_{ij} = \frac{1}{2} \left(\sigma_i + \sigma_j\right) \tag{3.33}$$

In the case of interaction between a polar p and a nonpolar n molecule the expressions are:

$$\mu_p^* = \frac{\mu_p}{\sqrt{\epsilon_p \sigma_p^3}} \tag{3.34}$$

$$\alpha_n^* = \frac{\alpha_n}{\sigma_n^3} \tag{3.35}$$

$$\xi = 1 + \frac{1}{4} \alpha_n^* \mu_p^* \sqrt{\frac{\epsilon_p}{\epsilon_n}} \tag{3.36}$$

$$\epsilon_{np} = \xi^2 \sqrt{\epsilon_p \epsilon_n} \tag{3.37}$$

$$\sigma_{np} = \frac{1}{2} \left(\sigma_n + \sigma_p\right) \xi^{-\frac{1}{6}} \tag{3.38}$$

where μ_p is the dipole moment of the polar molecule and α_n is the polarizability of the nonpolar molecule.

The internal component of the molecular heat capacities are defined based on the values of c_{pi} according to

$$\begin{aligned} c_{i,\text{int.}} &= 0; \qquad \text{for monoatomic species} \\ c_{i,\text{int.}} &= c_{pi} - \tfrac{5}{2}k_B \qquad \text{for non monoatomic species} \end{aligned} \tag{3.39}$$

The molecular specific heat at constant pressure c_{pi} is part of the thermodynamic properties required to perform transport calculations and should be available for the species present in the system.

The values to account for the transference of rotational energy into translational energy on colliding are $c_{i,\text{rot.}}$ and ζ_{ii}. These magnitudes and the expressions derived from experiments are studied in detail in reference [7]. The values of $c_{i,\text{rot.}}$ may be expressed as:

$$\begin{aligned} c_{i,\text{rot.}} &= k_B; \qquad \text{for linear molecules} \\ c_{i,\text{rot.}} &= \tfrac{3}{2}k_B; \qquad \text{for nonlinear molecules} \end{aligned} \tag{3.40}$$

where molecular linearity is assumed to be known a-priori, and has to be taken into account during the transport properties calculation. The expressions for the relaxation collision numbers are:

$$\zeta_{ij} = \zeta_{ii} = \zeta_{ii}\,(298)\,\frac{Z_{irot}\,(298)}{Z_{irot}\,(T)} \tag{3.41}$$

where

$$\frac{Z_{irot}\,(T)}{Z_{irot}^{\infty}} = 1 + \frac{\pi^{\frac{3}{2}}}{2}\left(\frac{\epsilon_i}{T}\right)^{\frac{1}{2}} + \left(\frac{\pi^2}{4} + 2\right)\left(\frac{\epsilon_i}{T}\right) + \pi^{\frac{3}{2}}\left(\frac{\epsilon_i}{T}\right)^{\frac{3}{2}} \tag{3.42}$$

where the values $\zeta_{ii}\,(298)$ are assumed to be known as part of the species database (guidelines for these magnitudes evaluation are shown in [7]). The expression (3.42), which is an extension of the expression Eq. (45) in [33], may be found in reference [34].

The remaining binary diffusion coefficients for the resonant exchange of internal energy are given by the expressions Eq. (3.43):

$$\begin{aligned} \mathscr{D}_{i\,\text{int.},j} &\sim \mathscr{D}_{ij}; \qquad i \neq j \\ \mathscr{D}_{i\,\text{int.},i} &\sim \mathscr{D}_{ii}; \qquad \text{for non-polar gases} \\ \mathscr{D}_{i\,\text{int.},i} &= \frac{\mathscr{D}_{ii}}{(1+\delta')}; \qquad \text{for polar gases} \end{aligned} \tag{3.43}$$

Reference [7] provides details on the evaluation of parameter δ', where distinction is made of the different types of polar molecules: *linear* dipoles and *symmetric top* dipoles. Neverthe-

less, a more simplified expression (3.44) is used in this work, taken from [35] and [36].

$$\delta^{'} = \frac{2985}{\sqrt{T^3}} \tag{3.44}$$

where T is the temperature in K.

3.4 Heat equation. Thermal conductivity

The average flow of energy is described by heat flow vector $\boldsymbol{q}$, which is made of the translational energy $\boldsymbol{q}_{tr}$ and the internal energy flux $\boldsymbol{q}_{int}$.

$$\boldsymbol{q} = \boldsymbol{q}_{tr} + \boldsymbol{q}_{int} \tag{3.45}$$

$$\boldsymbol{q}_{tr} = \sum_i \sum_I \int \frac{1}{2} m_i C_i^2 \boldsymbol{C}_i f_{iI} d^3c \tag{3.46}$$

$$\boldsymbol{q}_{int} = \sum_i \sum_I \int E_{iI} \boldsymbol{C}_i f_{iI} d^3c \tag{3.47}$$

Using the relation (3.15) by substitution and taking into account that integrands with odd functions of the components of $\boldsymbol{C}$ vanish and that only the perturbation part of f_{iI} contributes to the integral the heat flow becomes:

$$\boldsymbol{q}_{tr} = -\frac{1}{3} k_B \left[\boldsymbol{A}, \boldsymbol{A}\right] \nabla T - p \sum_{i=1}^{N} D_{Ti} \boldsymbol{d}_i + \frac{5}{2} k_B T \sum_{i=1}^{N} n_i \boldsymbol{V}_i \tag{3.48}$$

$$\boldsymbol{q}_{int} = k_B T \sum_{i=1}^{N} \bar{\mathcal{E}}_i \mathbf{V}_i \tag{3.49}$$

where $\bar{\mathcal{E}}_i = \dfrac{\bar{E}_i}{k_B T}$ is given by (3.10) and $\lambda' = \dfrac{1}{3} k_B \left[\boldsymbol{A}, \boldsymbol{A}\right]$ is the partial coefficient of thermal conductivity. The relation between the partial thermal conductivity and the thermal conductivity is given by (2.185) where the parameter λ' is obtained in terms of the coefficients $a_{10i}^{(1)}$ and $a_{01i}^{(1)}$.

$$\lambda' = \frac{5}{4} k_B \sum_{i=1}^{N} x_i \left(a_{10i}^{(1)} + a_{01i}^{(1)} \right) \tag{3.50}$$

Chapter 4

Collision Integrals evaluation

In this chapter, some topics related to integral collisions will be addressed. As previously described, they are an important issue in the transport properties evaluation. The integral collisions appear during the solution of the dynamic collision between articles. Collision integrals are necessary to generate the linear systems of equations to derive the transport coefficients.

4.1 Collision integrals mathematical description

An interaction potential for the mathematical description of the forces exerted between molecules is a key ingredient for the description of molecular collisions in the KTG. A very widely used potential for polar gases, which will be used in this work, and the selected for this work is the Stockmayer potential $(12, 6, 3)$,

$$\varphi(r) = 4\epsilon_{ij}\left[\left(\frac{\sigma_{ij}}{r}\right)^{12} - \left(\frac{\sigma_{ij}}{r}\right)^{6} + \delta_{ij}\left(\frac{\sigma_{ij}}{r}\right)^{3}\right] \tag{4.1}$$

where ϵ_{ij} is the Lennard-Jones potential well depth and σ_{ij} is the collision diameter. The Stockmayer potential combines the well known Lennard-Jones (AKA $12-6$) potential with a dipole-dipole interaction potential. The parameter δ_{ij} accounts the gases polarity

$$\delta_{ij} = \frac{1}{4}\mu_{ij}^{*}\zeta(\theta_i, \theta_i, \phi) \tag{4.2}$$

where the definition of ζ is

$$\zeta = 2\cos\theta_i\cos\theta_j - \sin\theta_i\sin\theta_j\cos\phi. \tag{4.3}$$

The parameters μ_i and μ_j are the dipole moments of the two interacting molecules with $\mu_{ij}^{*} = \mu_{ij}/(\epsilon_{ij}\sigma_{ij})^{\frac{1}{2}}$. The angles θ_i and θ_j are the angles of inclination of axes of the two

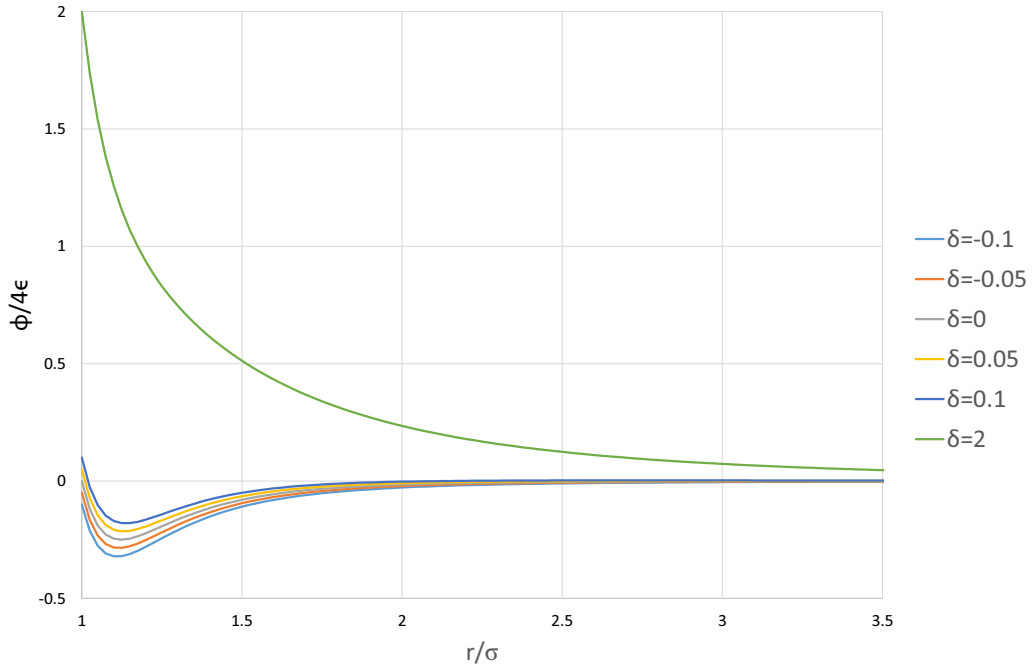

Figure 4.1: Scaled Stockmayer potential (12,6,3) $\phi/4\epsilon$ vs. the nondimensional distance r/σ for several values of the parameter δ that accounts for the dipole-dipole interaction.

dipoles to the line joining the centers of the molecules, and ϕ is the azimuthal angle between them.

The idea of Monchick and Mason [6], was to average the collision integrals for all the possible fixed relative orientation. The probability of each orientation is assumed equally probable and the collision integrals are

$$\left|\Omega^{(\ell,s)*}\right|_{\theta_1,\theta_2,\phi} = [(s+1)!]^{-1} \int_0^\infty \exp\left(-\tilde{g}^2\right) \left(\tilde{g}^2\right)^{s+1} Q^{(\ell)*} d\left(\tilde{g}^2\right) \tag{4.4}$$

where

$$Q^{(\ell)*} = \frac{2}{\sigma^2} \left[1 - \frac{1}{2}\frac{1+(-1)^\ell}{1+\ell}\right]^{-1} \int_0^\infty \left(1 - \cos^\ell \chi\right) b db, \tag{4.5}$$

$$\chi = \pi - 2b \int_{r_c}^\infty \left\{1 - \left(b^2/r^2\right) - \left[\varphi(r)/\frac{1}{4}mg^2\right]\right\}^{-\frac{1}{2}} \left(dr/r^2\right). \tag{4.6}$$

The parameter r_c is the distance of the closest approach and it depends on δ_{ij} and T^*. These integrals have to be computed numerically. Figure 4.2 is an example of intermediate results ($\delta = 0, \quad \ell = 1$), to show the mathematical complexity and why analytical resolution is not possible. The integrals and the intermediate results are calculated with nondimensional

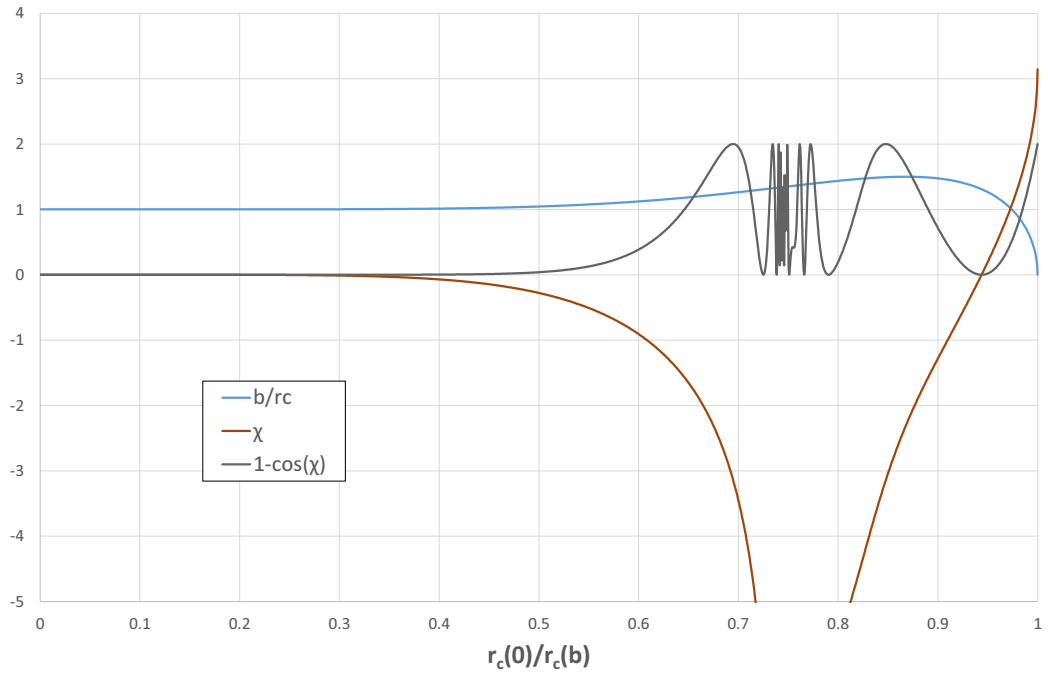

Figure 4.2: Intermediate results to calculate the collision integrals, ($\delta_{ij} = 0, \quad \ell = 1$). In blue, the nondimensional distance between two colliding particles. In brown, the χ integral resultant in the collision dynamic. In gray, the function $1 - \cos\chi$, necessary to obtain the parameter $Q^{(1)*}$.

parameters as the x axis $r_c\left(0\right)/r_c\left(b\right)$. Five points Gaussian integration formula for χ has been used. Further integration has to be done within the intervals where orbiting collision is possible.

For each pair of indexes (ℓ, s), each dipole configuration δ_{ij}, reduced temperature T^* and each dipole geometric position, the parameters $Q^{(\ell)*}$ (4.5) and $\left|\Omega^{(\ell,s)*}\right|_{\theta_1,\theta_2,\phi}$ (4.4) integral are obtained by numerical integration. The averaged value of the integral collision is obtained integrating the angle ϕ between 0 and 2π and $\cos\theta_1$, $\cos\theta_2$ between -1 and 1. The result must be divided between $2 \cdot 2 \cdot 2\pi$.

$$\Omega^{(\ell,s)*} = \frac{1}{8\pi} \int_{-1}^{1} \int_{-1}^{1} \int_{0}^{2\pi} \left|\Omega^{(\ell,s)*}\right|_{\theta_1,\theta_2,\phi} d\phi d\left(cos\theta_i\right) d\left(cos\theta_j\right) \tag{4.7}$$

With (4.7) the following expressions may be calculated

$$\begin{gathered}\Omega_{ij}^{(1,1)*}, \Omega_{ij}^{(2,2)*}, \Omega_{ij}^{(1,2)*}, \Omega_{ij}^{(1,3)*} \\ A_{ij}^{*} = \Omega_{ij}^{(2,2)*} / \Omega_{ij}^{(1,1)*} \\ B_{ij}^{*} = \left[5\Omega_{ij}^{(1,2)*} - 4\Omega_{ij}^{(1,3)*}\right] / \Omega_{ij}^{(1,1)*} \\ C_{ij}^{*} = \Omega_{ij}^{(1,2)*} / \Omega_{ij}^{(1,1)*}\end{gathered} \quad . \tag{4.8}$$

The above indexes and ratios appear in relations (3.23) to (3.29).

4.2 Monchick and Mason tables validity discussion

The collision integrals $\Omega_{ij}^{(1,1)*}$ and $\Omega_{ij}^{(2,2)*}$, and the ratios A^*, B^*, C^* were tabulated in [6] for monatomic and polar gases. The collision integrals and ratios, used in this work and coded in the software package MuTLib, are a direct electronic translation from the tables published in [6]. For a more compact form of the the tables, the reduced parameters δ^* and T^*, defined in 3.30 and 3.31 respectively, are used as input variables. Future MuTLib versions may use more accurate correlations which could be selected by the user from a collision integrals library.

The tables [6] were tested successfully against experiments in the normal range of combustion temperatures for pure diatomic gases, with less of 5% error in the range 300-3000K, [37]. However, further refinements in monatomic gases (specially noble gases) and extreme temperatures have been published [38]. There are also special modifications in the case of ionized gases, used in the astronomy field, for the study of planetary ionospheres, the solar corona and the solar interior [39], [40].

The package Chemkin uses additional modifications to the original tables as showed in Fig. 4.3. The polynomial approximations for A^*, B^* and C^* are taken from the software source code. However, a reference explaining the basis for the aforementioned polynomic modifications is lacking in the Chemkin software package, in fact, some other authors reference the software package itself when necessary.

In the package EGLib, $\Omega^{(1,1)*}$ values are imported from Chemkin calculations and the ratios A^*, B^* and C^* from Fig. 4.3 are recalculated using the polynomic approximations.

4.3 Tabulated values and polynomial approximations

In this sections the tables from [6] have been plotted in logarithmic scale for a better visualization. The polynomial approximations used in Chemkin package are also plotted for comparison.

In Fig 4.4 the values $\Omega^{(1,1)*}$ are represented together the Chemkin correlation for high reduced temperatures. Original values and the correlation are quite similar.

In Fig. 4.5 the ratio A^* is plotted for tabulated data and the Chemkin polynomial curve. The Chemkin curve fits reasonably in the interval $0.5 < T^* < 5$. Out of this interval the

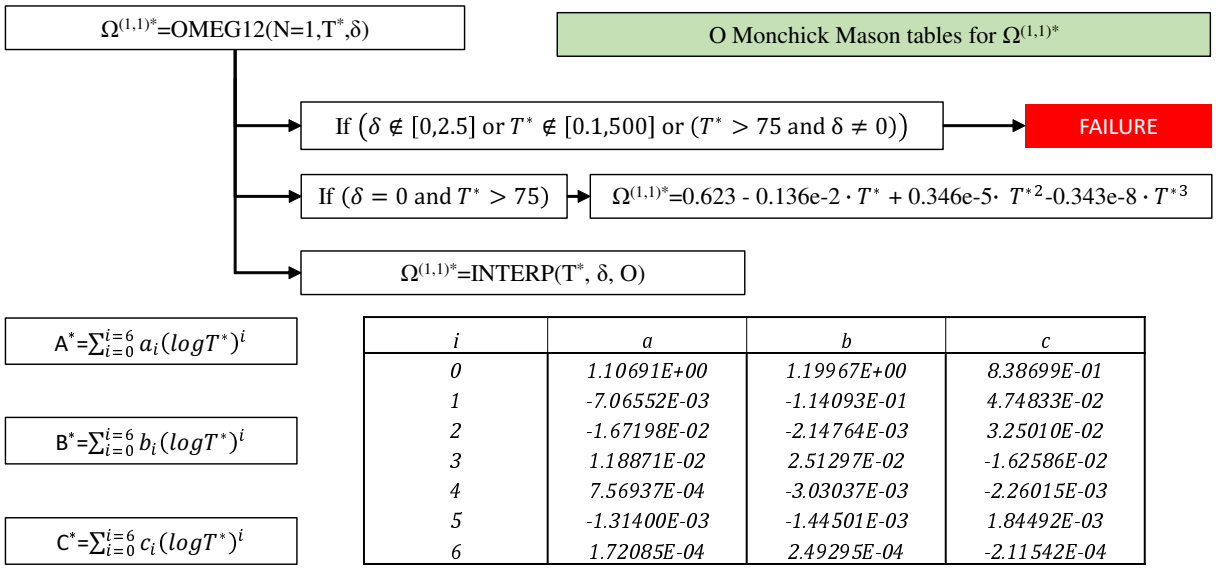

i	*a*	*b*	*c*
0	*1.10691E+00*	*1.19967E+00*	*8.38699E-01*
1	*-7.06552E-03*	*-1.14093E-01*	*4.74833E-02*
2	*-1.67198E-02*	*-2.14764E-03*	*3.25010E-02*
3	*1.18871E-02*	*2.51297E-02*	*-1.62586E-02*
4	*7.56937E-04*	*-3.03037E-03*	*-2.26015E-03*
5	*-1.31400E-03*	*-1.44501E-03*	*1.84492E-03*
6	*1.72085E-04*	*2.49295E-04*	*-2.11542E-04*

Figure 4.3: Chemkin scheme for the collision integrals calculation

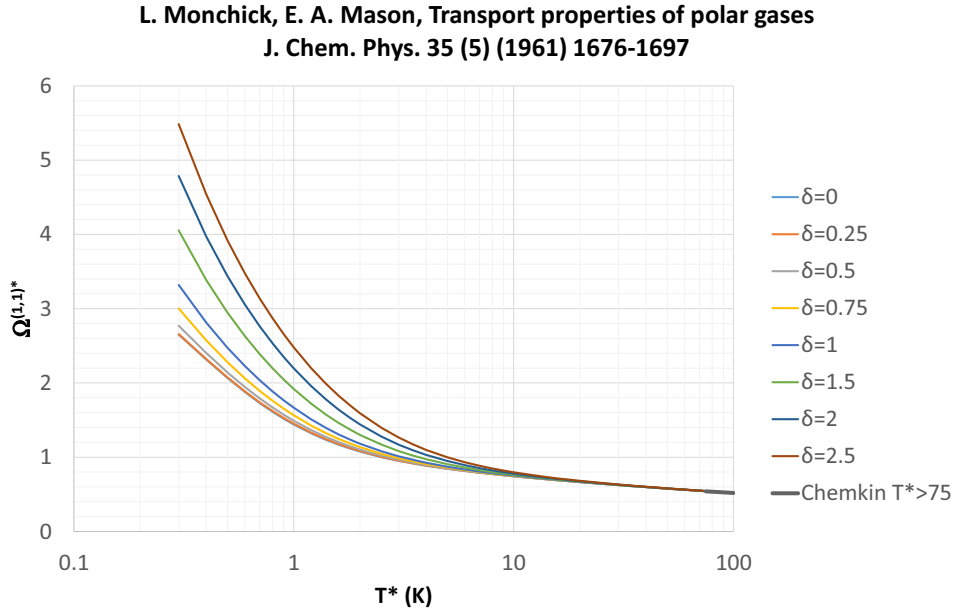

Figure 4.4: Reduced integral $\Omega^{(1,1)*}$. Plot of the Monchick and Mason tables.

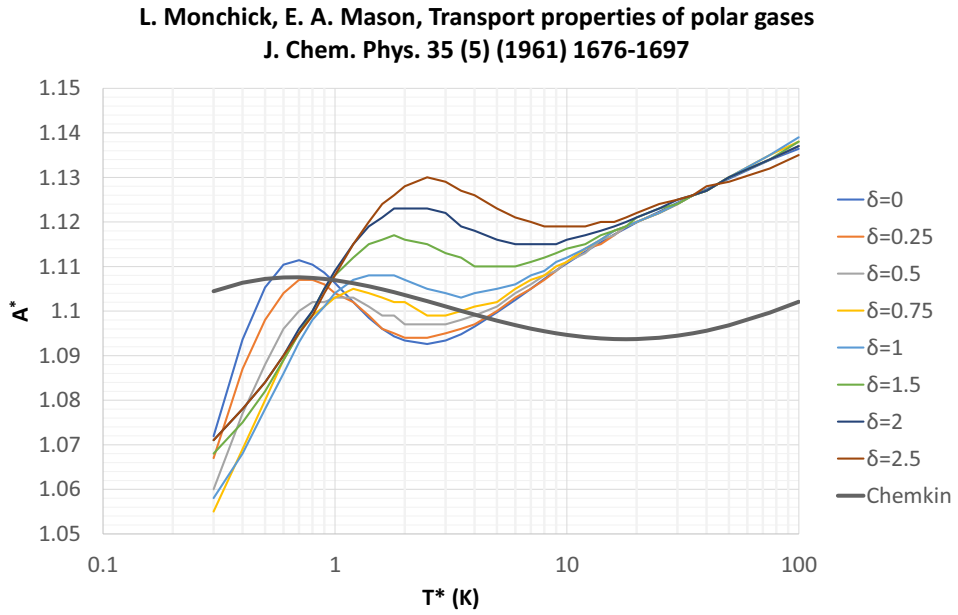

Figure 4.5: Reduced ratio A^*. Plot of the Monchick and Mason tables.

Monchick and Mason tables and the polynomial curve differ. For low values of T^*, the polynomial approximation is around a 4% over the tables values. For values $T^* > 10$ the polynomial approximation is around a 4% lower than the values in the tables.

In Figs. 4.6 and 4.7 the ratios B^* and C^* are plotted. The polynomial used in Chemkin lies in the middle of the Monchick and Mason tables for the most reduced temperatures in the range $1 < T^* < 10$. Out of this temperatures range differences up to 2% may be found.

To summarize, the Monchick and Mason approximation is adequate for the most common problems of combustion science and it is implemented in MuTLib.

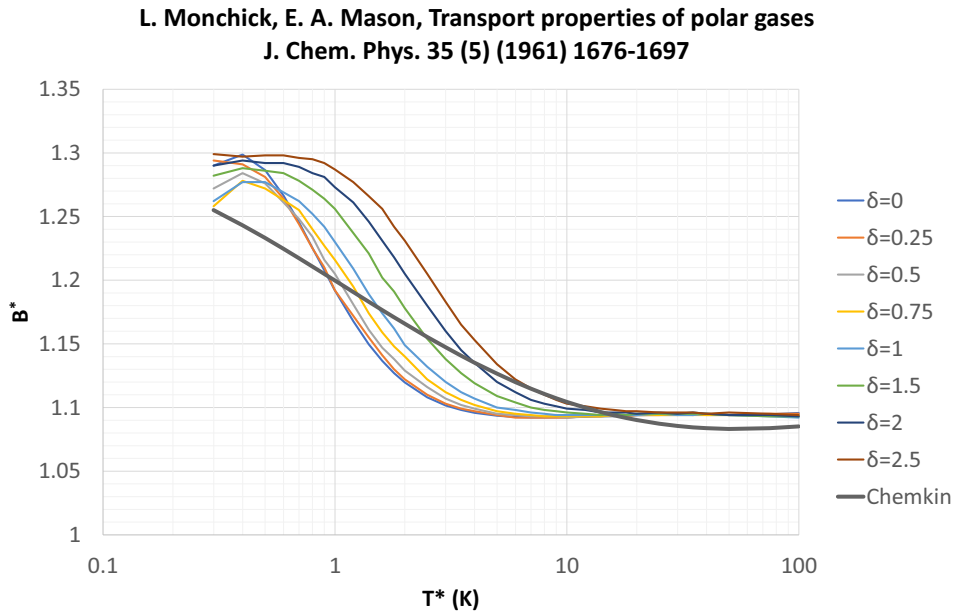

Figure 4.6: Reduced ratio B^*. Plot of the Monchick and Mason tables.

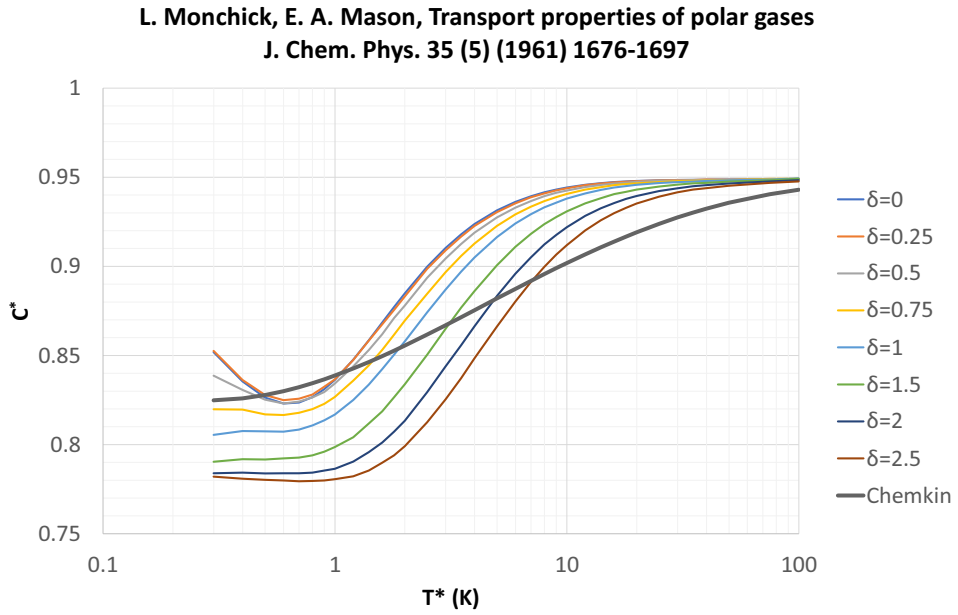

Figure 4.7: Reduced ratio C^*. Plot of the Monchick and Mason tables.

Chapter 5

Description of the multicomponent transport algorithm

This chapter describes the mathematical approach followed to calculate the transport coefficients from the kinetic theory of gases, Fick diffusion coefficients, thermal diffusion coefficients and thermal conductivity[41]. The strategy is an iterative algorithm that takes advantage of the use of the correct physical scales and the blockwise inversion.

5.1 Blockwise inversion strategy

The system of equations (3.19) may be written in a matrix form as:

$$\begin{bmatrix} \Lambda^{00,00} & \Lambda^{00,10} & 0 \\ \Lambda^{10,00} & \Lambda^{10,10} & \Lambda^{10,01} \\ 0 & \Lambda^{01,10} & \Lambda^{01,01} \end{bmatrix} \begin{Bmatrix} \mathbf{a}_{00}^{(1)} \\ \mathbf{a}_{10}^{(1)} \\ \mathbf{a}_{01}^{(1)} \end{Bmatrix} = \begin{Bmatrix} 0 \\ \mathbf{x} \\ \mathbf{x} \end{Bmatrix} \tag{5.1}$$

$$\sum_{j=1}^{N} y_j a_{00j}^{(1)} = 0 \tag{5.2}$$

The main idea behind the present algorithm for the calculation of the thermal diffusion coefficients has two parts. On one hand inspection of Eq. (5.1) shows that the coefficient matrix in the first block in this linear system (i.e., $\Lambda^{00,00}$ supplemented by Eq. (5.2)) is the same matrix that has to be inverted for the calculation of the Fick diffusion coefficients D_{ij}. Thus, the first part of the present algorithm is to solve Eqs. (5.2, 5.1) using the blockwise

matrix inversion formula

$$\left(\begin{array}{c|c} \mathbf{A} & \mathbf{B} \\ \hline \mathbf{C} & \mathbf{D} \end{array}\right)^{-1} = \left(\begin{array}{c|c} \mathbf{A}^{-1} + \mathbf{A}^{-1}\mathbf{B}(\mathbf{D} - \mathbf{C}\mathbf{A}^{-1}\mathbf{B})^{-1}\mathbf{C}\mathbf{A}^{-1} & -\mathbf{A}^{-1}\mathbf{B}(\mathbf{D} - \mathbf{C}\mathbf{A}^{-1}\mathbf{B})^{-1} \\ \hline -(\mathbf{D} - \mathbf{C}\mathbf{A}^{-1}\mathbf{B})^{-1}\mathbf{C}\mathbf{A}^{-1} & (\mathbf{D} - \mathbf{C}\mathbf{A}^{-1}\mathbf{B})^{-1} \end{array}\right) \tag{5.3}$$

which holds for any square matrix with entries $\mathbf{A}$, $\mathbf{B}$, $\mathbf{C}$, $\mathbf{D}$, as long as sub-matrices $\mathbf{A}$ and $\mathbf{D} - \mathbf{C}\mathbf{A}^{-1}\mathbf{B}$ are non-singular. In the present case, according to Eq. (5.1), the sub-matrices $\mathbf{A}$, $\mathbf{B}$, $\mathbf{C}$, $\mathbf{D}$ are defined by

$$\mathbf{A} = \Lambda^{00,00} \tag{5.4}$$

$$\mathbf{B} = \left[\begin{array}{cc} \Lambda^{00,10} & 0 \end{array}\right] \tag{5.5}$$

$$\mathbf{C} = \left[\begin{array}{c} \Lambda^{10,00} \\ 0 \end{array}\right] \tag{5.6}$$

$$\mathbf{D} = \left[\begin{array}{cc} \Lambda^{10,10} & \Lambda^{10,01} \\ \Lambda^{01,10} & \Lambda^{01,01} \end{array}\right]. \tag{5.7}$$

In the application of this strategy to the linear system under consideration the inverse of the first block ($\Lambda^{00,00}$ supplemented by Eq. (5.2), $\mathbf{A}$ in Eq. (5.3)) is already available from the calculation of D_{ij}.

The second part of the algorithm makes use of the observation that the second block that needs to be inverted to solve Eq. (5.1), i.e., $\mathbf{D} - \mathbf{C}\mathbf{A}^{-1}\mathbf{B}$ in Eq. (5.3), is diagonally dominant. Hence, by scaling this part of the system (blocks $\Lambda^{10,00}$, $\Lambda^{10,10}$, $\Lambda^{10,01}$, $\Lambda^{01,10}$and $\Lambda^{01,01}$) with the corresponding diagonal terms, the block $\mathbf{D} - \mathbf{C}\mathbf{A}^{-1}\mathbf{B}$ is written as $\mathbb{1} + A_T$ (see Eq. (5.20) below) and its inverse can be efficiently computed by means of the Neumann series [42] (i.e., the matrix version of the geometric series).

$$(\mathbb{1} + A_T)^{-1}_{ij} = \left(\sum_{r=0}^{\infty} (-A_T)^r\right)_{ij} \tag{5.8}$$

where we define matrix A_T, Eq. (5.20), by analogy with matrix A in Model 1 of [28]. This way the present algorithm makes full use of the information available from the calculation of the Fick diffusion coefficients D_{ij}, which is assumed to have been performed prior to the calculation of the thermal diffusion coefficients. On the other hand, the solution for D_{Ti} is written in terms of a Neumann series, in a similar way as it is done in Model 1 of [28]. The implementation of this general strategy is shown in full detail below.

5.2 Non-dimensionalization and scaling

The system of equations (5.1) may be scaled according to the following expressions:

$$\begin{aligned} F_{ij}^{rs,mn} &= \lambda_i^{rs}\mu_j^{mn}\frac{25k_Bn}{4}\Lambda_{ij}^{rs,mn} \\ \tilde{a}_{mnj} &= \frac{1}{2n}\frac{a_{mnj}^{(1)}}{\mu_j^{mn}} \qquad ; \qquad i,j=1,\ldots,N \\ \tilde{x}_{rsi} &= \frac{5}{2}\lambda_i^{rs} \end{aligned} \tag{5.9}$$

with:

$$\lambda_i^{00}=1 \qquad \lambda_i^{10}=\frac{x_i}{\dfrac{25k_Bn}{4}\Lambda_{ii}^{10,10}\mathscr{D}_{ii}} \qquad \lambda_i^{10}=\frac{x_i\left(\dfrac{c_{i,\text{int.}}}{k_B}\right)}{\dfrac{25k_Bn}{4}\Lambda_{ii}^{01,01}\left(\dfrac{c_{i,\text{int.}}}{k_B}\right)^2\mathscr{D}_{ii}} \qquad i=1,\ldots,N; \tag{5.10}$$

$$\mu_j^{00}=\frac{\mathscr{D}_{jN}}{x_j} \qquad \mu_j^{10}=\frac{\mathscr{D}_{jj}}{x_j} \qquad \mu_j^{10}=\frac{\mathscr{D}_{jj}\left(\dfrac{c_{j,\text{int.}}}{k_B}\right)}{x_j} \qquad j=1,\ldots,N; \tag{5.11}$$

where $c_{i,int}$ is the internal component of the molecular heat capacities for the species i. The reference species N has been selected as the species with highest mole fraction, in the same way as it is done in Model 1 and Model 1+M of [28]. This way we are able to make use of the results available from the calculation of D_{ij}. On the other hand, based on the observation that the second block in Eq. (5.1) is diagonally dominant, instead of using the reference species N to define the dimensionless variables, the reference scales in this part of the system are given by the corresponding diagonal terms. Note that factor $\dfrac{1}{x_j}$ is just a way to write the equations in a compact way. From the computational point of view, there is no division by magnitudes close to zero for vanishing mole fractions. Taking into account the nature of expressions F_{ijl} the resultant expressions related to the mole fractions are $\dfrac{x_ix_\ell}{x_j}\delta_{ij}$ and $\dfrac{x_ix_\ell}{x_j}\delta_{jl}$. In the first case $\dfrac{x_ix_\ell}{x_j}\delta_{ij}=x_l$ if $i=j$ and zero otherwise. As well, $\dfrac{x_ix_\ell}{x_j}\delta_{jl}=x_i$ if $j=l$ and zero otherwise. Note that for convenience the expressions $\dfrac{25k_Bn}{4}\Lambda_{ii}^{10,10}=\displaystyle\sum_{\ell=1}^{N}\frac{x_ix_\ell}{\mathscr{D}_{i\ell}}F_{ij\ell}^{10,10}$ and $\dfrac{25k_Bn}{4}\Lambda_{ii}^{01,01}\left(\dfrac{c_{i,\text{int.}}}{k_B}\right)^2=\displaystyle\sum_{\ell=1}^{N}\frac{x_ix_\ell}{\mathscr{D}_{i\ell}}\left(\frac{c_{i,\text{int.}}}{k_B}\right)^2F_{ij\ell}^{01,01}$ have been used.

Inserting the former definitions in Eq. (5.1), the KTG linear system is written in dimen-

sionless form as

$$\begin{bmatrix} F^{00,00} & F^{00,10} & 0 \\ F^{10,00} & F^{10,10} & F^{10,01} \\ 0 & F^{01,10} & \mathbb{1} \end{bmatrix} \begin{Bmatrix} \tilde{\mathbf{a}}_{00} \\ \tilde{\mathbf{a}}_{10} \\ \tilde{\mathbf{a}}_{01} \end{Bmatrix} = \begin{Bmatrix} \mathbf{0} \\ \tilde{\mathbf{x}}_{10} \\ \tilde{\mathbf{x}}_{01} \end{Bmatrix} \tag{5.12}$$

where the resultant last $2 \times N$ equations have been scaled with the diagonal terms to improve the convergence rate of the Neumann series used in the inversion of this part of the system. Note that for monatomic species $c_{i,\text{int.}} = 0$ and the correspondent equation $\sum_{j=1}^{N-1} F_{ij}^{01,10} \tilde{a}_{10j} + \tilde{a}_{01i} = \tilde{x}_{01i}$ only makes sense if $\tilde{a}_{01i} = 0$. In this case there are two options: direct elimination of the former equations from system (5.12) or make them compatible with (5.13) by means of

$$\begin{aligned} F_{ij}^{10,01} &= 0 \\ F_{ij}^{01,01} &= \delta_{ij} \text{ for monatomic species} \\ \tilde{x}_{01i} &= 0 \end{aligned} \tag{5.13}$$

Before using the blockwise inversion formula Eq. (5.3), the N^{th} equation in the linear system Eq. (5.12) (i.e., the last equation in the first block, which can be expressed as a linear combination of the $N-1$ previous equations) is substituted by the overall mass conservation condition Eq. (5.2), which is used to calculate the last entry of vector $\tilde{\mathbf{a}}_0$. Thus we find

$$\tilde{a}_{00N} = -\sum_{j=1}^{N-1} \frac{m_j}{m_N} \frac{\mathscr{D}_{jN}}{\mathscr{D}_{NN}} \tilde{a}_{00j} \tag{5.14}$$

and we define vector $\tilde{\mathbf{a}}_{00}^{-}$ as the vector containing the remaining values $\tilde{a}_{00j}$:

$$\tilde{a}_{00i}^{-} = \tilde{a}_{00i}; \qquad i = 1, \ldots, N-1 \tag{5.15}$$

Inserting this last result in Eq. (5.12), the KTG linear system for the thermal diffusion coefficients is finally written as Eq. (5.16)

$$\begin{bmatrix} \mathbb{1} + A & F^{00,10} & 0 \\ \hat{F}^{10,00} & F^{10,10} & F^{10,01} \\ 0 & F^{01,10} & \mathbb{1} \end{bmatrix} \begin{Bmatrix} \tilde{\mathbf{a}}_{00}^{-} \\ \tilde{\mathbf{a}}_{10} \\ \tilde{\mathbf{a}}_{01} \end{Bmatrix} = \begin{Bmatrix} \mathbf{0}^{-} \\ \tilde{\mathbf{x}}_{10} \\ \tilde{\mathbf{x}}_{01} \end{Bmatrix} \tag{5.16}$$

where

$$A_{ij} = F_{ij}^{00,00} - \frac{m_j}{m_N} \frac{\mathscr{D}_{jN}}{\mathscr{D}_{NN}} F_{iN}^{00,00} - \delta_{ij}; \qquad i,j = 1, \ldots, N-1 \tag{5.17}$$

$$\hat{F}_{ij}^{10,00} = F_{ij}^{10,00} - \frac{m_j}{m_N} \frac{\mathscr{D}_{jN}}{\mathscr{D}_{NN}} F_{iN}^{10,00}; \qquad i = 1, \ldots, N; \qquad j = 1, \ldots, N-1 \tag{5.18}$$

Eq. (5.16) is the final expression for the KTG linear system for D_{Ti} and λ'. The solution

of this system can be computed by means of the blockwise inversion formula Eq. (5.3). In this regard, the first sub-matrix that needs to be inverted is $\mathbb{1} + A$, where, as can be easily checked, A_{ij} (defined in Eq. (5.17)) is the same matrix A_{ij} given by Eq. (21) of [28]. Thus, the inverse of this block is already known from the calculation of the Fick diffusion coefficients (see Eq. (20) of [28]), since we are assuming that the calculation of D_{ij} has been completed prior to the calculation of D_{Ti} and λ'.

5.3 Final solution

According to the scaling used to derive Eq. (5.16), the new block matrix to be inverted using the blockwise matrix inversion formula (5.3) can be written as:

$$\left[D - CA^{-1}B\right]^{-1} = \begin{bmatrix} (\mathbb{1} + A_T)^{-1} & -(\mathbb{1} + A_T)\, F^{10,01} \\ -F^{01,10}\,(\mathbb{1} + A_T)^{-1} & \mathbb{1} + F^{01,10}\,(\mathbb{1} + A_T)^{-1}\, F^{10,01} \end{bmatrix} \tag{5.19}$$

where, by analogy with matrix A in Model 1 of [28], we define matrix A_T by means of

$$\mathbb{1} + A_T = F^{10,10} - \hat{F}^{10,00}\,(\mathbb{1} + A)^{-1}\, F^{00,10} - F^{10,01} F^{01,10} \tag{5.20}$$

Since this matrix is close to the identity it is reasonable to expect that the Neumann series inversion formula (Eq. (5.8)) can be used to define an approximate iterative algorithm with fast convergence rate. With this idea in mind, the thermal diffusion coefficients are given by means of

$$\left\{ \ \tilde{\mathbf{a}}^{-}_{00} \ \right\} = (\mathbb{1} + A)^{-1}\, F^{00,10}\,(\mathbb{1} + A_T)^{-1} \left(F^{10,01}\tilde{\mathbf{x}}_{01} - \tilde{\mathbf{x}}_{10}\right) \tag{5.21}$$

where $(\mathbb{1} + A)^{-1}$ is known from the calculation of the Fick diffusion coefficients and where $(\mathbb{1} + A_T)^{-1}$ can be computed in an iterative fashion using the Neumann series Eq. (5.8). For instance, to leading order (i.e., for $r = 0$) $(\mathbb{1} + A_T)^{-1} = \mathbb{1}$, whereas the first term ($r = 1$) would give $(\mathbb{1} + A_T)^{-1} = \mathbb{1} - A_T$. Note that the first iteration does not involve matrix multiplications.

Finally, the thermal diffusion coefficients can be easily calculated from the former result recalling Eqs. (3.20, 3.50, 5.11, 5.14). On the other hand, the thermal diffusion fluxes can be directly computed by means of

$$\mathbf{j}_{Ti} = -\rho \frac{m_i}{m} \mathscr{D}_{iN} \tilde{a}_{00i} \nabla \ln T \tag{5.22}$$

The coefficients $a^{(1)}_{10i}$ and $a^{(1)}_{01i}$ may be derived from the scaled parameters $\tilde{a}_{10i}$ and $\tilde{a}_{01i}$ that may be computed using the expressions:

$\mathbf{v}_1 = F^{10,01}\tilde{\mathbf{x}}_{01}$
$\mathbf{w} = \tilde{\mathbf{x}}_{10} - \mathbf{v}_1$
$\tilde{\mathbf{a}}_{10} = \mathbf{w}$

loop for the number of iterations
$\mathbf{v}_1 = F^{01,10}\mathbf{w}$
$\mathbf{v}_2 = F^{10,01}\mathbf{v}_1$
$\mathbf{v}_3 = F^{00,10}\mathbf{w}$
$\mathbf{v}_4 = (\mathbb{1} + A)^{-1}\,\mathbf{v}_3$
$\mathbf{v}_1 = \hat{F}^{10,00}\mathbf{v}_4$
$\mathbf{v}_5 = F^{10,10}\mathbf{w}$
$\mathbf{w} = \mathbf{v}_1 + \mathbf{v}_2 - \mathbf{v}_5 + \mathbf{w}$
$\tilde{\mathbf{a}}_{10} = \tilde{\mathbf{a}}_{10} + \mathbf{w}$
end of the loop

$\tilde{\mathbf{a}}_{01} = F^{01,10}\tilde{\mathbf{a}}_{10}$
$\tilde{\mathbf{a}}_{01} = \tilde{\mathbf{x}}_{01} - \tilde{\mathbf{a}}_{01}$
$\mathbf{v}_3 = F^{00,10}\tilde{\mathbf{a}}_{\mathbf{10}}$
$\tilde{\mathbf{a}}^{-}_{00} = -\,(\mathbb{1} + A)^{-1}\,\mathbf{v}_3$

Figure 5.1: Algorithm scheme for the calculation of vectors $\tilde{\mathbf{a}}^{-}_{00}$, $\tilde{\mathbf{a}}_{10}$ and $\tilde{\mathbf{a}}_{01}$ as matrix-vector multiplications

$$\left\{\ \tilde{\mathbf{a}}_{10}\ \right\} = -\,(\mathbb{1} + A_T)^{-1}\,(F^{10,01}\tilde{\mathbf{x}}_{01} - \tilde{\mathbf{x}}_{10}) \tag{5.23}$$

$$\left\{\ \tilde{\mathbf{a}}_{01}\ \right\} = \tilde{\mathbf{x}}_{01} + F^{01,10}\,(\mathbb{1} + A_T)^{-1}\,(F^{10,01}\tilde{\mathbf{x}}_{01} - \tilde{\mathbf{x}}_{10}) \tag{5.24}$$

It will be noted that aforementioned matrix inversion $(\mathbb{1} + A)^{-1}$ is not strictly needed to obtain the vectors $\left\{\ \tilde{\mathbf{a}}^{-}_{00}\ \right\}$, $\left\{\ \tilde{\mathbf{a}}_{10}\ \right\}$ and $\left\{\ \tilde{\mathbf{a}}_{01}\ \right\}$ with a desired level of convergence. From the computational point of view it is more efficient to simply implement algorithms with successive matrix-vector multiplications, see Figure 5.1. For that purpose the expressions (5.20) and (5.8) must be taken into account.

5.4 Transport algorithm convergence

First of all, the matrix resultant in the scaled system of equations (5.12) will be studied. The order of the different blocks will be analyzed. The diagonal blocks have to be not very far from identity and the off-diagonal blocks have to be close to zero to ensure the procedure convergence. The selected approach with Neumann series will be efficient as long as the matrix to invert is close to identity.

The ratios between binary diffusion coefficients appear in the expressions for the system

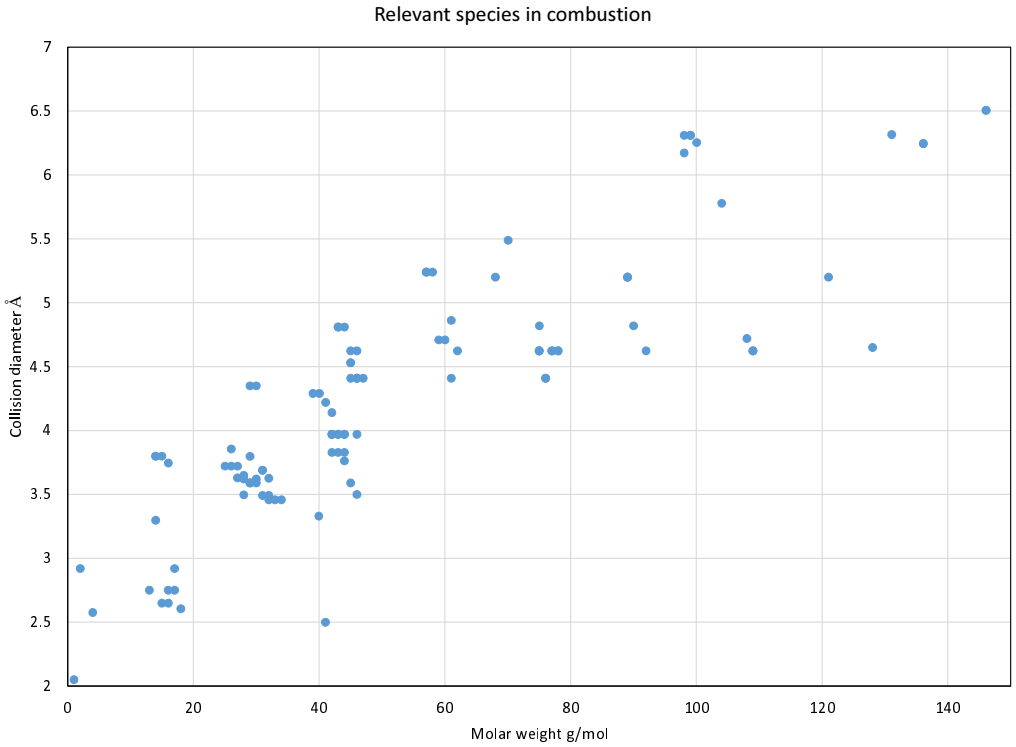

Figure 5.2: Collision diameter vs. molar weight for the main species used in combustion, extracted from tables in [2].

coefficients. These ratios depend on, collision diameters, mole masses and collision integrals. Data from reference [6] show that collision diameters values are around $2 - 7.5\mathring{A}$ for different species commonly used in combustion. Also, for common ranges of temperature, the collision integrals values $\Omega^{(1,1)*}$ are in the range of $0.5 - 4$ (this curves are shown in Figure 4.4).

The terms $\frac{\mathscr{D}_{ij}}{\mathscr{D}_{k\ell}}$ may be expressed as (5.25).

$$\frac{\mathscr{D}_{ij}}{\mathscr{D}_{k\ell}} = \left(\frac{\sigma_{k\ell}}{\sigma_{ij}}\right)^2 \frac{\Omega^{(1,1)*}_{k\ell}}{\Omega^{(1,1)*}_{ij}} \sqrt{\frac{m_{k\ell}}{m_{ij}}} \tag{5.25}$$

The values of the collision diameter σ against the mole weight for most of the species used in combustion has been plotted in Fig. 5.2.

The ratio between binary coefficients may be approximated by

$$\frac{\mathscr{D}_{ij}}{\mathscr{D}_{k\ell}} \sim \left(\frac{\sigma_{k\ell}}{\sigma_{ij}}\right)^2 \frac{\Omega^{(1,1)*}_{k\ell}}{\Omega^{(1,1)*}_{ij}} \sqrt{\frac{\frac{m_\ell m_k}{m_\ell + m_k}}{\frac{m_i m_j}{m_i + m_j}}} = \left(\frac{\sigma_{k\ell}}{\sigma_{ij}}\right)^2 \frac{\Omega^{(1,1)*}_{k\ell}}{\Omega^{(1,1)*}_{ij}} \sqrt{\frac{m_\ell}{m_i}} \sqrt{\frac{1 + \frac{m_i}{m_j}}{1 + \frac{m_\ell}{m_k}}} \tag{5.26}$$

with

$$0.5 < \frac{\Omega_{k\ell}^{(1,1)*}}{\Omega_{ij}^{(1,1)*}} < 4 \tag{5.27}$$

If the molecular weight of the species i,j,$k$and ℓ are similar the order of magnitude

$$\frac{\mathscr{D}_{ij}}{\mathscr{D}_{k\ell}} \sim \frac{\Omega_{k\ell}^{(1,1)*}}{\Omega_{ij}^{(1,1)*}} \tag{5.28}$$

In the following derivations a chemical species will be considered dilute if $x_m \dfrac{\mathscr{D}_{ij}}{\mathscr{D}_{k\ell}} \to 0$. The approximation to estimate orders of magnitude is that $\dfrac{\mathscr{D}_{ij}}{\mathscr{D}_{k\ell}} \sim 1$.

5.4.1 Estimated values of the terms associated to parameters F

In this section the different blocks of the scaled system of equation will be analyzed. As mentioned above the typical orders of magnitude will be checked to ensure that the resultant matrix to invert is not very different from identity.

Estimated values of the terms associated to $F^{00,00}$

$$F_{ij}^{00,00} = \sum_{\ell=1}^{N} \frac{\mathscr{D}_{jN}}{\mathscr{D}_{i\ell}} \frac{x_i x_\ell}{x_j} (\delta_{ij} - \delta_{j\ell}) \ ; \qquad i,j = 1,\ldots,N. \tag{5.29}$$

If $i = j$. Approximations can be done in the case that $\mathscr{D}_{iN} \sim \mathscr{D}_{i\ell}$.

$$F_{ii}^{00,00} = \sum_{\substack{\ell=1 \\ (\ell \neq i)}}^{N} \frac{\mathscr{D}_{iN}}{\mathscr{D}_{i\ell}} x_\ell \qquad F_{ii}^{00,00} \sim \sum_{\substack{\ell=1 \\ (\ell \neq i)}}^{N} x_\ell. \tag{5.30}$$

If the chemical species i is dilute $x_l \sim 1$ the diagonal terms are around unity. If $i \neq j$

$$F_{ij}^{00,00} = -x_i \frac{\mathscr{D}_{jN}}{\mathscr{D}_{ij}} \qquad F_{ii}^{00,00} \sim -x_i. \tag{5.31}$$

For a dilute species $F_{ij}^{00,00} \sim 0$. Hence, the resultant matrix row is almost a diagonal matrix row for dilute species.

Estimated values of the terms associated to $F^{00,10}$

Values $C_{i\ell}^*$ are around $\dfrac{9}{10}$ for every species, tables from [6], figure 4.7.

$$F_{ij}^{00,10} = \sum_{\ell=1}^{N} \frac{\mathscr{D}_{jj}}{\mathscr{D}_{i\ell}} \frac{x_i x_\ell}{x_j} \left(\frac{5}{2} - 3C_{i\ell}^* \right) \frac{m_{i\ell}}{m_j} (\delta_{ij} - \delta_{j\ell}) . \tag{5.32}$$

If $i = j$

$$F_{ii}^{00,10} = \sum_{\substack{\ell=1 \\ (\ell \neq i)}}^{N} x_\ell \frac{\mathscr{D}_{jj}}{\mathscr{D}_{i\ell}} \frac{m_\ell}{2\,(m_i + m_\ell)} \left(5 - 6C_{i\ell}^*\right) \qquad F_{ii}^{00,10} \sim -\frac{1}{10} \sum_{\substack{\ell=1 \\ (\ell \neq i)}}^{N} x_\ell. \tag{5.33}$$

If $i \neq j$

$$F_{ij}^{00,10} = -x_i \frac{\mathscr{D}_{jj}}{\mathscr{D}_{ij}} \frac{m_i}{2\,(m_i + m_j)} \left(5 - 6C_{i\ell}^*\right) \quad F_{ij}^{00,10} \sim \frac{x_i}{10} \tag{5.34}$$

Hence, the values of matrix $F^{00,10}$ will be small in a general way, independently if the species is dilute or not.

Estimated values of the terms associated to $F^{10,00}$

The procedure in this case is similar to $F^{00,10}$ but the scaling factor for each addend is $\frac{\mathscr{D}_{jN}}{\mathscr{D}_{i\ell}}$ instead $\frac{\mathscr{D}_{jj}}{\mathscr{D}_{i\ell}}$. Moreover, the global summation is scaled with $\frac{1}{F_{ii}^{10,10}}$.

$$F_{ij}^{10,00} = \frac{\displaystyle\sum_{\ell=1}^{N} \frac{\mathscr{D}_{jN}}{\mathscr{D}_{i\ell}} \frac{x_i x_\ell}{x_j} \left(\frac{5}{2} - 3C_{i\ell}^*\right) \frac{m_{i\ell}}{m_i} \left(\delta_{ij} - \delta_{j\ell}\right)}{F_{ii}^{10,10}} \tag{5.35}$$

and the scaling terms $F_{ii}^{10,10}$ are

$$\begin{aligned} F_{ii}^{10,10} = 2A_{ii}^* x_i + & \sum_{\substack{\ell=1 \\ (\ell \neq i)}}^{N} \frac{\mathscr{D}_{ii}}{\mathscr{D}_{i\ell}} x_\ell \left\{ 4A_{i\ell}^* + \left[\left(\frac{25}{4} - 3B_{i\ell}^* \right) \frac{m_\ell}{m_i} + \frac{15}{2} \frac{m_i}{m_\ell} \right] \right\} \frac{m_{i\ell}^2}{m_i m_\ell} \\ & + \frac{20}{3} x_i \frac{A_{ii}^* c_{i,\mathrm{rot.}}}{\pi k_B \zeta_{iI}} + \frac{20}{3} \sum_{\substack{\ell=1 \\ (\ell \neq i)}}^{N} \frac{\mathscr{D}_{ii}}{\mathscr{D}_{i\ell}} x_\ell \left(\frac{A_{i\ell}^* c_{i,\mathrm{rot.}}}{\pi k_B \zeta_{i\ell}} + \frac{A_{i\ell}^* c_{\ell,\mathrm{rot.}}}{\pi k_B \zeta_{\ell i}} \right) \frac{m_{i\ell}^2}{m_i m_\ell}. \end{aligned} \tag{5.36}$$

The values of A_{ij}^* are slightly over 1 as can be seen in Figure 4.5. The parameter $\zeta_{i\ell}$ may be approximated by the rotational collision index from figure 5.3 and takes values from 0 to 3. The parameter $\frac{c_{i,\mathrm{rot.}}}{k_B}$is 1 or $\frac{3}{2}$. Therefore the approximation $\frac{A_{i\ell}^* c_{i,\mathrm{rot.}}}{\pi k_B \zeta_{i\ell}} \sim \frac{1}{6}$ is an idea of the order of magnitude. The values of B_{ij}^* are around 1 from figure 4.6. Assuming $m_i \sim m_\ell$ and $\mathscr{D}_{iN} \sim \mathscr{D}_{i\ell}$ the order of magnitude of the scaling factor is

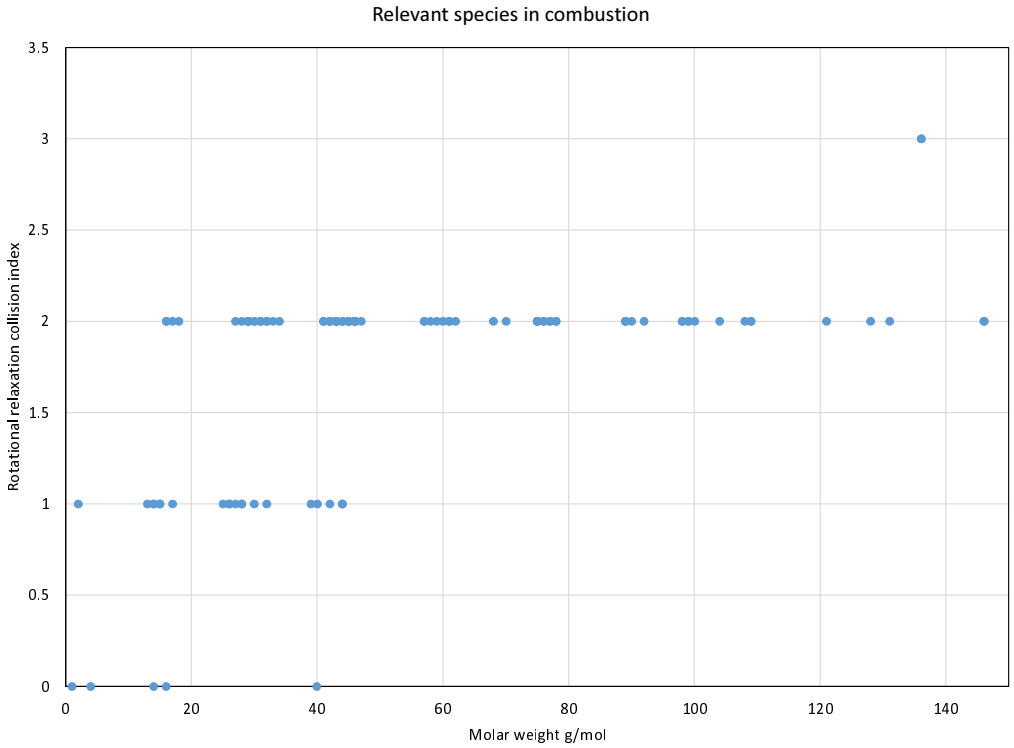

Figure 5.3: Rotational relaxation collision index ζ vs. molar weight for the main species used in combustion, extracted from tables in [2]

$$F_{ii}^{10,10} \sim \frac{28}{9}x_i + \sum_{\substack{\ell=1 \\ (\ell \neq i)}}^{N} \frac{611}{144}x_\ell. \tag{5.37}$$

If $i = j$, the definition (5.35) drives to

$$F_{ii}^{10,00} = \frac{\sum_{\substack{\ell=1 \\ (\ell \neq i)}}^{N} x_\ell \frac{\mathscr{D}_{iN}}{\mathscr{D}_{i\ell}}\left(\frac{5}{2} - 3C_{i\ell}^*\right)\frac{m_\ell}{(m_i+m_\ell)}}{F_{ii}^{10,10}} \qquad F_{ii}^{10,00} \sim \frac{-\frac{1}{10}\sum_{\substack{\ell=1 \\ (\ell \neq i)}}^{N} x_\ell}{\frac{28}{9}x_i + \sum_{\substack{\ell=1 \\ (\ell \neq i)}}^{N} \frac{611}{144}x_\ell}. \tag{5.38}$$

It is clear that $\left|F_{ii}^{10,00}\right| \ll 1$. For the non diagonal elements $i \neq j$

$$F_{ij}^{10,00} = \frac{-x_i \frac{\mathscr{D}_{iN}}{\mathscr{D}_{i\ell}}\frac{m_i}{(m_i+m_j)}\left(\frac{5}{2} - 3C_{i\ell}^*\right)}{F_{ii}^{10,10}} \qquad F_{ij}^{10,00} \sim \frac{\frac{1}{10}x_i}{\frac{28}{9}x_i + \sum_{\substack{\ell=1 \\ (\ell \neq i)}}^{N} \frac{611}{144}x_\ell} \tag{5.39}$$

Again, the expected values are lower than one $\left|F_{ij}^{10,00}\right| \ll 1$

Estimated values of the terms associated to $F^{10,10}$

As in the case of $F^{10,00}$, the global scaling factor is $\frac{1}{F_{ii}^{10,10}}$. In this case, the scaling factor for each addend is $\frac{\mathscr{D}_{jj}}{\mathscr{D}_{i\ell}}$.

$$\begin{aligned} F_{ii}^{10,10}\ F_{ij}^{10,10} = & \sum_{\ell=1}^{N} \frac{\mathscr{D}_{jj}}{\mathscr{D}_{i\ell}}\frac{x_i x_\ell}{x_j}\left\{4A_{i\ell}^*\left(\delta_{ij}+\delta_{j\ell}\right) + \right. \\ & \left. \left[\left(\tfrac{25}{4} - 3B_{i\ell}^*\right)\tfrac{m_\ell}{m_j} + \tfrac{15}{2}\tfrac{m_j}{m_\ell}\right]\left(\delta_{ij}-\delta_{j\ell}\right)\right\}\tfrac{m_{i\ell}^2}{m_i m_\ell} \\ & + \frac{20}{3}\sum_{\ell=1}^{N} \frac{\mathscr{D}_{jj}}{\mathscr{D}_{i\ell}}\frac{x_i x_\ell}{x_j}\frac{m_{i\ell}^2}{m_i m_\ell}A_{i\ell}^*\left(\delta_{ij}+\delta_{j\ell}\right)\left(\frac{c_{i,\mathrm{rot.}}}{\pi k_B \zeta_{i\ell}} + \frac{c_{\ell,\mathrm{rot.}}}{\pi k_B \zeta_{\ell i}}\right). \end{aligned} \tag{5.40}$$

If $i = j$

$$F_{ii}^{10,10} = 1. \tag{5.41}$$

If $i \neq j$

$$F_{ij}^{10,10} \sim \frac{-\frac{163}{144}x_i}{\frac{28}{9}x_i + \sum\limits_{\substack{\ell=1 \\ (\ell \neq i)}}^{N} \frac{611}{144}x_\ell}. \tag{5.42}$$

The off diagonal terms are small and the matrix $F^{10,00}$ is closed to the identity.

Estimated values of the terms associated to $F^{10,01}$

The expression for these terms are:

$$F_{ij}^{10,01} = \frac{-\sum\limits_{\ell=1}^{N} \frac{\mathscr{D}_{jj}}{\mathscr{D}_{i\ell}} \frac{x_i x_\ell}{x_j} \frac{10 m_j A_{i\ell}^*}{(m_i + m_\ell)} (\delta_{j\ell} + \delta_{ij}) \frac{c_{j,\text{rot.}}}{\pi k_B \zeta_{j\ell}}}{F_{ii}^{10,10}}. \tag{5.43}$$

If $i = j$

$$F_{ij}^{10,01} \sim \frac{\frac{2}{3}x_i + \sum\limits_{\substack{\ell=1 \\ (\ell \neq i)}}^{N} \frac{1}{3}x_\ell}{\frac{28}{9}x_i + \sum\limits_{\substack{\ell=1 \\ (\ell \neq i)}}^{N} \frac{611}{144}x_\ell}. \tag{5.44}$$

If $i \neq j$

$$F_{ij}^{10,01} \sim \frac{-\frac{1}{3}x_i}{\frac{28}{9}x_i + \sum\limits_{\substack{\ell=1 \\ (\ell \neq i)}}^{N} \frac{611}{144}x_\ell} \tag{5.45}$$

All the terms are small and therefore this matrix is closed to zero.

Estimated values of the terms associated to $F^{01,10}$

The expression for these terms are:

$$F_{ij}^{01,10} = \frac{-\sum_{\ell=1}^{N} \frac{\mathscr{D}_{jj}}{\mathscr{D}_{i\ell}} \frac{x_i x_\ell}{x_j} \frac{10 m_i A_{i\ell}^*}{(m_i+m_\ell)} (\delta_{j\ell}+\delta_{ij}) \frac{c_{i,\text{rot.}}}{\pi k_B \zeta_{i\ell}}}{F_{ii}^{01,01}}. \tag{5.46}$$

The scaling terms $F_{ii}^{01,01}$ are

$$F_{ii}^{01,01} = \sum_{\ell=1}^{N} \frac{\mathscr{D}_{ii}}{\mathscr{D}_{i\ell}} x_\ell \frac{25}{4} \left\{ \frac{c_{i,\text{int.}}}{k_B} \frac{\mathscr{D}_{i\ell}}{\mathscr{D}_{i\,\text{int.},\ell}} + \frac{12}{5} \frac{m_i A_{i\ell}^*}{m_\ell} \frac{c_{i,\text{rot.}}}{\pi k_B \zeta_{i\ell}} \right\}. \tag{5.47}$$

The approximations $\frac{\mathscr{D}_{i\ell}}{\mathscr{D}_{i\,\text{int.},\ell}} \sim 1$ and $\frac{c_{i,\text{int.}}}{k_B} \sim \frac{5}{2}$ may be considered. If $i = j$

$$F_{ij}^{01,10} \sim \frac{\frac{2}{3}x_i + \sum_{\substack{\ell=1 \\ (\ell \neq i)}}^{N} \frac{1}{3} x_\ell}{\sum_{\ell=1}^{N} \frac{145}{8} x_\ell}. \tag{5.48}$$

If $i \neq j$

$$F_{ij}^{01,10} \sim \frac{-\frac{1}{3}x_i}{\sum_{\ell=1}^{N} \frac{145}{8} x_\ell} \tag{5.49}$$

All the terms are small and therefore this matrix is close to zero.

Estimated values of the terms associated to $F^{01,01}(\mathbb{1}+A)^{-1}$

By definition, this matrix is the identity

$$F_{ij}^{01,01} = \frac{\sum_{\ell=1}^{N} \frac{\mathscr{D}_{jj}}{\mathscr{D}_{i\ell}} \frac{x_i x_\ell}{x_j} \frac{25}{4} \left\{ \frac{c_{i,\text{int.}}}{k_B} \frac{\mathscr{D}_{i\ell}}{\mathscr{D}_{i\,\text{int.},\ell}} + \frac{12}{5} \frac{m_i A_{i\ell}^*}{m_\ell} \frac{c_{i,\text{rot.}}}{\pi k_B \zeta_{i\ell}} \right\} \delta_{ij}}{\sum_{\ell=1}^{N} \frac{\mathscr{D}_{ii}}{\mathscr{D}_{i\ell}} x_\ell \frac{25}{4} \left\{ \frac{c_{i,\text{int.}}}{k_B} \frac{\mathscr{D}_{i\ell}}{\mathscr{D}_{i\,\text{int.},\ell}} + \frac{12}{5} \frac{m_i A_{i\ell}^*}{m_\ell} \frac{c_{i,\text{rot.}}}{\pi k_B \zeta_{i\ell}} \right\}}. \tag{5.50}$$

If $i = j$

$$F_{ij}^{01,01} = 1. \tag{5.51}$$

If $i \neq j$

$$F_{ij}^{01,01} = 0. \tag{5.52}$$

5.4.2 Convergence analysis

The described procedure contains two matrix inversions, $(\mathbb{1} + A)^{-1}$ and $(\mathbb{1} + A_T)^{-1}$. The convergence problem of $(\mathbb{1} + A)^{-1}$ is analyzed in references [28, 30]. The inversion of matrices close to identity may be done by the Neumann series approximation and $(\mathbb{1} + A_T)^{-1}$ is suited to it. The Neumann series inversion of (5.8) is convergent as long as the norm of matrix A_T is $\|A_T\| < 1$, and has fast convergence rate if $\|A_T\| \ll 1$.

If the previous estimations are correct (section §5.4), the matrices , $F^{10,10}$, $\hat{F}^{10,00}$, $F^{00,10}$, $F^{10,01}$, $F^{01,10}$ and $\mathcal{E}^{10,10}$ from (5.53) are close to zero and the norm is small.

$$F^{10,10} = \mathbb{1} + \mathcal{E}^{10,10} \tag{5.53}$$

The matrix A_T is therefore expected to be reasonably small, because is derived with operations involving small matrices.

$$A_T = \mathcal{E}^{10,10} - \hat{F}^{10,00} \left(\mathbb{1} + A\right)^{-1} F^{00,10} - F^{10,01} F^{01,10} \tag{5.54}$$

Thus, the fast inversion convergence rate is then reached as a consequence of the scaling procedure.

Chapter 6

Transport algorithm efficiency

This chapter tries to cope the operations count of the presented algorithm. In general, this an iterative approach and the speed is very competitive. What is valuable is that the global number of operations be the lowest for a desired level of accuracy. In this chapter the operation count of the present algorithm is analyzed. It is important to have in mind that, regarding the algorithm performance, it is not necessary to be the fastest at each iteration if accuracy is reached at a lower number of iterations.

6.1 Operation count

The number of operations implied in the present algorithm is addressed below. It will be compared against other well known algorithms, including a direct $LDL^T$and two iterative conjugate gradient algorithms, with and without preconditioning. It will be assumed that the matrix system and the right hand side of the linear system are given. No considerations are made about the operations needed to build the linear system of equations, only the number of operations needed to reach the solution is accounted for. The approach is very generic and the numbers of operations are estimated approximately, although minor order numbers of operations will be kept. Any of the algorithms used for comparison may be optimized or customized for the current problem and the number of operations may differ slightly. Thus, the main purpose here is only to provide a general idea of the algorithm cost in terms of the different numbers of additions and multiplications needed in each case. For instance, for preconditioning we have considered a left matrix-vector multiplication, where a dense preconditioning matrix is assumed and no sparsity issues are taken into account.

The sequence of matrix-vector multiplications in (5.23) $(\mathbb{1} + A_T)^{-1} \left(\tilde{\mathbf{x}}_{10} - F^{10,01}\tilde{\mathbf{x}}_{01}\right)$ are repeated in the expressions (5.21) and (5.24) from right to left. A single matrix-vector multiplication of order N takes $MV = 2N^2 - N$ operations. The computation of the vector $F^{10,01}\tilde{\mathbf{x}}_{01} - \tilde{\mathbf{x}}_{10}$ requires $N + MV$ operations. Taking into account the expression (5.20),

the resultant vector $-\left(\mathbb{1}+A_T\right)\left(F^{10,01}\tilde{\mathbf{x}}_{01}-\tilde{\mathbf{x}}_{10}\right)$ requires ca. $7MV+4N$ operations. The value is approximated because some matrix and vector dimensions are of order $N-1$ in (5.20). Thus, for a number of Neumann steps r the number of operations needed to obtain $\left(\mathbb{1}+A_T\right)^{-1}\left(F^{10,01}\tilde{\mathbf{x}}_{01}-\tilde{\mathbf{x}}_{10}\right)$ is ca. $6rMV+3rN+MV+N$, and to get the solution for the three vectors $\tilde{\mathbf{a}}_{00}^{-}$, $\tilde{\mathbf{a}}_{10}$ and $\tilde{\mathbf{a}}_{01}$ around $6rMV+4MV+3rN+3N$ operations are necessary.

6.2 Comparison with existing methods

A direct inversion of a system of $3N$ equations with LDL^T factorization takes $\frac{(3N)^3}{3}=9N^3$ operations [43]. In the case of a matrix multiplication for the whole $3N$ system, the matrix-vector multiplication takes $12N^2-N$, avoiding the null terms. A general iterative conjugate gradient algorithm (not optimized for this particular system) requires $30rN+r\left(12N^2-N\right)$ operations for the solution of a $3N$ system of equations (see, e.g., [43] (10.2.16)). With pre-conditioning, an additional $3N$ matrix-vector multiplication for the right hand side and one additional $3N$ matrix-vector multiplication in each iteration are considered. The operation count results for each of the aforementioned solution algorithms are summarized in Table 6.1, as a function of the number of iterations r. The expressions shown in Table table 6.1 are plotted in Figure figure 6.1. It is important to remark that the conjugate gradient operation count shown in this work corresponds to a generic conjugate gradients (CG) algorithm, not to EGLib, which is specifically optimized for this particular system, leading to a lower computational load. As can be seen, the performance of the present algorithm (see orange lines) is better than the direct method. With the first iteration $r=1$, the direct algorithm is slower than MuTLib algorithm for any number of species. For higher levels of iteration $r=2$ and $r=3$, direct method (blue lines) is better for small numbers of species, under 10. The operation count of MuTLib is slightly better than a generic conjugate gradient algorithm for low numbers of species and slightly worse for high numbers of species. However, the operation count of MuTLib with the recommended iteration level $r=1$, is better than conjugate gradient for $r\geq 2$ for any number of species. On the other hand Figure 6.1 shows that the performance of MuTLib is better than a generic preconditioned conjugate gradient regardless of iteration level and number of species.

Algorithm	Number of operations
MuTLib algorithm	$12rN^2 + 8N^2 - 3rN - N$
LDL^T	$9N^3$
Conjugate gradient	$12rN^2 + 29rN$
Preconditioned conjugate gradient	$30rN^2 + 18N^2 + 26rN - 3N$

Table 6.1: Number of operations needed to solve a system of N species for several iterative algorithms as a function of the number of iterations r.

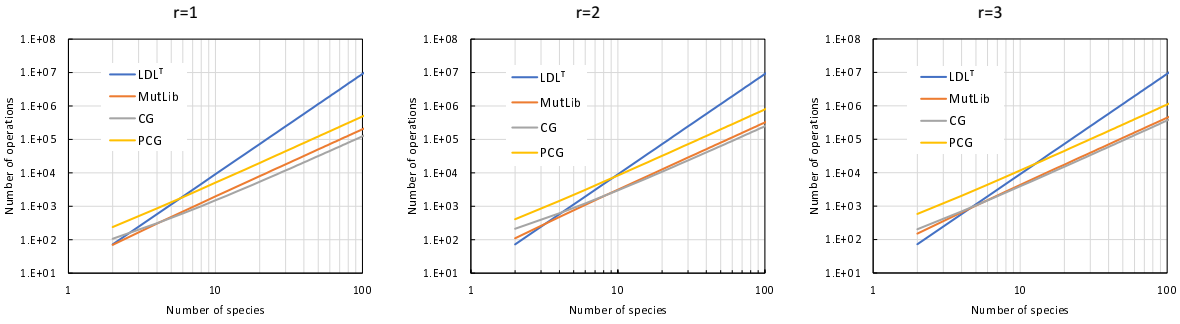

Figure 6.1: Operation count needed to solve the transport system for N species according to MuTLib, a direct method LDT^T, an iterative conjugate gradient method (CG) and a preconditioned conjugate gradient method (PCG) as a function of the number of species for numbers of iterations r =1, 2, 3.

Chapter 7

Transport algorithm accuracy

The performance of the present approximate method is illustrated below in two particular cases of interest in combustion: a hydrogen premixed flame and a methane counterflow diffusion flame. We will focus on the accuracy of the results for the thermal diffusion fluxes D_{Ti} and partial thermal conductivity λ' vs. number of terms included in the iterative algorithm. To this end the package Chemkin with full multicomponent transport description (including Soret transport) has been used to determine the mole fraction and temperature profiles as a function of position in each flame configuration. Thus, the transport properties in the mixture are computed by Chemkin according to KTG [6] and provide the rigorous results for D_{Ti} and λ' as functions of position (termed D_{Ti} (exact KTG) and λ' (exact KTG) below). Then, based on the mole fraction and temperature profiles provided by Chemkin, the thermal diffusion coefficients D_{Ti} and partial thermal conductivity λ' are re-calculated according to the present iterative algorithm and the corresponding results (termed D_{Ti} (approximate model) and λ' (approximate model) below) are compared to the corresponding rigorous KTG values. To this end we define the absolute error in D_{Ti} and λ' as

$$\begin{aligned} \Delta D_{Ti} &= |D_{Ti}\,(\text{approximate model}) - D_{Ti}\,(\text{exact KTG})| \\ \Delta\lambda' &= |\lambda'\,(\text{approximate model}) - \lambda'\,(\text{exact KTG})| \end{aligned} \tag{7.1}$$

and will base our accuracy analysis in terms of the maximal absolute errors as a function of position, normalized by the maximal value of each corresponding rigorous KTG magnitude

$$\begin{aligned} \varepsilon_i &= \frac{\max\left(\Delta D_{Ti}\right)}{\max|D_{Ti}\,(\text{exact KTG})|} \\ \varepsilon_{\lambda'} &= \frac{\max\left(\Delta\lambda'\right)}{\max|\lambda'\,(\text{exact KTG})|} \end{aligned} \tag{7.2}$$

The same accuracy analysis will be also performed with the thermal diffusion fluxes and partial thermal conductivity computed by means of the mixture averaged approximation

(Appendix A from additional material), and the corresponding normalized errors ε_i and $\varepsilon_{\lambda'}$ are also shown.

The calculation of the thermal diffusion coefficients and partial thermal conductivity involves the calculation of the Fick diffusion coefficients. Hence, to focus on the accuracy of the Neumann series used for the inversion of the new sub-matrix $\mathbb{1}+A_T$ (Eq. (5.20)), in the results shown below the calculation of the Fick diffusion coefficients has been performed in an analytic way. As a consequence the inverse of matrix $\mathbb{1}+A$ is given by the corresponding exact result, which is equivalent to the leading order result of model 1+M in the optimized implementation shown in [30]. Thus, in the convergence analysis shown below the normalized relative errors ε_i and $\varepsilon_{\lambda'}$ are shown as a function of the number of terms included in the Neumann series expansion used to calculate the inverse of the thermal diffusion sub-matrix $(\mathbb{1}+A_T)$ according to the present approximate algorithm (i.e., the maximal *finite* value considered for index r in Eq. (5.8)).

7.1 Results for premixed hydrogen flames

We consider a uni-dimensional hydrogen flame deflagration in air at 1atm and 300K as a function of the equivalence ratio ϕ, with chemical kinetics described by the seven-step combustion mechanism [44]. As a consequence only 8 species are present, numbered according to: H2, O2, H2O, O, OH, H, HO2, N2, with nitrogen as the reference species. As a particular case, Fig. 7.1 (major species) and Fig. 7.2 (radicals) show the results found for each chemical species as a function of position in a stoichiometric ($\phi = 1$) premixed hydrogen flame. Figures 7.1(a), 7.2(a) show the mole fraction and temperature profiles. Figures 7.1(b) and 7.2(b) show the thermal diffusion coefficients as a function of position for different algorithm approximations and mixture averaged. Figures 7.1(c), 7.2(c) show the relative errors found for different MuTLib algorithm approximations, mixture averaged and the available EGLib approximation. As can be seen in Figs. 7.1(c), 7.2(c), the convergence rate of the present algorithm is remarkable, yielding results which are quite accurate including only the first order term ($r = 1$) in the Neumann series expansion (Eq. (5.8)). On the other hand, Figs. 7.1(c), 7.2(c) also show that the mixture averaged approximation is quite inaccurate in this particular case (errors of MA approximation are out of range in Figs. 7.1(c), 7.2(c)). This result could be expected, since the mixture averaged approximation is a good approximation only in the dilute limit. Regarding the accuracy of EGLib, although for some species (H2, O, OH, H) the differences are almost as good as the MuTLib approximation for $r = 2$, the results for O2, H2O, HO2 and N2 with EGLib are similar to the MuTLib approximation for $r = 1$.

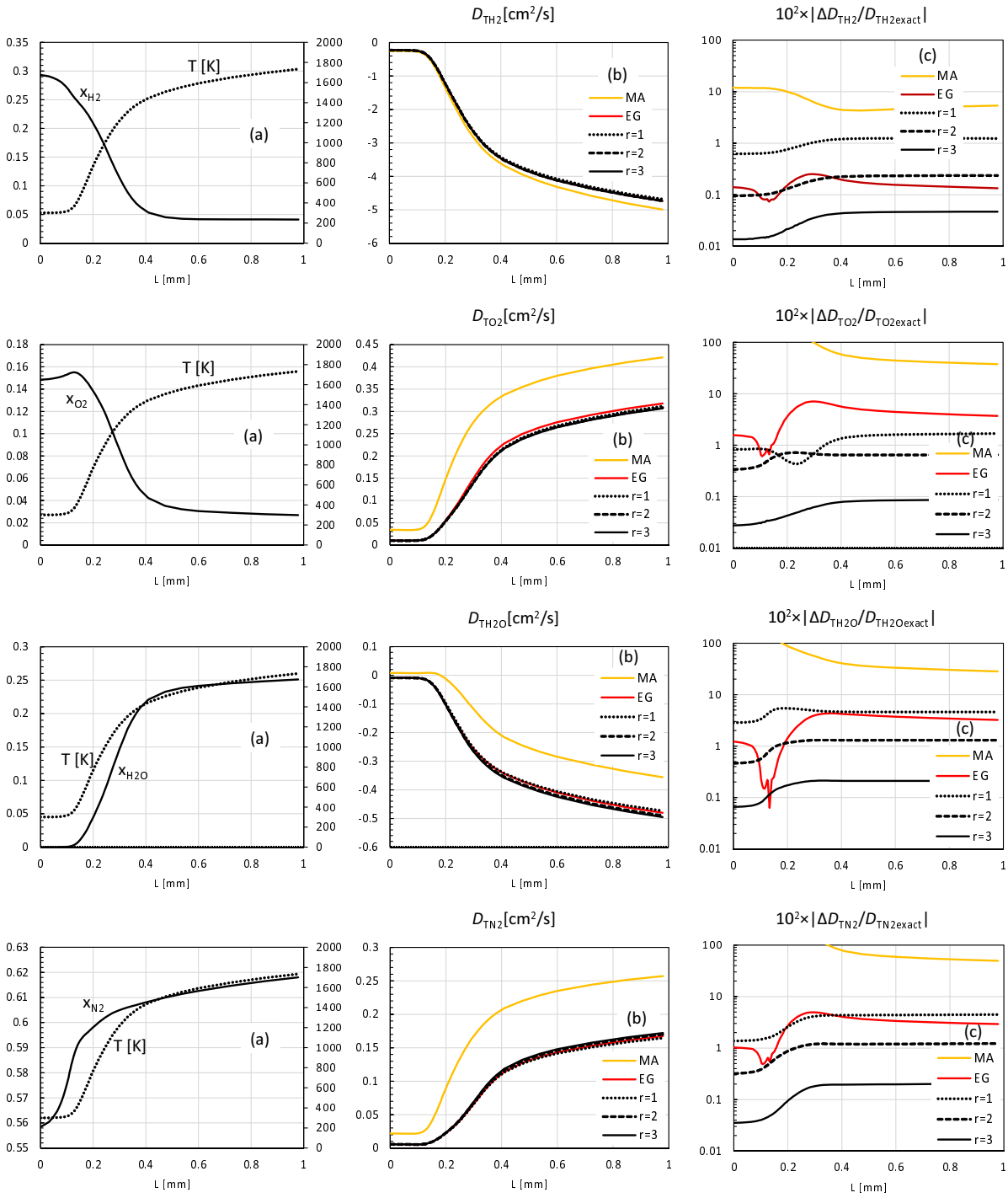

Figure 7.1: Results for the major species in a stoichiometric ($\phi = 1$) premixed hydrogen flame vs. distance L. Left column (a): mole fraction and temperature profiles. Center column (b): thermal diffusion coefficients. Right column (c): thermal diffusion coefficients percentage errors. The results for D_{Ti} (b) and $10^2 \times |\Delta D_{Ti}/D_{Tiexact}|$ (c) are shown for several maximal values of index r considered in the truncated Neumann series expansion (Eq. (5.8)). The results for D_{Ti} (b) using the mixture averaged (MA) approximation are shown in yellow lines. The results for $10^2 \times |\Delta D_{Ti}/D_{Tiexact}|$ (c) using the EGLib (EG) $r = 3$ approximation are also shown using red lines.

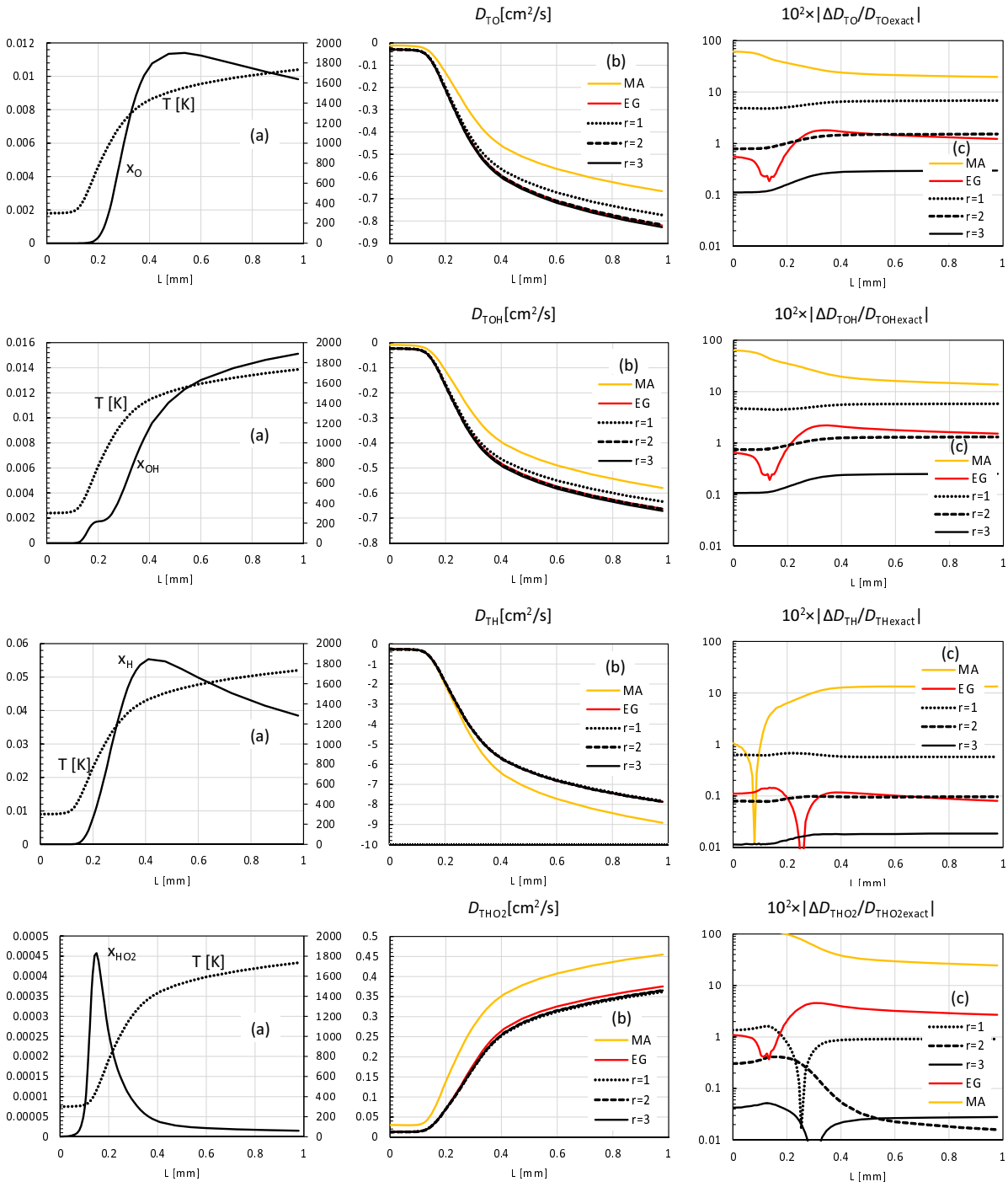

Figure 7.2: Results for the intermediate species in a stoichiometric ($\phi = 1$) premixed hydrogen flame vs. distance L. Left column (a): mole fraction and temperature profiles. Center column (b): thermal diffusion coefficients. Right column (c): thermal diffusion coefficients percentage errors. The results for D_{Ti} (b) and $10^2 \times |\Delta D_{Ti}/D_{Tiexact}|$ (c) are shown for several maximal values of index r considered in the truncated Neumann series expansion (Eq. (5.8)). The results for D_{Ti} (b) using the mixture averaged (MA) approximation are shown in yellow lines. The results for $10^2 \times |\Delta D_{Ti}/D_{Tiexact}|$ (c) using the EGLib (EG) $r = 3$ approximation are also shown using red lines.

In addition to the thermal diffusion coefficients, the thermal diffusion fluxes may be plotted as presented in Figs. 7.3 and 7.4. In this case the right column represents the fluxes difference in absolute values.

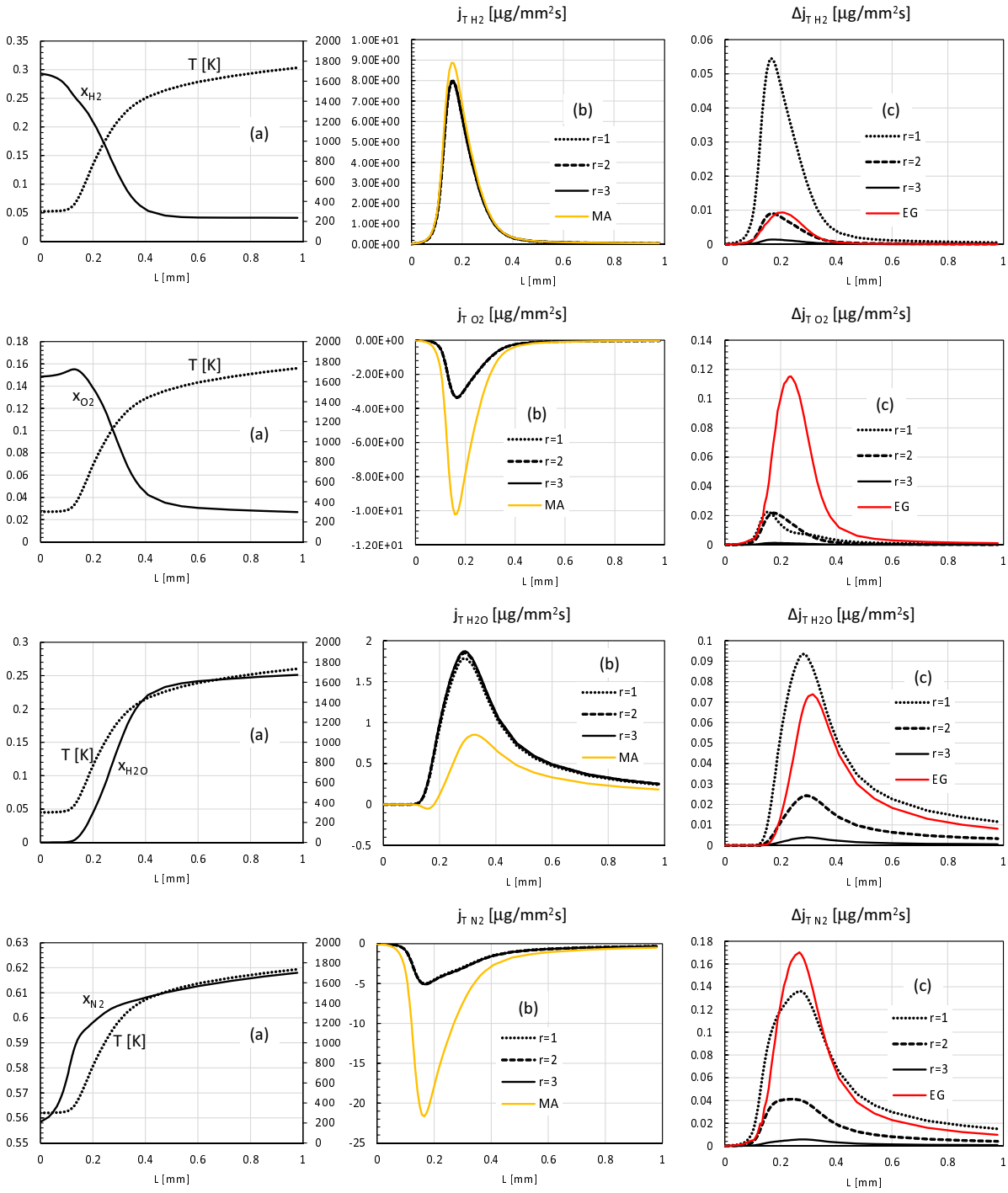

Figure 7.3: Results for the major species in a stoichiometric ($\phi = 1$) premixed hydrogen flame vs. distance L. Left column (a): mole fraction and temperature profiles. Center column (b): thermal diffusion fluxes. Right column (c): thermal diffusion fluxes absolute errors. The results for j_{Ti} (b) and Δj_{Ti} (c) are shown for several maximal values of index r considered in the truncated Neumann series expansion (Eq. (5.8)). The results for j_{Ti} (b) using the mixture averaged (MA) approximation are shown in yellow lines. The results for Δj_{Ti} (c) using the EGLib (EG) $r = 3$ approximation are also shown using red lines.

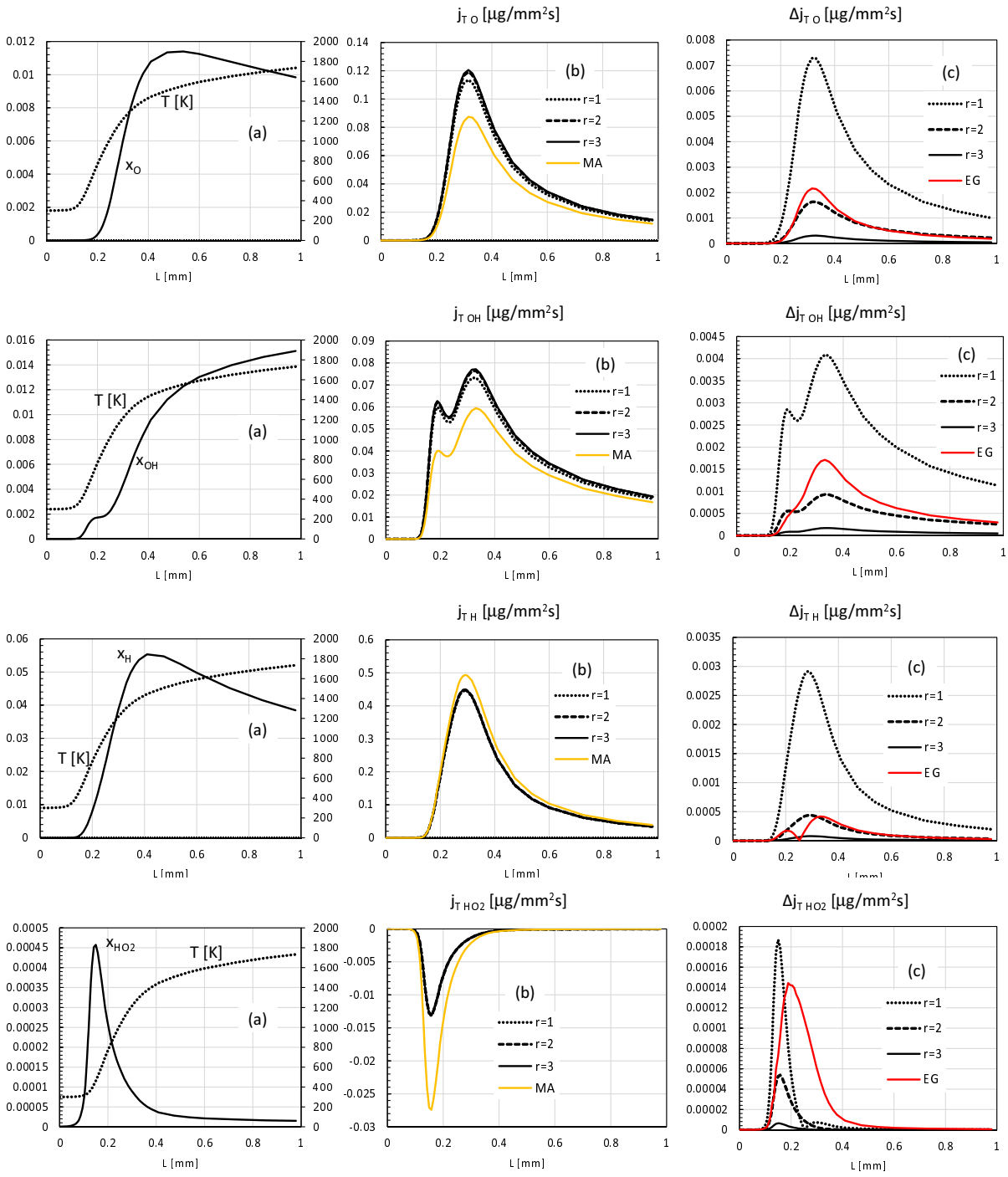

Figure 7.4: Results for the intermediate species in a stoichiometric ($\phi = 1$) premixed hydrogen flame vs. distance L. Left column (a): mole fraction and temperature profiles. Center column (b): thermal diffusion fluxes. Right column (c): thermal diffusion fluxes absolute errors. The results for j_{Ti} (b) and Δj_{Ti} (c) are shown for several maximal values of index r considered in the truncated Neumann series expansion (Eq. (5.8)). The results for j_{Ti} (b) using the mixture averaged (MA) approximation are shown in yellow lines. The results for Δj_{Ti} (c) using the EGLib (EG) $r = 3$ approximation are also shown using red lines.

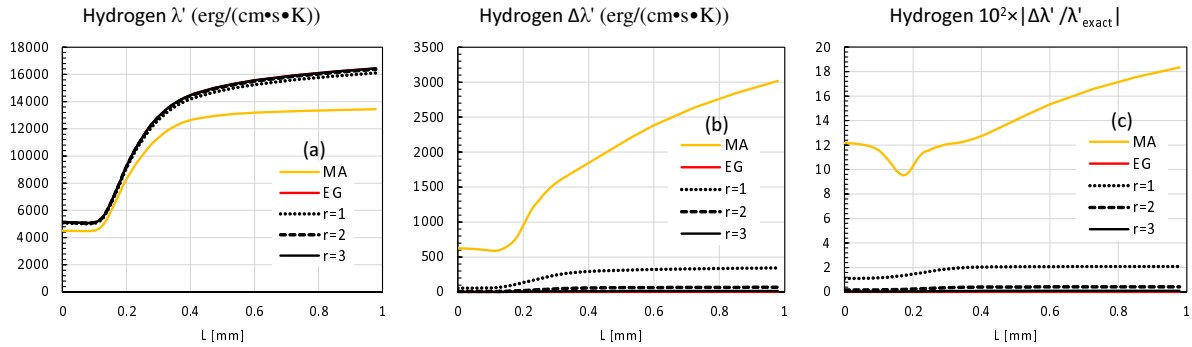

Figure 7.5: Partial thermal conductivity in a stoichiometric ($\phi = 1$) premixed hydrogen flame vs. distance L. Left column (a): partial thermal conductivity values. Center column (b): partial thermal conductivity absolute errors . Right column (c): partial thermal conductivity percentage errors. The results are shown for several maximal values of index r considered in the truncated Neumann series expansion (Eq. (5.8)). The results using the mixture averaged (MA) approximation are shown in yellow lines. The results using the EGLib (EG) $r = 3$ approximation are also shown using red lines.

Figure (7.5) shows the results for the partial thermal conductivity. As in the former results, we find that the mixture averaged approximation is again quite inaccurate, while the EGLib results for three conjugate gradient iterations (with preconditioning in the last one) provide almost the exact values. In this case the results found with the present MuTLib algorithm are not as accurate as those found using EGLib. However, the accuracy of MuTLib for the partial thermal conductivity is around 2% for $r = 1$, which is remarkably accurate.

Figures 7.6, 7.7 and 7.8 show the normalized relative errors ε_i and $\varepsilon_{\lambda'}$ (Eq. (7.2)) vs. maximal value of r in Eq. (5.8) found according to the present algorithm, as well as the mixture averaged approximation. In the present analysis we have considered values of the equivalence ratio ϕ covering the whole range between the lean-flame (Fig. 7.6) and the rich-flame (Fig. 7.8) limits, while the results for a stoichiometric flame are shown in Fig. 7.7. As can be seen, the present algorithm is quite accurate and has very fast convergence rate. In all the cases considered the first order term of the Neumann series (Eq. (5.8)) provides maximal relative errors of order 10% (often lower than 10%), and this error decreases by ca. an order of magnitude with each new term included in the truncated Neumann series.

Figures 7.6, 7.7 and 7.8 also show that the present iterative algorithm is considerably more accurate than the mixture averaged approximation, even if the Neumann series is truncated at the first order term ($r = 1$). Regarding the comparison of relative errors among the different species, it should be noted that the present definition of the normalized relative errors ε_i (Eq. (7.2)) penalizes those species with lowest thermal diffusion coefficients. Therefore the species H2 and H have lower relative errors in Figs. 7.6, 7.7, 7.8 according to both, the present model and the mixture averaged approximation.

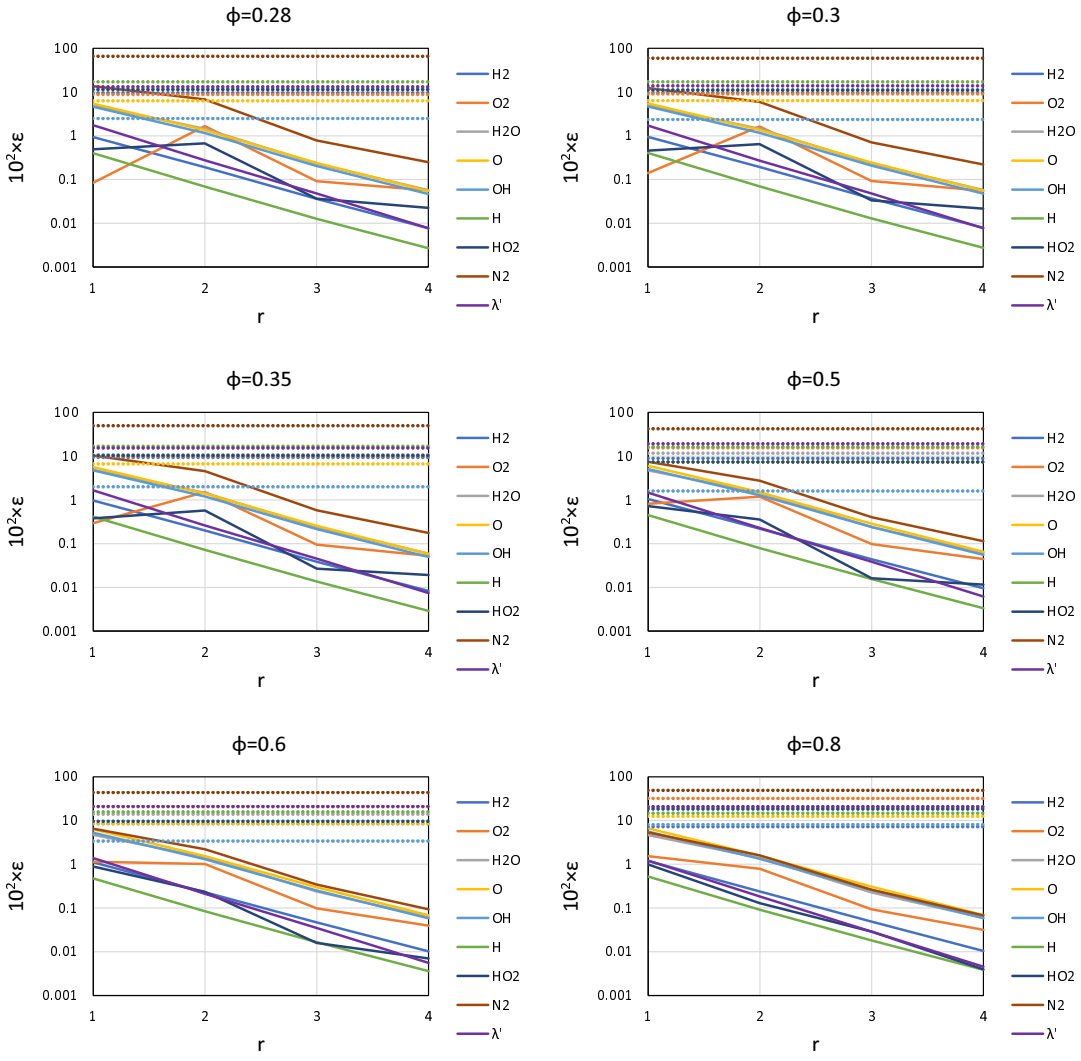

Figure 7.6: Normalized relative errors ε_i and $\varepsilon_{\lambda'}$ (Eq. (7.2)) found vs. maximal r considered in the truncated Neumann series (Eq. (5.8)) for lean hydrogen premixed flames. Dotted horizontal lines: corresponding results found with the mixture averaged approximation.

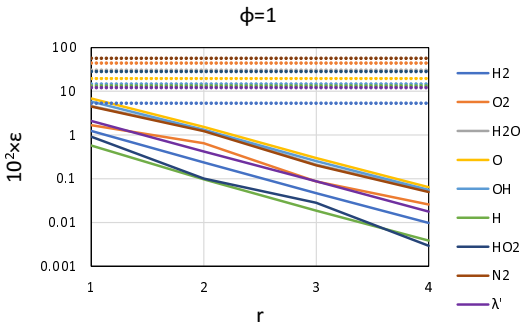

Figure 7.7: Relative errors found vs. r for stoichiometric flames. Dotted horizontal lines = Mixture Averaged Model. Continuous lines= present algorithm.

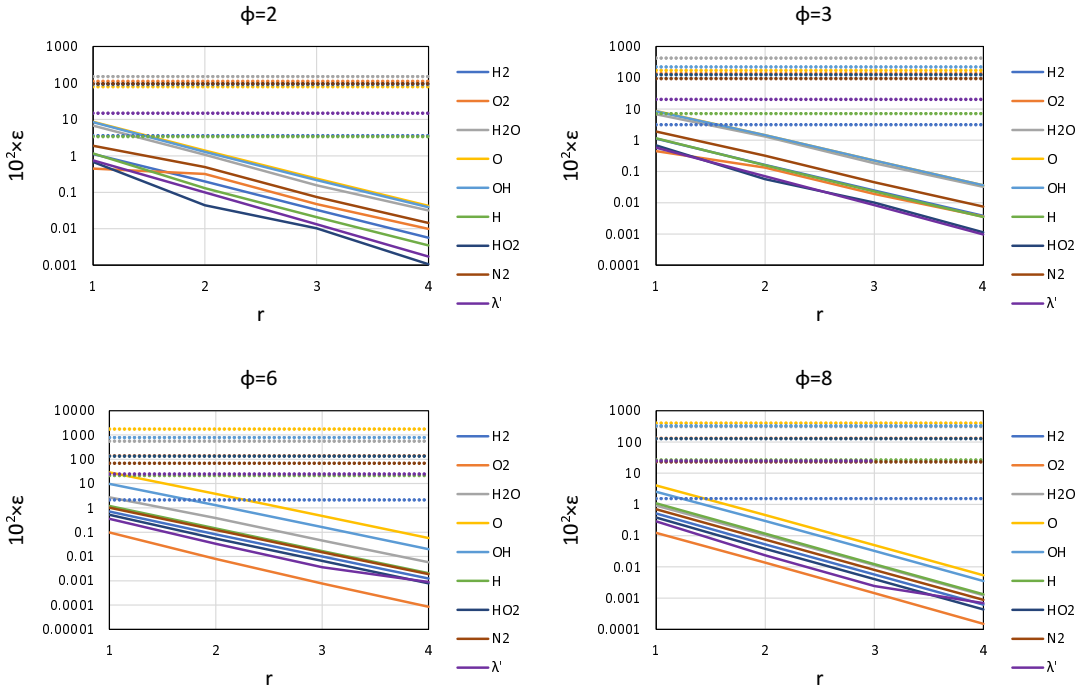

Figure 7.8: Relative errors found vs. r for rich flames. Dotted horizontal lines = Mixture Averaged Model. Continuous lines = present algorithm.

We recall that an apparent linear decrease of ε_i and $\varepsilon_{\lambda'}$ vs. r in the semi-log Figs. 7.6, 7.7, 7.8 corresponds to an exponential convergence rate of the present algorithm. Hence, the results for the normalized relative errors ε_i and $\varepsilon_{\lambda'}$ in Figs. 7.6, 7.7, 7.8 seem to fit to the general exponential decrease formula

$$\varepsilon = \varepsilon_1 e^{-\alpha(r-1)} \tag{7.3}$$

where the prefactor ε_1 provides the accuracy of the present model truncated at the first order term ($r = 1$), while the exponent α provides the convergence rate. The results of this fit are shown in Fig. 7.9 for each particular chemical species vs. the equivalence ratio. The most relevant feature of the present algorithm that can be seen in Fig. 7.9 is an overall relative error of order 10% at the first order term and an exponential convergence rate with a relative error reduction close to an order of magnitude for each new term included in the truncated Neumann expansion (Eq. (5.8)). We also remark that the accuracy and convergence rate of the present algorithm is not as dependent on equivalence ratio as it happens to Model 1 and Model 1+M of [28] for the Fick diffusion fluxes. In the present algorithm this has been accomplished by means of the diagonal term scaling of the KTG system (Eqs. ((5.10)-(5.11))).

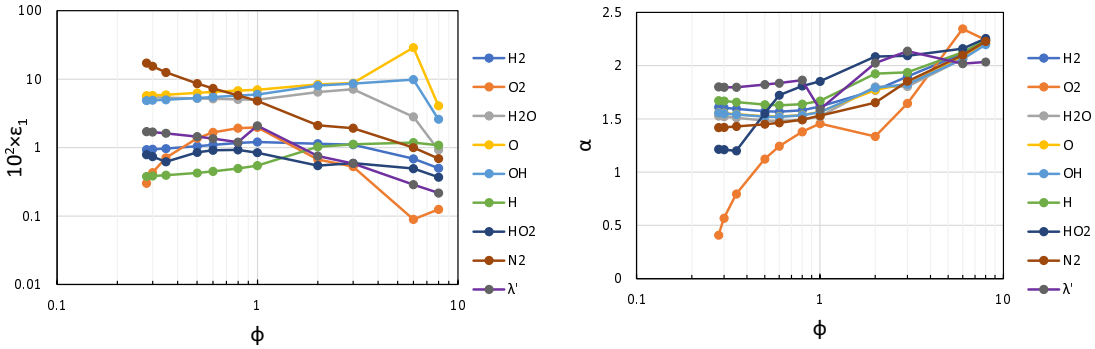

Figure 7.9: Results for maximal relative error ε_i fitted to the formula $\varepsilon = \varepsilon_1 e^{-\alpha(r-1)}$ vs. ϕ for all species. Left: 10^2 $\times$ first order term error ε_1. Right: exponent α.

7.2 Results for methane counterflow diffusion flames

To show the performance of the present algorithm in the case of a diffusion flame we consider a counterflow diffusion flame configuration. Two counterflow jets are simulated, with methane as fuel at $x = 0$mm and air as oxidizer at $x = 20$mm. The initial compositions are summarized in Table 7.1. The chemical mechanism of [2] is used, involving 58 species and 270 reactions. The stagnation point is fixed at $x = 10$mm with strain rate $a = 100\text{s}^{-1}$. The Chemkin boundary conditions must be iterated to simulate the desired condition and to obtain the mole fractions and temperature as a function of distance. The basis of the steady flame model used in this section is described in reference [45].

Figure 7.10 shows the results for the species with higher thermal diffusion flux, CH4, O, H2O and N2. According to the present results we find that in this case the first order term of the present iterative algorithm is already more accurate than both, mixture averaged approximation and EGLib package.

	Fuel	Oxidizer
Temperature	$T = 320\text{K}$	$T = 1350\text{K}$
Mole fractions	$x_{\text{CH4}} = 0.33$ $x_{\text{O2}} = 0.15$ $x_{\text{N2}} = 0.52$	$x_{\text{H2O}} = 0.15$ $x_{\text{O2}} = 0.12$ $x_{\text{N2}} = 0.73$

Table 7.1: Case of temperature conditions and mole fractions of fuel and oxidizer for a methane counterflow diffusion flame.

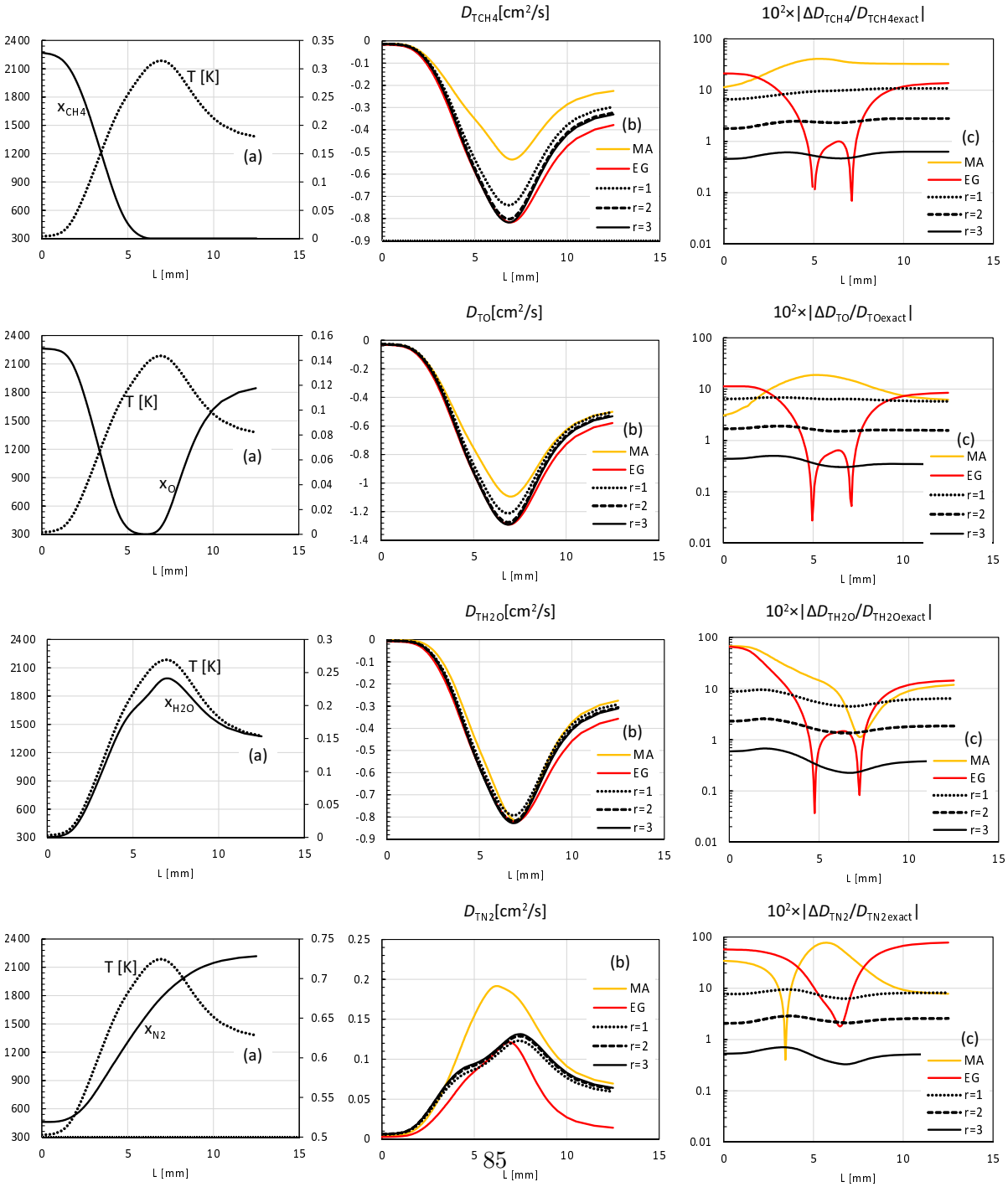

Figure 7.10: Results vs. axial distance L for the major species CH4, O, H2O and N2; mole fraction x and temperature T (a), thermal diffusion coefficients (b) and thermal diffusion coefficients percentage error (c) as compared to exact (KTG) values for different approximation

Figure 7.11 presents the results for the species O2, H2, CO2 and CO with meaningful thermal diffusion flux. The accuracy increases with the number of iterations considered in the truncated Neumann series expansion (Eq. (5.8)), as could be expected. As can be seen, the shape of the curves is similar in all the cases, which could also be expected since the thermal diffusion fluxes are proportional to the temperature gradient in all the cases.

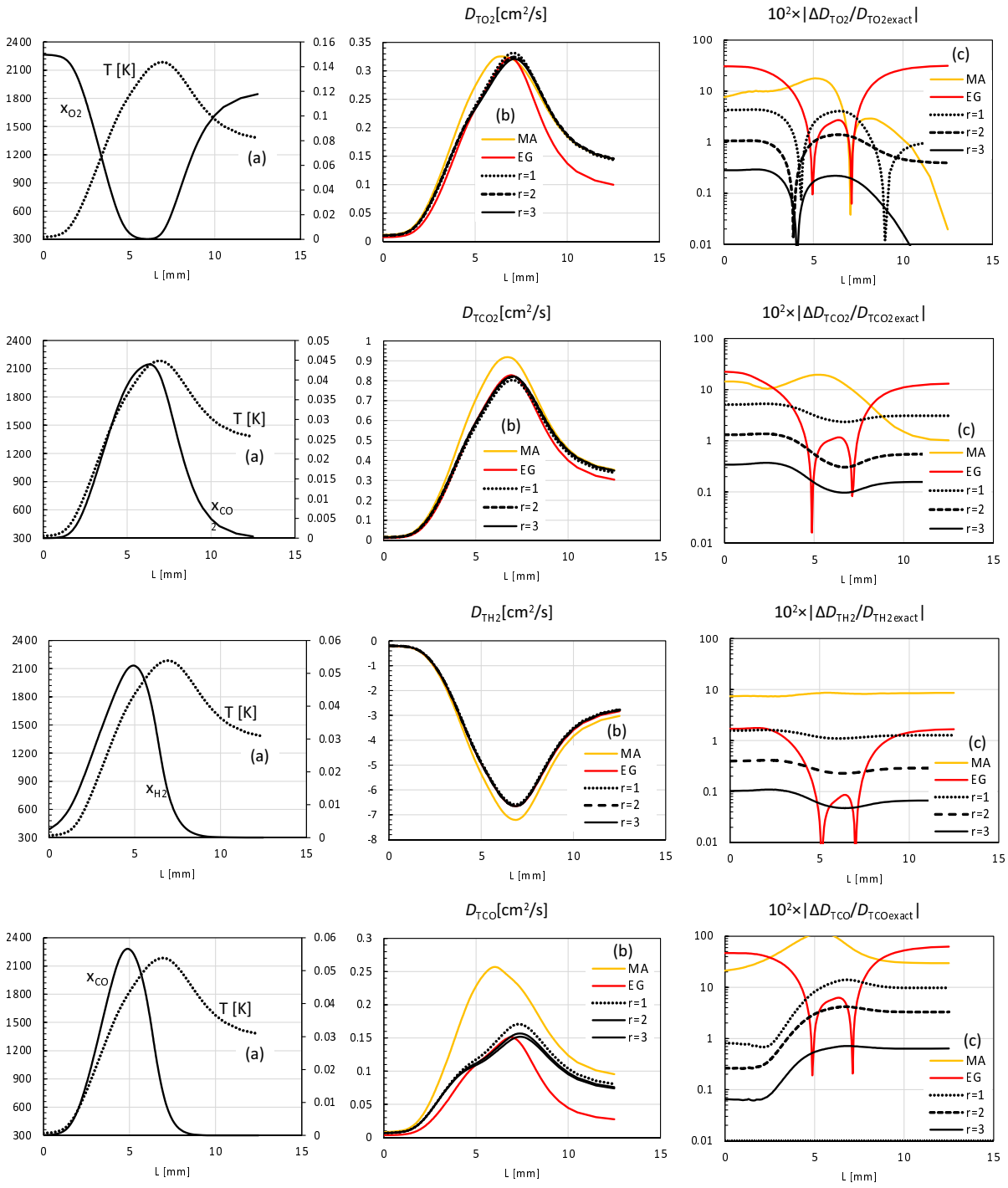

Figure 7.11: Results for species O2, CO2, H2 and CO vs. axial distance L; mole fraction x and temperature T (a), thermal diffusion coefficients (b) and thermal diffusion coefficients percentage error (c) as compared to exact (KTG) values for different approximation terms, mixture averaged approximation (yellow lines) and EGLib with $r = 3$ (red lines).

The figures for the thermal diffusion fluxes are Figs. 7.12 and 7.13.

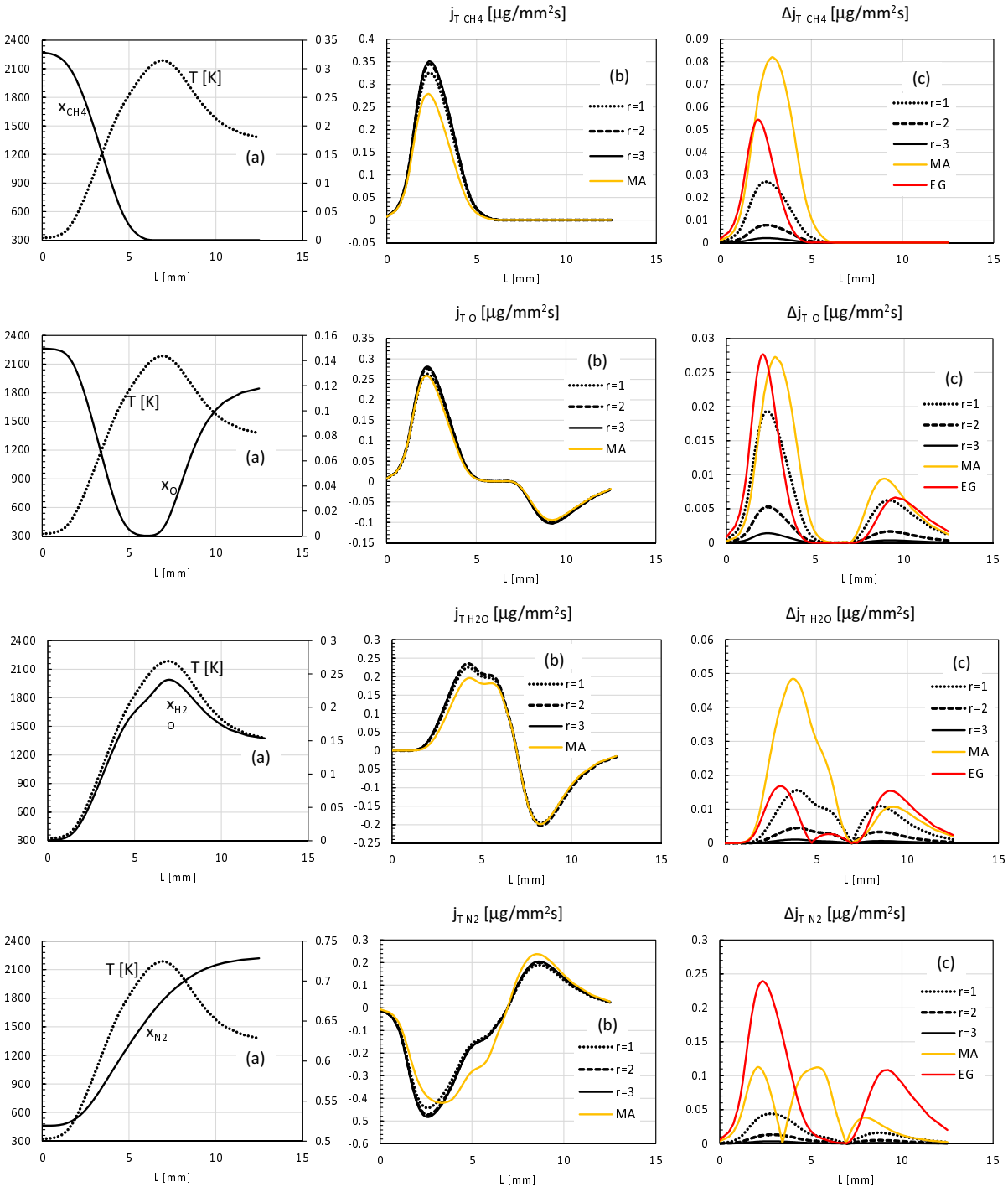

Figure 7.12: Major results vs. axial distance L for species CH4, O, H2O and N2; mole fraction x and temperature T (a), diffusion flux j (b) and absolute diffusion flux error Δj (c) as compared to exact (KTG) values for different approximation terms, mixture averaged approximation (yellow lines) and EGLib (EG $r = 3$, red lines).

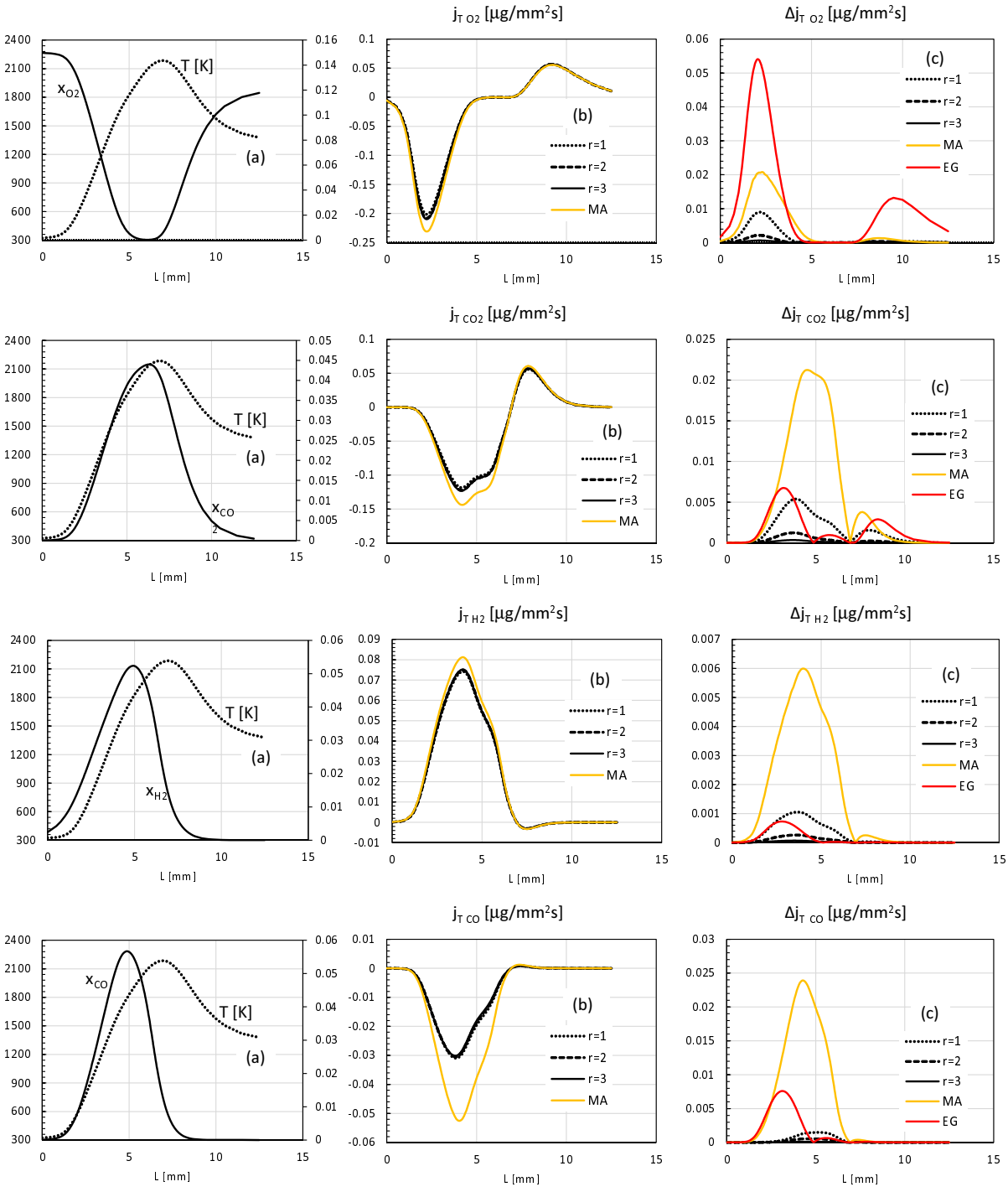

Figure 7.13: Intermediate results vs. axial distance L for species O2, CO2, H2 and CO; mole fraction x and temperature T (a), diffusion flux j (b) and absolute diffusion flux error Δj (c) as compared to exact (KTG) values for different approximation terms, mixture averaged approximation (yellow lines) and EGLib (EG, $r = 3$, red lines).

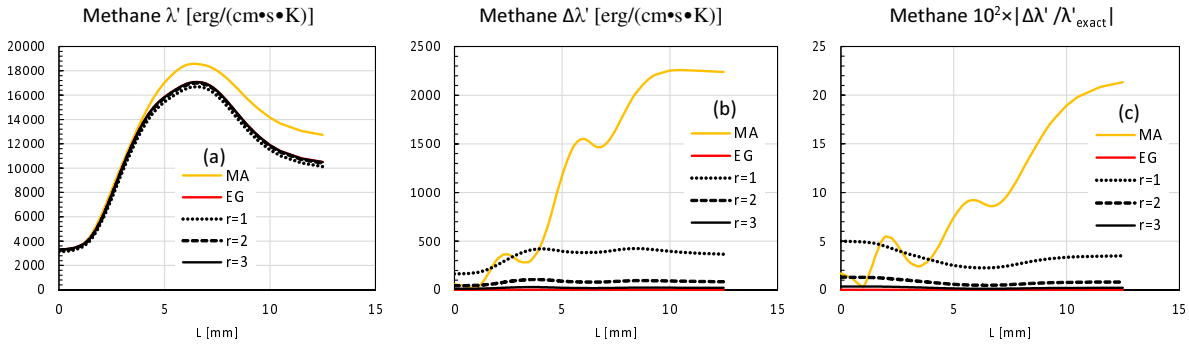

Figure 7.14: Partial thermal conductivity in a methane diffusion flame vs. distance L. Left column (a): partial thermal conductivity values. Center column (b): partial thermal conductivity absolute errors . Right column (c): partial thermal conductivity percentage errors. The results are shown for several maximal values of index r considered in the truncated Neumann series expansion. The results using the mixture averaged (MA) approximation are shown in yellow lines. The results using the EGLib (EG) $r = 3$ approximation are also shown using red lines.

Figure (7.14) shows the results for the partial thermal conductivity. As can be seen, the mixture averaged approximation is very inaccurate, while EGLib (which includes three preconditioned conjugate gradient iterations) provides results which are indistinguishable from the exact values. As can be seen in Fig. 7.14, the results found with the present algorithm (with $r = 1, 2, 3$) are not as accurate as those found with EGLib. However, the relative errors found with MuTLib including only the first Neumann series iteration (r=1) is less than 5% (remaining around 3% in most of the integration domain), which is a remarkable result.

Figure 7.15 shows the relative errors for the species CH4, O, H2O, N2, O2, CO2, H2, CO and the thermal conductivity for the present iterative algorithm and mixture averaged. As in the case of the premixed hydrogen flame, the error decays exponentially and therefore the error curves look linear in semi-logarithmic scales. As can be seen in Fig. 7.15, the relative errors may be fitted to the exponential decrease formula Eq. (7.3), in a similar way as it was done in the case of a premixed hydrogen flame. The results from this fit show that ε_1 values range from 1.11% (H2) to 14.8% (N2). In the case of the convergence rate exponent α, the results are very similar for all species, ranging between 1.35 (λ') and 1.53 (H2). Hence, the accuracy and convergence rate of the present algorithm in the methane counterflow diffusion flame configuration is comparable to the corresponding results found in the premixed hydrogen flame configuration.

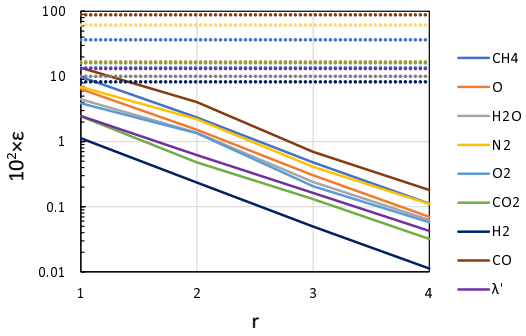

Figure 7.15: Normalized relative errors ε_i and $\varepsilon_{\lambda'}$ (Eq. (7.2)) found vs. maximal r considered in the truncated Neumann series (Eq. (5.8)) for methane counterflow diffusion flames. Dotted horizontal lines: corresponding results found with the mixture averaged approximation.

Chapter 8

Conclusions

8.1 Results summary

An algorithm for an efficient and accurate multicomponent thermal diffusion coefficients calculation based on the kinetic theory of gases (KTG) is described. This is possible by using the proper scaled parameters and a detailed examination of the different matrices that must be inverted in the resultant system of linear equations, derived from the KTG. The terms involving inelastic collisions and relaxation times for the internal degrees of freedom in polyatomic gases are considered and the resonant exchange of rotational energy is also accounted for in the case of polar gases, in addition to the classical Chapman-Enskog expressions. Thus, the present model considers the same physical effects included in the full multicomponent transport description considered in the Chemkin package.

In the case of a multicomponent mixture with N chemical species, the proposed algorithm makes use of the $N-1 \times N-1$ matrix inversion needed for the calculation of the Fick's diffusion coefficients, a problem addressed in Model 1 and Model 1+M of reference [28]. Based on these results, the calculation of the thermal diffusion coefficients involves a new $2N \times 2N$ (or $(N+P)\times(N+P)$, where P is the number of non monatomic molecules) matrix inversion, which is diagonally dominant. As a consequence, scaling this system by the corresponding diagonal terms allows for a fast convergence rate iterative algorithm, based on the Neumann series.

The accuracy and convergence rate of this new algorithm have been successfully analyzed. The results are compared against the mixture averaged calculations and the transport package developed by Ern and Giovangigli, EGLib, for two examples of practical interest: a premixed hydrogen flame and a methane counterflow diffusion flame. We show that the proposed new iterative algorithm at the first order term is already more accurate than the mixture average approximation in all the cases considered. On the other hand, it is shown that the first order term of the present algorithm (i.e., without the need of additional matrices multiplication)

is comparable to the results based on the EGLib library including three conjugate gradient iterations (the iteration level provided in the library) for the hydrogen combustion example, and much more accurate for the methane combustion flame. Regarding convergence rate beyond the first order term, we find that each new term in the new iterative algorithm provides a relative error reduction in thermal diffusion fluxes close to an order of magnitude, making it a very accurate and efficient algorithm.

During the preparation of this work different presentations have been performed to show the progress in the field to the combustion community:

- O. Córdoba and M. Arias-Zugasti
  Efficient Calculation of Multicomponent Thermal Diffusion Coefficients based on Kinetic Theory
  Oral presentation at the 11th Mediterranean Combustion Symposium, MCS11. Tenerife, España, 16/06/2019-20/06/2019. urlhttps://mcs11.unizar.es

- O. Córdoba and M. Arias-Zugasti
  Accurate and efficient calculation of multicomponent thermal diffusion fluxes based on kinetic theory
  Oral presentation at the 3rd HPC Spanish Combustion Workshop. Barcelona, España, 02/07/2021.

- B. Naud, O. Córdoba and M. Arias-Zugasti
  Application of an efficient and accurate multicomponent transport approximation
  Oral presentation at the 1st Spanish Fluid Mechanics Conference. Cádiz, España, 19/06/2022-22/06/2022. urlhttps://https://sfmc22.uca.es/

- O. Córdoba and M. Arias-Zugasti
  Convergence rate and dependence on polyatomic effects of recent accurate and efficient multicomponent transport iterative algorithm
  Oral presentation at the 1st Spanish Fluid Mechanics Conference. Cádiz, España, 19/06/2022-22/06/2022. urlhttps://https://sfmc22.uca.es/

A paper with the core of this work has also been published

- O. Córdoba and M. Arias-Zugasti
  Accurate and efficient calculation of multicomponent thermal diffusion coefficients and partial thermal conductivity based on kinetic theory,
  `https://doi.org/10.1016/j.combustflame.2022.112202`. Combustion and Flame 244, 112202-1-15, 2022. Reference [41].

As a general conclusion the present algorithm for the thermal diffusion coefficients, together with the results shown in [28] for the Fick's diffusion coefficients, provide an extremely efficient

and accurate method for the calculation of molecular mass transport coefficients in mixtures with large numbers of components, which will be of interest for the numerical simulation of detailed combustion mechanisms involving large numbers of chemical species. The aforementioned new algorithms have been implemented in the C++ software library package MuTLib (Multicomponent Transport Library) for the transport properties calculations in third party applications, which is available as additional material of [41].

8.2 Transport algorithm optimization. Recommendations for future works

During the investigation presented a few issues that may improve the efficiency and accuracy of the obtained results have been found .

The first issue is related to the collision integrals. The only option implemented in MuTLib is the direct reading of Monchick and Mason tables. A future improvement is the implementation of more accurate curves, tables or correlations. The idea is to provide the library user with multiple options to cope different necessities for transport calculations.

The second issue is to check the nature of the system of equations and, provided the mole fraction dependency, search for simplifications. For the species with mole fractions under a threshold many terms could be automatically equaled to zero and faster calculations may be performed. Related to this, a Model 1+M in the same way it was done for the Fick diffusion [28] may increase the algorithm efficiency.

The last issue is the study of the blocks in the resultant system of linear equations when there are values with different orders of magnitude. In particular, something similar to 5.4 when there are species with very different molecular weight and meaningful mole fractions.

The mentioned investigation areas will be the subject of a forthcoming publication.

Bibliography

[1] J. H. Ferziger and H. G. Kaper. *Mathematical Theory of Transport Processes in Gases.* North-Holland, 1972.

[2] Combustion Research Group at UC San Diego. The San Diego mechanism. Chemical-Kinetic Mechanisms for Combustion Applications. https://web.eng.ucsd.edu/mae/groups/combustion/mechanism.html.

[3] S. Chapman and T. G. Cowling. *The Mathematical Theory of Non-Uniform Gases.* Cambridge University Press, Cambridge UK, third edition, 1985.

[4] J. O. Hirschfelder, C. F. Curtiss, and R. B. Bird. *The Molecular Theory of Gases and Liquids.* Wiley, New York NY, second edition, 1964.

[5] C. S. Wang-Chang and G. E. Uhlenbeck. Transport phenomena in polyatomic gases. Technical report, University of Michigan, 1959.

[6] L. Monchick and E. A. Mason. Transport properties of polar gases. *The Journal of Chemical Physics*, 35(5):1676–1697, 1961.

[7] E. A. Mason and L. Monchick. Heat conductivity of polyatomic and polar gases. *The Journal of Chemical Physics*, 36(6):1622–1639, 1962.

[8] L. Monchick, K. S. Yun, and E. A. Mason. Formal kinetic theory of transport phenomena in polyatomic gas mixtures. *The Journal of Chemical Physics*, 39(3):654–669, 1963.

[9] F. A. Williams. *Combustion Theory.* CRC Press, second edition, 1994.

[10] D. E. Rosner. *Transport Processes in Chemically Reacting Flow Systems.* DOVER, Mineola NY, 2000.

[11] Faizan Habib Vance, Philip de Goey, and Jeroen A. van Oijen. The effect of thermal diffusion on stabilization of premixed flames. *Combustion and Flame*, 216:45–57, 2020.

[12] J. Schlup and G. Blanquart. Validation of a mixture-averaged thermal diffusion model for premixed lean hydrogen flames. *Combustion Theory and Modelling*, 22(2):264–290, 2018.

[13] J. De Charentenay and A. Ern. Multicomponent transport impact on turbulent premixed H2/O2 flames. *Combustion Theory and Modelling*, 6(3):439–462, 2002.

[14] C. Bruno, V. Sankarana, H. Kollab, and J. H. Chen. Impact of multi-component diffusion in turbulent combustion using direct numerical simulations. *Combustion and Flame*, 162:4313–4330, 2015.

[15] Nancy J. Brown, Lucas A.J. Bastien, and Phillip N. Price. Transport properties for combustion modeling. *Progress in Energy and Combustion Science*, 37(5):565–582, 2011.

[16] Frederick R. W. McCourt, Jan J. M. Beenakker, Walter E. Köhler, and Ivan Kuscer. *Nonequilibrium Phenomena in Polyatomic Gases. Volume 1: Dilute Gases.* 1990.

[17] W. A. Wakeham, M. A. Assael, J. K. Atkinson, J. Bilek, J. M.N.A. Fareleira, A. D. Fitt, A. R.H. Goodwin, and C. M.B.P. Oliveira. Thermophysical property measurements: The journey from accuracy to fitness for purpose. *International Journal of Thermophysics*, 28(2):372–416, 2007.

[18] G. Dixon-Lewis. Flame structure and flame reaction kinetics II. Transport phenomena in multicomponent systems. *Proceedings of the Royal Society of London Series. A-Mathematical and Physical Sciences*, 307(1488):111–135, 1968.

[19] W. W. Jones and J. P. Boris. An algorithm for multispecies diffusion fluxes. *Computers and Chemistry*, 5(2-3):139–146, 1981.

[20] E. S. Oran and J. P. Boris. Detailed modeling of combustion systems. *Progress in Energy and Combustion Science*, 7(1):1–72, 1981.

[21] A. Ern and V. Giovangigli. Impact of detailed multicomponent transport on planar and counterflow hydrogen/air and methane/air flames. *Combustion Science and Technology*, 149(1):157–181, 1999.

[22] V. Giovangigli. *Multicomponent Flow Modeling.* Birkhäuser, Boston, 1999.

[23] V. Giovangigli. Multicomponent transport in laminar flames. *Proceedings of the Combustion Institute*, 35(1):625–637, 2015.

[24] V. Giovangigli. Convergent iterative methods for multicomponent diffusion. *IMPACT of Computing in Science and Engineering*, 3(3):244–276, 1991.

[25] A. Ern and V. Giovangigli. Projected iterative algorithms with application to multicomponent transport. *Linear Algebra and Its Applications*, 250:289–315, 1997.

[26] A. Ern and V. Giovangigli. *Multicomponent Transport Algorithms*. Springer - Verlag, 1994.

[27] Y. Xin, W. Liang, W. Liu, T. Lu, and C. K. Law. A reduced multicomponent diffusion model. *Combustion and Flame*, 162(1):68–74, 2015.

[28] M. Arias-Zugasti, P. L. García-Ybarra, and J. L. Castillo. Efficient calculation of multicomponent diffusion fluxes based on kinetic theory. *Combustion and Flame*, 163:540–556, 2016.

[29] P. L. Garcia-Ybarra, C. Nicoli, and P. Clavin. Soret and dilution effects on premixed flames. *Combustion Science and Technology*, 42(1-2):87–109, 1984.

[30] B. Naud and M. Arias-Zugasti. Accurate multicomponent Fick diffusion at a lower cost than mixture-averaged approximation: Validation in steady and unsteady counterflow flamelets. *Combustion and Flame*, 219:120–128, 2020.

[31] D. Burnett. The distribution of velocities in a slightly non-uniform gas. *Proceedings of the London Mathematical Society*, 39:385–430, 1935.

[32] D Burnett. The distribution of molecular and the mean motion in a non-uniform gas. *Proceedings of the London Mathematical Society*, 40:382–435, 1935.

[33] J. G. Parker. Rotational and vibrational relaxation in diatomic gases. *Physics of Fluids*, 2(4):449–462, 1959.

[34] C. A. Brau and R. M. Jonkman. Classical theory of rotational relaxation in diatomic gases. *The Journal of Chemical Physics*, 52(2):477–484, 1970.

[35] Robert J. Kee. Theory Manual C HEMKIN ® Software. *Design*, (May):1–273, 2004.

[36] Robert J. Kee, Michael E. Coltrin, Peter Glarborg, and Huayang Zhu. *Chemically Reacting Flow Theory, Modeling, and Simulation*. Wiley, second edition, 2018.

[37] E. L. Heck, A. S. Dickinson, and V. Vesovic. Testing the Mason-Monchick approximation for transport properties of pure diatomic gases. *Chemical Physics Letters*, 204(3-4):389–392, 1993.

[38] Michael J. Wright, Helen H. Hwang, and David W. Schwenke. Recommended collision integrals for transport property computations part 1: Air Species. *AIAA Journal*, 43(1):2558–2564, 2005.

[39] L. Monchick and E. A. Mason. A reconsideration of thermal diffusion in ionized gases: Quantal and dynamic shielding effects. *Physics of Fluids*, 28(11):3341–3348, 1985.

[40] Michael J. Wright, Helen H. Hwang, and David W. Schwenke. Recommended collision integrals for transport property computations part 2: Mars and venus entries. *AIAA Journal*, 45(1):281–288, 2007.

[41] Oscar Córdoba and Manuel Arias-zugasti. Efficient Calculation of Multicomponent Thermal Diffusion Coefficients Based on Kinetic Theory. *Combustion and Flame*, 244:1–15, 2022.

[42] K. Chen. *Matrix Preconditioning Techniques and Applications*. Cambridge University Press, Cambridge UK, 2005.

[43] Gene H. Golub and Charles F. Van Loan. *Matrix Computation*. The Johns Hopkins University Press, third edition, 1996.

[44] D. Fernández-Galisteo, A. L. Sánchez, A. Liñán, and F. A. Williams. One-step reduced kinetics for lean hydrogen-air deflagration. *Combustion and Flame*, 156(5):985–996, 2009.

[45] R. J. Kee, J. A. Miller, G. H. Evans, and G. Dixon-Lewis. A computational model of the structure and extinction of strained, opposed flow, premixed methane-air flames. *Symposium (International) on Combustion*, 22(1):1479–1494, 1989.

[46] J. Stefan. Sitzungsberichte Akad. Wiss. *Wien, II*, 68:325, 1874.

[47] C. R. Wilke. Diffusional properties of multicomponent gases. *Chemical Engineering Progress*, 46(2):95–104, 1950.

[48] D. F. Fairbanks and C. R. Wilke. Diffusion coefficients in multicomponent gas mixtures. *Industrial and Engineering Chemistry*, 42(3):471–475, 1950.

[49] P. Paul and J. Warnatz. A re-evaluation of the means used to calculate transport properties of reacting flows. *Symposium (International) on Combustion*, 27(1):495–504, 1998.

[50] E. Anderson, Z. Bai, C. Bischof, S. Blackford, J. Demmel, J. Dongarra, J. Du Croz, A. Greenbaum, S. Hammarling, A. McKenney, and D. Sorensen. *LAPACK Users' Guide*, volume 1. SIAM, Philadelphia, Pennsylvania, USA, third edition, 1999.

Nomenclature

Abbreviations

A	perturbation matrix for Fick's diffusion calculation
A_T	perturbation matrix for thermal diffusion calculation
$c_{\text{int.}}$	internal component of the molecular heat capacity
c_p	molecular heat capacity at constant pressure
$c_{\text{rot.}}$	rotational component of the molecular heat capacity
c_v	molecular heat capacity at constant volume
D	Fick difussion coefficient
$\mathscr{D}$	binary diffusion coefficient
$\mathscr{D}_{\text{int.}}$	binary diffusion coefficient for internal energy
DNS	Direct Numerical Simulation
D_T	thermal difussion coefficient
EGLib	Ern Giovangigli Library
$\mathbf{j_T}$	thermal diffusion flux
KTG	Kinetic Theory of Gases
m	molecular mass
MA	Mixture Averaged
MuTLib	Multicomponent Transport Library
n	number density

p	pressure
$\mathcal{R}$	universal gas constant
r.s.	rigid sphere
T	absolute temperature
$\mathbf{v}$	mixture hydrodynamic velocity (barycentric)
x	mole fraction

Greek Symbols

$\mathbf{c}$	particule velocity
δ	Kronecker delta function
ϵ	well depth Lennard Jones potential
η	dynamic viscosity
γ	adiabatic coefficient
λ	thermal conductivity
λ'	partial thermal conductivity
μ	dipole moment
ϕ	equivalence ratio
ϕ	equivalence ratio
$\mathbf{r}$	position
σ	collision cross section
t	time
ζ	collision number

Subscripts

(n)	Chapman-Enskog approximation index

Superscripts

$-$	Magnitude average
(n)	Chapman-Enskog approximation index

Appendix A

Mixture averaged diffusion approximation

The general formulas used in the calculation of the diffusion coefficients according to this simplified model are quoted below. As is well known, the mixture averaged approximation allows for the calculation of the transport properties in multicomponent mixtures avoiding the need to solve the several linear systems that arise from the KTG. The calculation of the thermal diffusion coefficients according to this simplified model makes use of the mixture averaged Fick diffusion coefficients. These coefficients were originally defined as shown in Eq. (A.1) [46, 47, 48]

$$D_{i-\mathrm{mix}} = (1 - x_i) \left[\sum_{\substack{j=1 \\ j \neq i}}^{N} \frac{x_j}{\mathscr{D}_{ij}} \right]^{-1} \quad ; \qquad \mathbf{j}_i = -\rho \frac{m_i}{m} \frac{1 - y_i}{1 - x_i} D_{i-\mathrm{mix}} \mathbf{d}_i. \tag{A.1}$$

Although this formula is still in wide use (see, e.g., [9, 48]), the slightly simplified definition provided later by [3]

$$\tilde{D}_{i-\mathrm{mix}} = (1 - y_i) \left[\sum_{\substack{j=1 \\ j \neq i}}^{N} \frac{x_j}{\mathscr{D}_{ij}} \right]^{-1} \quad ; \qquad \mathbf{j}_i = -\rho \frac{m_i}{m} \tilde{D}_{i-\mathrm{mix}} \mathbf{d}_i \tag{A.2}$$

has become more common in combustion (see, e.g., [49, 12]). Both expressions are totally equivalent and are related by

$$\tilde{D}_{i-\mathrm{mix}} = \frac{1-y_i}{1-x_i} D_{i-\mathrm{mix}}. \tag{A.3}$$

For a more comprehensive discussion on the different conventions for the multicomponent diffusion coefficients see [28]. In this work we will make use of Eq. (A.2). With this choice in mind, the mixture averaged thermal diffusion coefficients are given by [49]

$$D_{Ti-\mathrm{mix}} = \frac{k_{Ti}}{x_i} \tilde{D}_{i-\mathrm{mix}} \tag{A.4}$$

where k_{Ti} is the thermal diffusion ratio for species i in the mixture. Nevertheless, the reader should be warned that many authors define k_{Ti} as in Eq. (A.4) including an additional factor given by the local mass density ρ_i, to avoid the corresponding singularity found in the dilute limit [3, 49, 12]. In those cases the expression for the flux vector is modified accordingly.

Following [3, 12], the mixture averaged thermal diffusion ratios k_{Ti} are given by

$$k_{Ti} = \frac{m^2}{\mathcal{R}\rho} \sum_{j=1}^{N} \frac{1.2C_{ij}^* - 1}{\mathscr{D}_{ij}} \frac{y_i b_j + y_j b_i}{m_i + m_j} \tag{A.5}$$

where b_i is given by

$$b_i = \lambda_i \left[1 + \frac{1.065}{2\sqrt{2}x_i} \sum_{\substack{j=1 \\ j \neq i}}^{N} x_j \Phi_{ij} \right]. \tag{A.6}$$

In the former expression the pure species thermal conductivity λ_i may be approximated by

$$\lambda_i = \frac{15}{4} \frac{\mathcal{R}\eta_i}{m_i} \tag{A.7}$$

where the viscosity η_i is given by

$$\eta_i = \frac{5}{16} \frac{\sqrt{\pi m_i k_B T}}{\pi \sigma_i^2 \Omega_{ii}^{(2,2)*}} \tag{A.8}$$

The former expression depends on the reduced collision integrals $\Omega_{ii}^{(2,2)*} = A_{ii}^* \Omega_{ii}^{(1,1)*}$, which are provided by [6] for most species of interest in combustion. Finally, the values Φ_{ij} are given

by

$$\Phi_{ij} = \frac{\left[1 + \left(\frac{\eta_i}{\eta_j}\right)^{1/2} \left(\frac{m_j}{m_i}\right)^{1/4}\right]^2}{\left[1 + \frac{m_i}{m_j}\right]^{1/2}} \tag{A.9}$$

As can be seen, the evaluation of the mixture averaged thermal diffusion coefficients is considerably more involved than the corresponding mixture averaged Fick diffusion coefficients, but it is still considerably simpler than the rigorous evaluation of these transport properties according to KTG.

Appendix B

MuTLib Multicomponent Transport Library. Users' guide, version 0.3

B.1 Introduction

MutLib is a C++ library with classes and functions to calculate transport variables. The ideas behind the implemented algorithms may be found in references [28, 30] and "Accurate and efficient calculation of multicomponent thermal diffusion coefficients and partial thermal conductivity based on kinetic theory", pending to be published.

B.2 License

MutLib is a freely-available software package. It can be included in commercial software packages. We only ask that that proper credit be given to the authors, for example by citing the MutLib Users' Guide. The license used for the software is the modified BSD license.

Like all software, it is copyrighted. It is not trademarked, but we do ask the following: if you modify the source for these routines we ask that you change the name of the routine and comment the changes made to the original.

We will gladly answer any questions regarding the software. If a modification is done, however, it is the responsibility of the person who modified the routine to provide support.

B.3 Installation

The source code of the library is supplied for customized compilations. For this purpose a makefile is provided to create a libMutLib.a file. This file is a group of the different object files generated during the compilation. The installation has been successfully tested in Ubuntu OS and Windows 10, with GNU gcc compiler (mingw-w64 in the case of Windows) The LAPACK

library is required for direct matrix inversion when needed, [50]. Therefore, the third party executables must be linked to MutLib and LAPACK libraries.

The package is delivered in a compressed tar file MutLib.tar. Any software to extract files is valid. In a console the following command may work:

$tar - xvfMutLib.tar$

The list of the compressed files is as follows:

example.cpp
kineticdata.cpp
kineticdata.h
LICENSE
Makefile.example
Makefile.MutLib
omega.cpp
species.cpp
species.h
thermodata.cpp
thermodata.h
transport.cpp
transport.h
tran.dat
therm.dat

To build the library the following command generates the file libMutLib.a

$make - fMakefile.MutLib$

The file *therm.dat*contains the necessary coefficients to calculate the thermodynamic properties, such as the specific heat at constant pressure c_p. It must be written in NASA format for thermo mechanical tables. The file *tran.dat* contains data relevant in kinetic theory fore the different species usually present in mixtures. Examples of these files may be found in [2] . The files in this site contain data for usual species used in combustion, however, the files can be edited to add more species.

B.4 Library structure and setup

There are four main classes to perform transport calculations:

1. class *Species*. Contains the relevant information in the mixture. The name of the species, the molar weight, the mole fractions, pressure and temperature. The class prototype may be viewed in the file *species.h*.

2. class *Thermodata*. Contains the information related to the NASA thermodynamic polynomials. The methods deliver thermodynamic data of the desired species. The class prototype may be viewed in the file *thermodata.h*.

3. class *Kineticdata*. Contains data related to the kinetic theory of gases. The class prototype may be viewed in the file *kineticdata.h*.

4. class *Transport*. Stores the the transport properties of the mixture. The methods provide calculated Fick and Soret diffusion fluxes and the partial thermal conductivity. The class prototype may be viewed in the file *transport.h*.

The classes Kineticdata and Thermodata are set by a file reading. The following sentences must be executed only once at the beginning of the program.

thermodata.ReadFile("*therm.dat*");

kineticdata.ReadFile("*tran.dat*");

The mixture definition is the next step. Each species may be added to the *Species* class. It is necessary to search for the indexes in the kinetic and thermodynamic databases.

indexK = *kineticdata.CheckName*(*speciesName*);

indexT = *thermodata.CheckName*(*speciesName*);

species.AddSpecie(*speciesName*, *molarMass*, *indexK*, *indexT*);

Temperature and pressure is also setup in the *Species* class:

species.temp=288.15;

species.press=101325;

The next step is to pass the generated information to the *Transport* class:

transport.SetUp(*species*, *kineticdata*, *thermodata*);

The *Transport* class is now ready to calculate and recover the desired information:

transport.Calculate();

Depending on the user interest the required information may be different. Next code instructions will deliver Fick diffusion fluxes, Soret diffusion fluxes and partial thermal conductivity.

transport.GetFickFluxes(*vectorOfMoleFractionGradients*);

transport.GetSoretFluxes(*gradientOfTemperatureLogarithm*);

transport.GetThCond();

The function Calculate may not use default values and different arguments are available to fit the calculation. The next is the method prototype.

```
//Main driver
void Calculate(
    bool            exact=false,    //boolean to set exact Fick diffusion
                                    //coefficients
    unsigned int    Fickr=1,        //Fick diffusion Neumann steps
    int             FickM=0,        //M number of species in model 1+M for
                                    //Fick diffusion coefficients
    double          FickThr=.1,     //Molar fraction threshold in model 1+M
                                    //for Fick diffusion coefficients
                                    //activated with FickM<0
    unsigned int    Soretr=1);      //Soret diffusion Neumann steps
```

B.5 Units

The following units have been considered during the development and must be taken into account by the user.

Magnitude	*Units*
Temperature	K
Pressure	Pa
Molar weight	g/mol
Flux	$\mu g/s$
Mole fraction gradient	$1/mm$
Temperature gradient	K/mm
Thermal conductivity	$J/\left(m \cdot s \cdot K\right)$

B.6 Usage example

In this section a very simple case of a binary mixture is presented. The diffusion fluxes are printed in two different conditions of the mixture.To build the example executable the following command generates the file *example.exe*.

$make - f\ Makefile.example$

The call to the executable produces the next output:

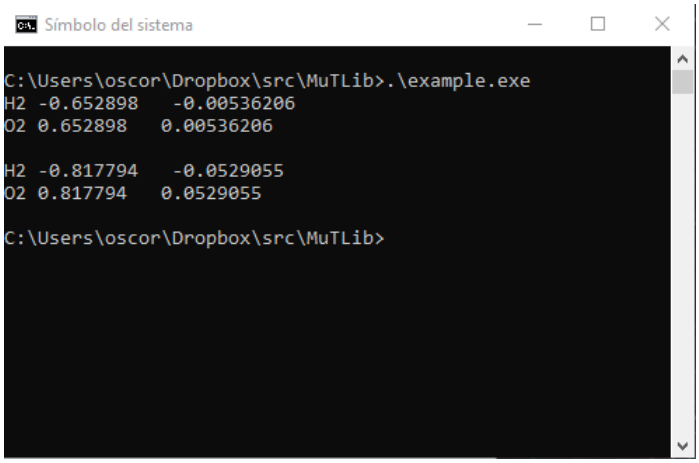

The next figures show the source code of the file example.cpp

```cpp
#include <iostream>
#include <transport.h>

using namespace std;

int main(){

    Species     species;
    ThermoData  thermodata;
    KineticData kineticdata;
    Transport   transport;

    if (!kineticdata.ReadFile("tran.dat")){
        cout<<"Error reading file tran.dat"<<endl;
        exit(0);
    }
    if (!thermodata.ReadFile("therm.dat")){
        cout<<"Error reading file therm.dat"<<endl;
        exit(0);
    }

    string name;
    int indexK;
    int indexT;

    name="H2"; //Molar weight 1g/mol Mole fraction 0.5
    indexK=kineticdata.CheckName(name);
    indexT=thermodata.CheckName(name);
    if (indexK==-1 || indexT==-1){
        cout<<"Error, species "<<name<<" not found"<<endl;
        exit(0);
    }
    species.AddSpecie(name,.5,indexK, indexT);

    name="O2"; //Molar weight 32g/mol Mole fraction 0.5
    indexK=kineticdata.CheckName(name);
    indexT=thermodata.CheckName(name);
    if (indexK==-1 && indexT==-1){
        cout<<"Error, species "<<name<<" not found"<<endl;
        exit(0);
    }
    species.AddSpecie(name,.5,indexK, indexT);

    //Sets pressure and temperature
    species.temp=288.15; //teperature in K
    species.press=101325;//pressure in Pa

    //Sets up the transport class
    transport.SetUp(&species, &kineticdata, &thermodata);

```

```
51      transport.Calculate();
52
53      vector<double>drive;
54      drive.resize(2,1.);
55      double gradLogT=1;
56
57      vector<double> FickFluxes;
58      vector<double> SoretFluxes;
59      FickFluxes=transport.GetFickFluxes(drive);
60      SoretFluxes=transport.GetSoretFluxes(gradLogT);
61
62      cout<<species.GetName(0)<<" "<<FickFluxes[0]<<"   "<<SoretFluxes[0]<<endl;
63      cout<<species.GetName(1)<<" "<<FickFluxes[1]<<"   "<<SoretFluxes[1]<<endl;
64
65      cout<<endl;
66      species.temp=1000.;
67      species.SetMolFrac(0,0.7);
68      species.SetMolFrac(1,0.3);
69      transport.Calculate();
70      FickFluxes=transport.GetFickFluxes(drive);
71      SoretFluxes=transport.GetSoretFluxes(gradLogT);
72      cout<<species.GetName(0)<<" "<<FickFluxes[0]<<"   "<<SoretFluxes[0]<<endl;
73      cout<<species.GetName(1)<<" "<<FickFluxes[1]<<"   "<<SoretFluxes[1]<<endl;
74
75
76      return 0;
77  }
78
```